U. S. DEPARTMENT OF COMMERCE
W. Averell Harriman, Secretary
NATIONAL BUREAU OF STANDARDS
E. U. Condon, Director

MARCH 1948
VOLUME 40
NUMBER 3

JOURNAL OF RESEARCH

of the

NATIONAL BUREAU OF STANDARDS

Contents

RP		Page
1865.	Measurement of water in gases by electrical conduction in a film of hygroscopic material and the use of pressure changes in calibration. Elmer R. Weaver and Ralph Riley. (Price 25 cents)	169
1866.	Electric quadrupole coupling of the nuclear spin with the rotation of a polar diatomic molecule in an external electric field. U. Fano. (Price 15 cents)	215
1867.	Preliminary study on portions of the systems Na_2O-CaO-Al_2O_3-Fe_2O_3 and Na_2O-CaO-Fe_2O_3-SiO_2. William R. Eubank and Robert H. Bogue. (Price 15 cents)	225
1868.	Theory and design of a cavity attenuator. J. J. Freeman. (Price 15 cents)	235
1869.	Theory of Wagner ground balance for alternating-current bridges. Richard K. Cook. (Price 10 cents)	245
1870.	Correlations of the gel strength of paste walls and the shelf life of electric dry cells. Walter J. Hamer. (Price 15 cents)	251

For sale by the Superintendent of Documents, U. S. Government Printing Office, Washington 25, D. C. - Price 50 cents
$4.50 per year on subscription

UNITED STATES GOVERNMENT PRINTING OFFICE, WASHINGTON : 1948

U. S. Department of Commerce
National Bureau of Standards

Research Paper RP1865
Volume 40, March 1948

Part of the Journal of Research of the National Bureau of Standards

Measurement of Water in Gases by Electrical Conduction in a Film of Hygroscopic Material and the Use of Pressure Changes in Calibration

By Elmer R. Weaver and Ralph Riley [1]

The electrical conductivity of a thin film of such a material as phosphoric acid changes over a wide range with changes in the concentration of water in the atmosphere with which it is in contact. By adjusting the pressures of a sample of gas of known and one of unknown composition, they can be made to have the same concentration of water, shown by the production of equal resistances of the detecting film. Apparatus and procedures for making such adjustments and calculating analyses are given in detail, and numerous applications are described. The method has the merits of simplicity, speed, and great sensitivity. Only small samples are needed, and few substances interfere.

I. Introduction

1. General Method

The measurement of water vapor in gases by observing the resistance of thin films of electrolyte has been employed occasionally at the National Bureau of Standards for a variety of purposes during a period of nearly 30 years. The essentials of the method are extremely simple. A thin film of liquid, which may be such a material as phosphoric or sulfuric acid or a solution containing one or more acids, bases, or salts with a binding material such as gelatin or a high-polymer plastic, is spread over the surface of a solid insulator between metallic electrodes. The electrolyte tends to reach equilibrium with the water vapor in the atmosphere that surrounds it and to form a solution, the electrical resistance of which is a measure of the water vapor in the atmosphere. We need, in addition, some sort of instrument for measuring or comparing electrical resistances and a means of calibrating the film by comparison with a gas of known moisture content. Polarization makes necessary the use of alternating current for the measurement.

The method was devised initially [1] [2] to detect very small concentrations of water vapor in gases entering a catalytic reaction in which water is a poison. The material first tried for the conducting film was a salt, calcium chloride; but it was soon found that the salt became a nonconducting solid at a humidity far higher than that to be detected, and numerous other electrolytes were tried. Among them phosphoric and sulfuric acids were found most useful, because they served to detect the smallest concentrations of water vapor. However, films of these materials changed resistance so rapidly that it seemed hardly worthwhile to calibrate them by comparison with known atmospheres, laboriously prepared.

The method therefore fell into disuse except for qualitative work until F. W. Dunmore [2, 3] employed it successfully for much higher humidities in connection with meteorological observations. He used a salt, lithium chloride, as the electrolyte in a plastic film of very high resistivity, but one which held its calibration well. The need during the war for a method of determining rapidly very small quantities of water vapor in aviator's oxygen led to the development of a means of calibrating a sensitive film at the time of its use so quickly and simply that little need remained for a permanent calibration. This at

[1] The senior author has been unable to learn the whereabouts of Mr. Riley, who served as a civilian at Pearl Harbor during the latter part of the war. The senior author is therefore entirely responsible for the text of the present paper, but most of the observations on which it is based were made by Mr. Riley, who also contributed much of the constructive thought that went into the development of the method.

[2] Figures in brackets indicate the literature references at the end of this paper.

774908—48

once greatly extended the possible applications of the method, several of which will be suggested later in this paper.

2. Principle Involved in Calibration by the Adjustment of Pressure

As a rough approximation, deviations from which will be discussed later, the resistance of a given film is independent of the gases other than water vapor with which it is in contact and depends only on the amount of water contained in unit volume. If a sample of gas, such as oxygen or air, of known water content per unit volume is passed over the film it will assume a certain resistance. If a second sample of gas of unknown water content is then passed over the film, the resistance will usually be different, but it may be restored to its original value by compressing or expanding the second sample until it contains the same quantity of water per unit volume (more exactly until the water vapor has the same fugacity) as the first sample. When this condition is reached, we note the pressure and readily compute what the water content would be in a unit volume at any other pressure (usually, but not always, 1 atmosphere). If the unknown gas is initially at atmospheric pressure, it may be more convenient to change the pressure of the standard gas until the same resistance is produced by both.

As a simple illustration of the first procedure, let us say that the first sample of gas used as a standard is known to contain 2 mg of water per liter, and that the second sample causes the detecting film to have the same resistance as the first (and that it therefore also contains 2 mg of water per liter) when at a pressure of 100 atmospheres. If the second sample of gas is now expanded to 1 atmosphere, it has about 100 times the volume but the same total quantity of water as before expansion, and the water content is, therefore, 0.02 mg per liter. The second procedure may be illustrated by the following example. A cylinder of oxygen known to contain 8 micrograms (0.008 mg) of water per liter when expanded to atmospheric pressure was used as the standard gas. The resistance produced by exposing the film to a sample of freon at atmospheric pressure was matched by adjusting the oxygen to 18 psig (pounds per square inch gage) or a total pressure of 2.2 atmospheres. Then the freon at atmospheric pressure contained 2.2 times as much water as did the oxygen at atmospheric pressure, or 18 micrograms per liter.

Frequently it is convenient, in order to make the best use of available gages, to set one gas to an arbitrary pressure of no interest in itself and to match it by adjusting the pressure of the other. For brevity, the process of adjusting the pressure of one or both gases to produce the same electrical resistance of the detector will be called comparing the gases. In general four pressures are involved in a comparison:

P_s, the pressure at which the standard gas contains a known concentration of water vapor, S.

P_c, the comparison pressure at which the standard gas is matched with the electrical resistance produced by the unknown gas at pressure P_x.

P_x, defined by the preceding statement.

P_w, the pressure at which we wish to know the concentration of water in the unknown gas.

The water content, C, of the standard gas at the comparison pressure is

$$C=S\frac{P_c}{P_s}. \tag{1}$$

Since it is known that the unknown gas has this same water content at the matching pressure P_x, the water content, W, at pressure P_w of the unknown gas is derived from C, just as C was derived from S:

$$W=C\frac{P_w}{P_x}=\frac{SP_cP_w}{P_sP_x} \tag{2}$$

Having determined the value of W we can obviously use the newly analyzed gas as the standard to determine W_1, the water content of still another unknown gas at P_{w_1} after matching it electrically at pressure P_{x_1} against the new standard at Pw, thus:

$$W_1=W\frac{P_{w_1}}{P_{x_1}}=S\frac{P_cP_wP_{w_1}}{P_sP_xP_{x_1}} \tag{3}$$

There is obviously no limit to the number of steps of this kind that can be taken, but because some error is involved in each comparison, the results soon lose significance.

A gas that contains an approximately known concentration of water, to be used as the first or the only standard, can be obtained easily by saturating compressed air (or other compressed gas that may be available) with water vapor at any convenient pressure. S then represents the concentration of water vapor in equilibrium with

liquid water at the temperature of the measurement, and P_s is the pressure in the saturator. S and W may be expressed in any units, not necessarily in micrograms per liter, pounds per thousand cubic feet, or other units of mass per unit of volume; they may also be expressed as partial pressures, relative humidities, or percent by volume. Since only ratios of pressures are involved in the computation of W and S, any unit of pressure may be used, provided it is kept clearly in mind that total pressures are involved, not gage pressures (above atmospheric).

In the application of the method that has been most extensively made—determining the moisture content of compressed gases—it is convenient to use as the standard gas air, oxygen, or nitrogen saturated at about 35-atmospheres pressure and expanded to 1 atmosphere. The water content of the unknown gas is to be determined at 1 atmosphere. Hence, if pressures are expressed in atmospheres, P_e and P_w of eq 2 are both unity, and the equation becomes

$$W=\frac{S}{P_s P_z}, \tag{4}$$

in which S is the concentration of water in a vapor space in equilibrium with liquid water.

In the method of use described, the pressure gages are the measuring instruments. We are usually not at all concerned with the actual value of the electrical resistance of the sensitive film, and the electical instruments are used only to show that two resistances, corresponding to measured pressures, are the same; but in some cases, especially when following changing concentrations of water vapor, it is impracticable to make a separate calibration through the adjustment of pressure for every variation of humidity, and readings of the electrical instruments are recorded and interpreted, usually by interpolation between values determined by pressure readings. The electrical circuit is then truly used as a measuring instrument and not merely as a null-point indicator.

In the foregoing description of principles, it was necessary to qualify many of the statements with the words about, approximate, etc. The corrections to be made to produce more accurate results and the sources of error will be discussed after the construction of the instrument and its operation have been described.

II. Description of Apparatus Employed

1. General Arrangement and Procedure

The general method which has been outlined above may be employed with apparatus of great variety. For certain purposes the equipment may be designed for pressures either above or below atmospheric, and many of the parts may be made of glass, metal, or plastic in numerous arrangements. Since the principal application of the method in the past has been to the testing of compressed oxygen, the apparatus designed specifically for and preferred for that purpose will be that first described, and alternative constructions and accessories will follow.

The essential electrodes, the separating insulation on which the conducting film is spread, and their support will be called collectively the detector. The electrical equipment used for showing equality of resistance of the film under different conditions will be called the indicator. The indicator consists essentially of two parts, the indicating circuit involving an adjustable bridge with its power supply and amplifying device and an indicating instrument, which will be called more briefly the galvanometer, although its name plate is more likely to bear the word microammeter. The other necessary parts of the equipment are a pressure-tight enclosure for the detector called the cell, a saturator, two pressure gages, four valves, a cylinder of compressed nitrogen, air, or other gas, and connecting tubing. A high-pressure regulator and a computer are desirable but not indispensable.

The preferred arrangement of gas connections is shown diagrammatically in figure 1. When

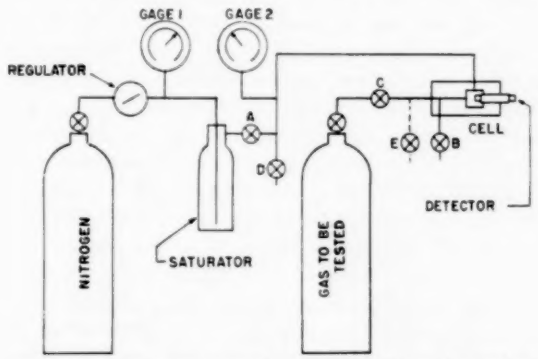

FIGURE 1.—*Diagram of mechanical connections for testing compressed gas.*

used for oxygen testing, the regulator on the nitrogen cylinder is set to deliver gas to the saturator at a pressure of about 500 psi, as shown by gage 1. The saturated gas is admitted in a slow stream to the cell through valve A and, after passing over the detector, is discharged through valve B, which is generally left wide open. When the detector has reached equilibrium, the indicating circuit is adjusted so that the galvanometer needle is on-scale and the reading is noted. Valves A and B are then closed, and the gas to be tested is admitted to the cell through valve C and discharged through valve D. These two valves are manipulated so that with the gas flowing at a moderate rate, the galvanometer balances at the reading previously noted. The reading of gage 2 is then recorded. The reading of gage 1 while gas was passing through the saturator is P_s, of eq 4, and the reading of gage 2 is P_x.

In the arrangement illustrated, slight leakage of gas through valves A or C, which it is hard to avoid with complete certainty, does not affect the result, because in each case the leaking gas is discharged without reaching the detector. Nitrogen is indicated as the gas to be saturated, because it is usually as available at an oxygen plant, where most of the testing is done, as is oxygen or compressed air, and it does not corrode the steel bottle used as a saturator. Except for the rusting of the saturator, air or oxygen is as satisfactory as nitrogen. If only one cylinder of gas is to be tested, it may first be attached to the saturator to provide the standard gas and then connected as the gas to be tested. If a high-pressure regulator is not available and gage 1 has a sufficient range, the full pressure of the cylinder may be applied to the saturator, but this ultimately results in the waste of compressed gas and a certain amount of inconvenience or a reduced accuracy in the reading of pressures.

The actual arrangement of apparatus in the model of the instrument most used, which was adopted by the Army Air Forces and is preferred by the authors for simplicity and accessibility, is shown in profile in figure 2. The valves are lettered as in figure 1. A spare valve, E, controlling entrance to the system at the same point as valve C, has been found very convenient for the attachment of a gage more sensitive than gage 2 (0 to 3000 psi) or of a secondary standard,

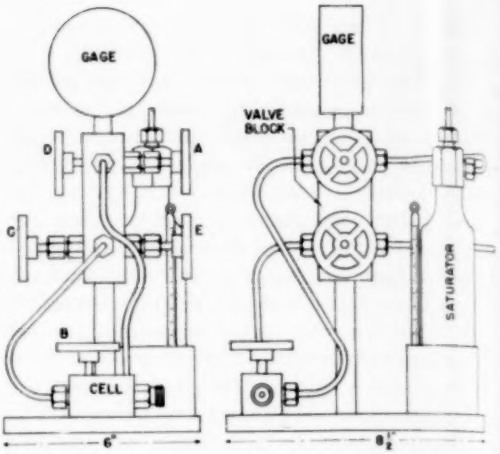

FIGURE 2.—*Front and side elevations of portable instrument.*

a cylinder of gas drier than can be obtained from the saturator. Valve E is not needed for the routine testing of oxygen under the Army-Navy specification, however.

Four of the valves are mounted in a single valve block for simplicity of support. Dimensions and further details are shown in cross section in figure 3. The block is made of heavy metal to conduct heat as readily as possible to the points of expansion of the gas through the principal valves. The cell is connected to the valve block only through considerable lengths of small metal tubing to minimize the effects of expansion on the temperature of the detector. Valve B is placed directly on the cell to minimize the pressure drop from detector to outlet when the standard gas is to be used as 1 atmosphere without measurement or corrections. It is quick-opening, and its passages are large for the same reason.

Details of construction of the various parts will now be discussed.

2. Detector

(a) Detector Currently Used for Oxygen Testing

In figure 4 is shown the detector preferred by the authors because of its compactness and ease of handling when recoating or transferring from a place of use to a cell for calibration. It is the form that has been used in most of the oxygen testing apparatus and also in most of the experimental work to be described. Unless otherwise specified, it may be considered to be the detector

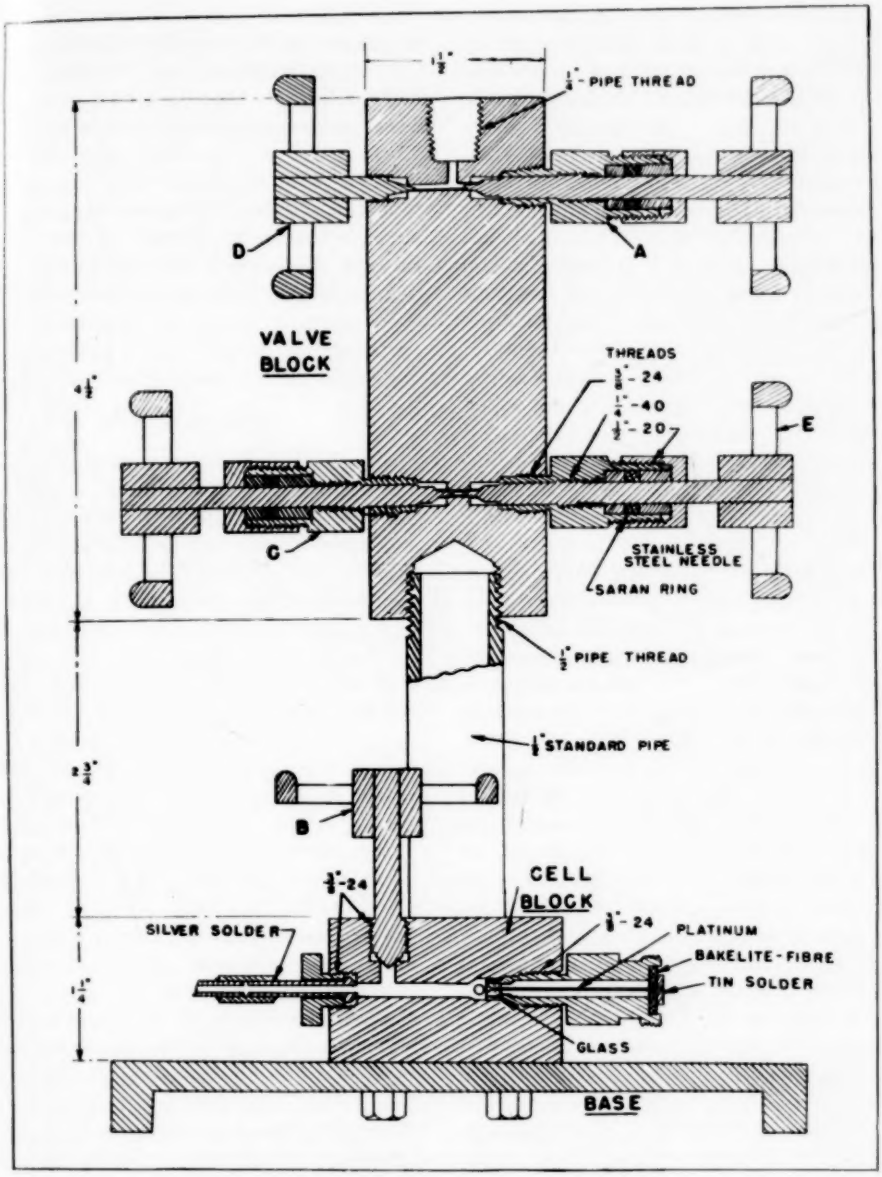

FIGURE 3.—*Section of valve block and cell block of portable instrument.*

eferred to throughout the remainder of this paper. t is made as follows: The end of a platinum wire f about 0.5-mm diameter is fused to form a bead bout 1.5 mm in diameter. A larger bead of lass, made for sealing to platinum, is fused over he end of the wire and then into a short length f thin-walled platinum tubing about 3 mm in

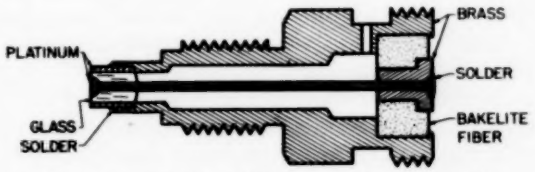

FIGURE 4.—*Detail of detector most frequently used.*

diameter. The glass readily wets the metal and should be allowed to flow slowly into the tube by capillarity at as low a temperature as practicable in order to avoid the formation of bubbles by the decomposition of the glass. The platinum sleeve is then soldered into a brass or stainless steel fitting that can be screwed into the cell. Both soft- and hard-soldering have been employed with about an equal percentage of failures, which are much too numerous. During soft-soldering, the platinum sleeve is heated quickly and tends to break away from the glass, as it would not do if glass and metal were slowly heated together. When the unit has cooled down, the break is not repaired but remains an invisible crack into which the liquid electrolyte is eventually forced by high pressures. When the tip is hard-soldered, cracking is even more likely to take place during the initial heating, but the glass can be heated enough to repair the break by fusion. In the meantime, the central wire may get badly out of place. In spite of these difficulties, several detectors have been made by the authors without the aid of jigs, annealing chambers, or other special arrangements.

After assembling, the end of the detector is ground off with an abrasive powder to approximately the middle of the platinum bead. From time to time the surface is examined under a lens, and all pits left by bubbles are ground out if practicable. An optical polish is not needed and probably not even desirable. The degree of roughness of the finish does not seem to make much difference; it will probably be satisfactory to make the finish such that the surface appears dull but without visible roughness to the unaided eye. A finishing abrasive with grains 20 microns in diameter is probably about right.

The purpose of fusing the bead on the end of the small wire is, of course, to increase the length and diminish the width of the space between electrodes. The use of a wire of smaller diameter than is wanted at the surface saves platinum, but its principal purpose is to minimize the chance of cracking the glass around it during heating and cooling. An attempt to use smaller platinum tubing for the outer electrode resulted in a higher percentage of failures.

It is very important that no soldering flux get to the back of the electrodes and their insulation, and that the glass be free from cracks extending from one electrode to the other. When such cracks occur, not only is the sensitive film shunted by a resistance slowly variable with changes of humidity, which introduces lag but might be tolerated, but there is also a continuous fluctuation of resistance, irregular both in period and magnitude. In the worst case observed, the fluctuations, which occurred from once in 8 or 10 seconds to three or four times a second, were sufficiently violent to cause off-scale deflections of the galvanometer in each direction. This particular detector appeared perfect when examined in diffused daylight even under a low-power microscope, but strong illumination showed interference colors from a transverse fissure well below the surface.

(b) Detectors of Other Forms

The first detector was made by twisting two wires close together around a glass tube and painting the eletrolytic film between them. This was soon abandoned because, as it evaporated, the solution of electrolyte tended to be drawn by capillarity under the curving surface of the wire and to leave most of the conducting material in relatively thick deposits partially covered by the wire where it was slow to reach equilibrium with the gas. Platinizing the closed end of a glass tube and etching a gap in the platinum coating was found to be easier than the use of wires and to result in a nearly smooth surface easy to coat with a relatively uniform film of the electrolyte. Electrical connections were made through platinum wires sealed through the glass before platinizing. Detectors of this form are quite satisfactory for use in glass apparatus at low pressure. For use in metal, the platinum coated tube was soldered into a brass bushing [1].

With the electrical instruments used until recently, resistances of the coated detector were too high to be easily measured in the low range of humidities, and there was a premium on making the gap between electrodes as long and narrow as possible. A detector, made for the Army-National Geographic Society stratosphere flight of the *Explorer II* in 1935, but not used because the electrolytic coating did not hold its calibration well enough, was made by platinizing a glass tube about 1½ in. in diameter and 1 ft long and cutting the coating into two helical strips with a sharp-edged grinding wheel. The result was a line separation between electrodes about 0.1 mm wide and 3 m long. In his first radio-sonde hygrom-

ter, F. W. Dunmore [2] ground helical grooves into a glass tube in the same way but employed wires laid in the grooves as conductors instead of a platinum coating between grooves. Later [3] he employed wires wound on a polystyrene-coated metal tube.

The earlier detectors were not strong enough to withstand the high pressures required in oxygen testing, and several other types have been tried for high-pressure work in addition to the one described in section II, 2, (a). Figure 5 illustrates

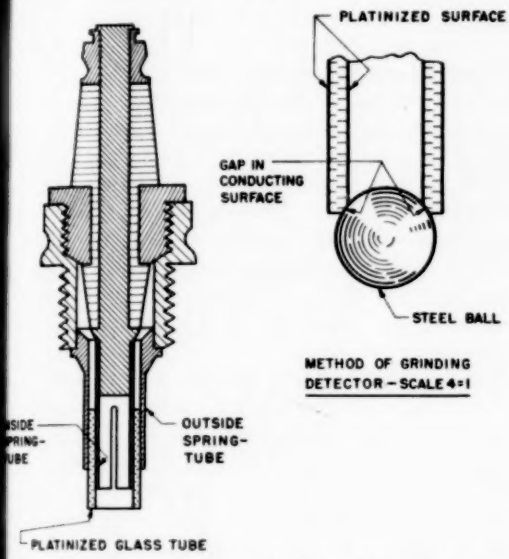

FIGURE 5.—*Detail of detector made from a high-test aviation spark plug, type 437.*

the one that is simplest to make. The spark-points of an aviation spark plug (which does not depend on the strength of porcelain to prevent bursting under pressure, the fault of the usual automobile spark-plug), are replaced by coaxial tubes of thin metal, the outer ends of which are split into segments that can be bent to make secure spring contacts with the inside and outside of a glass tube inserted between them. The glass tube need not be more than 2 cm long. Internal and external diameters of 6 and 8 mm are convenient. The tube is left open at both ends. One end is dipped into a platinizing solution made by dissolving 1 g of platinic chloride in 10 ml of 99.5-percent alcohol and adding 2.5 ml of (U. S. P. collodion) and heated above a Bunsen flame, at first gently but finally to the initial softening point of the glass. Usually there is no trouble from lack of adherence of the platinum, and one dipping is enough. Adherence can be improved by very slightly etching the glass with hydrofluoric acid before coating. A rounded piece of metal, conveniently a bearing-ball soldered to a piece of metal tubing, is used with a little fine abrasive to grind the platinum coating from the edge at which the cylindrical inner surface of the tube intersects the plane surface of its end, as shown in the small insert in figure 5. The initially continuous platinum coating is thus divided into two conductors separated by a ground-glass surface 0.2 to 0.5 mm wide, which is then coated with the conducting film. The end of the tube that is not platinized should be fire-polished ever so slightly. If the glass is left sharp, it may shave shreds of metal from the holders and cause puzzling short circuits. If fire-polishing results in an easily noticeable change of diameter of the tube, it may be difficult to slide over the inside spring-tube, and the contact with the inside platinum coating is likely to be poor.

Because they are so easily constructed, several detectors in various forms were made of metal, usually stainless steel, with plastic instead of glass insulation. Lucite (methyl methacrylate) and two or three other plastics were tried. The detectors were quite usable but generally and somewhat vaguely less satisfactory than detectors with glass insulation. They seemed to be sluggish in response, particularly after they had been in use for some time, an effect attributed to some penetration of the electrolyte into the plastic where it was relatively but not entirely unresponsive to changes of humidity. Other effects were attributed to poor adherence of the coating to the plastic. These unsatisfactory results must not be considered conclusive against plastic insulators. The polystyrene used successfully by Dunmore was not tried because no machinable pieces were at hand, nor were Saran, Nylon, or other promising materials tried.

One form of detector, with plastic insulation shown in section in figure 6 will be described since it is extremely easy to make. It is not well suited to high-pressure use but was designed for installation in sheet-metal containers within which the humidity is to be determined from time to time. The detector consists merely of two metal washers with a thin sheet of insulating material between

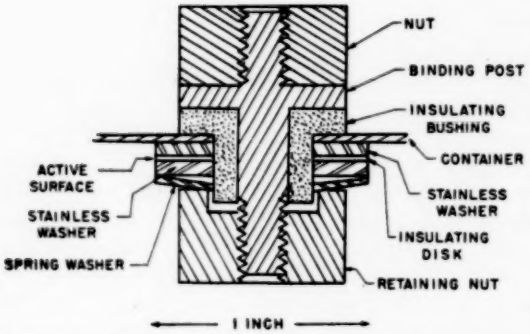

FIGURE 6.—*Detail of simple detector with plastic insulation.*

them, held together by a central bolt and spring washer. An insulating bushing surrounds the bolt. The diameter shown, 1 in., is probably the largest there will ever be occasion to use. The same construction can be employed with a diameter of only a few millimeters. The edges of the washers and sheet insulation are painted with the film of electrolyte. Several sheet insulating materials of different compositions and thicknesses were tried with equal success so far as could be judged from the limited study made. Commercial cellophane, 0.03 mm thick, appeared to be as good as anything. Brass washers were used, and the electrolytic coating was a solution of lithium chloride and cullulose acetate in acetone containing a little alcohol and water. This coating adhered perfectly for a year but, as F. W. Dunmore [3] observed, with copper wire and lithium chloride, the metal corroded. Stainless steel washers with a sheet of Saran (polymerized vinylidene chloride) melted between them, and others with polystyrene insulation, are now being tried.

3. Electrical Indicator

In the initial study of the method [1] and the occasional uses made of it from 1919 to 1935, a simple Wheatstone bridge and alternating-current galvanometer were employed with 60-cycle alternating current from the power supply. The electrical system designed in 1935 by Frank Wenner was essentially the same, except that power was supplied from batteries and a motor-driven reversing commutator. F. W. Dunmore used Wenner's system in the laboratory, but for meteorological work the detector was made the resistance element of an oscillating circuit, the frequency of which was the measure of the resistance of the detector.

It was a common characteristic of these indicating systems, except the last, that they responded satisfactorily only to comparatively large currents through the detector. This placed a premium on detectors of large size to accommodate an opening between electrodes of sufficient length and on thick coatings of slow response. In Dunmore's hygrometer, the current is direct (though interrupted), and extremely low current densities between electrodes are necessary, if interference by polarization is to be avoided. This necessitates much the same design as though a larger alternating current were required.

F. W. Gross, of the Bureau's Electrical Instruments Section, designed for the authors an indicator in which alternating voltage was supplied from an independent battery-operated oscillator, and the unbalance voltage of the bridge was amplified through vacuum tubes. The original circuit has been modified several times, usually in the direction of simplification, by E. C. Creitz and the authors. Four of the resulting circuits are illustrated in figures 7 to 10. The circuit of figure 7 is thoroughly satisfactory, except when it is to be used as a measuring and not merely as an indicating instrument (cf. the next to last paragraph of section I, 2). It is the circuit that has been most used and is still preferred for most work by the authors. The variable resistance, V, in the arm of the bridge adjacent to the detector is commonly changed only in large steps to within an order of magnitude of the resistance of the detector. The galvanometer reading is then brought on-scale by adjusting the point of contact on resistance R, and further electrical measurement is limited to observing the position of the galvanometer needle.

The circuit shown in figure 8 permits a fairly accurate measurement of the electrical resistance of the detector and is employed when for any reason the electrical equipment, rather than a combination of pressure gages, is to be used as the measuring instrument. It was used in the studies of the resistance of films, rate of attainment of equilibrium, etc., to be reported.

Figure 9 shows a simplification of the circuit of figure 7 that appears to be entirely satisfactory for most purposes and is less expensive. The

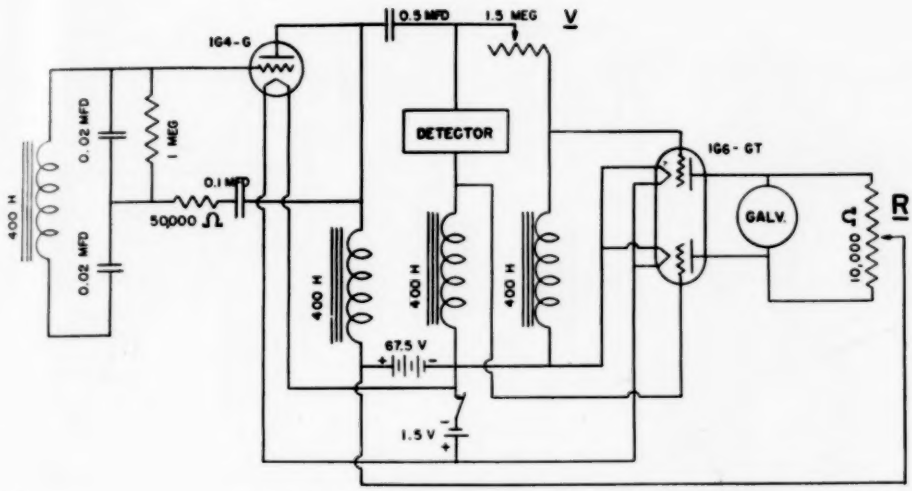

FIGURE 7.—*Diagram of indicating circuit.*

Used when gages are employed as primary measuring instruments.

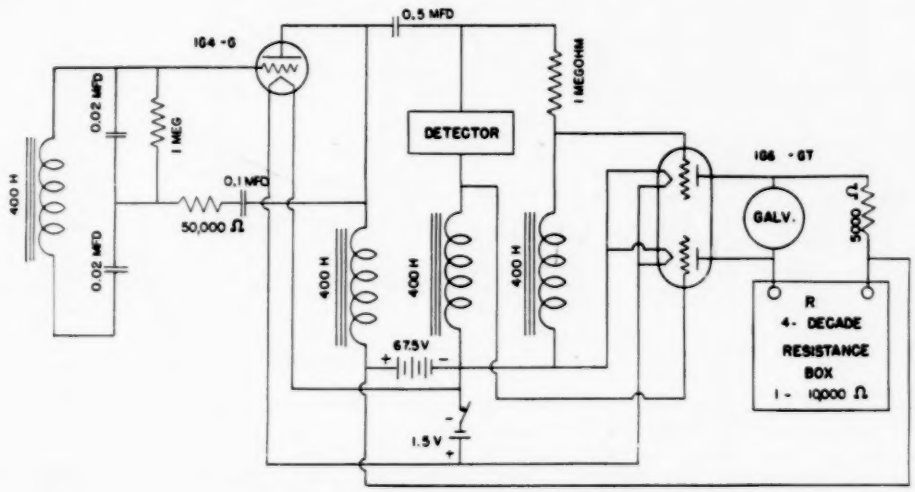

FIGURE 8.—*Diagram of measuring circuit.*

Most used when measurements depend on electrical calibration.

odifications consist of the substitution of three megohm fixed resistances for the two choke-ils and the variable resistance V in the bridge ntaining the detector, and of a fixed and a riable resistance for the single variable resist-re R of figure 6. The modified circuit is com-ratively recent, has been only crudely assem-d and has not been used very often for that ason.

Figure 10 shows a circuit, designed by E. C. Creitz, which uses 60-cycle alternating current and thus eliminates batteries. Readings made with it have appeared to be less steady than with the battery-operated circuits, which are preferred in consequence. The low frequency also causes the galvanometer needle to vibrate visibly. The oscillator of figures 7 to 9 has a frequency of about 400 cycles per second.

The galvanometer is a direct-current instrument that receives alternate pulses in opposite direc-

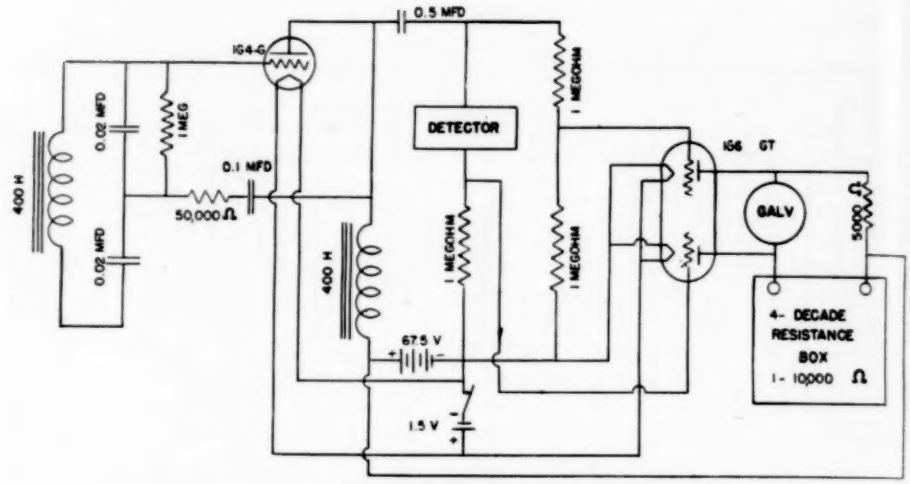

FIGURE 9.—*Diagram of simplified measuring circuit.*

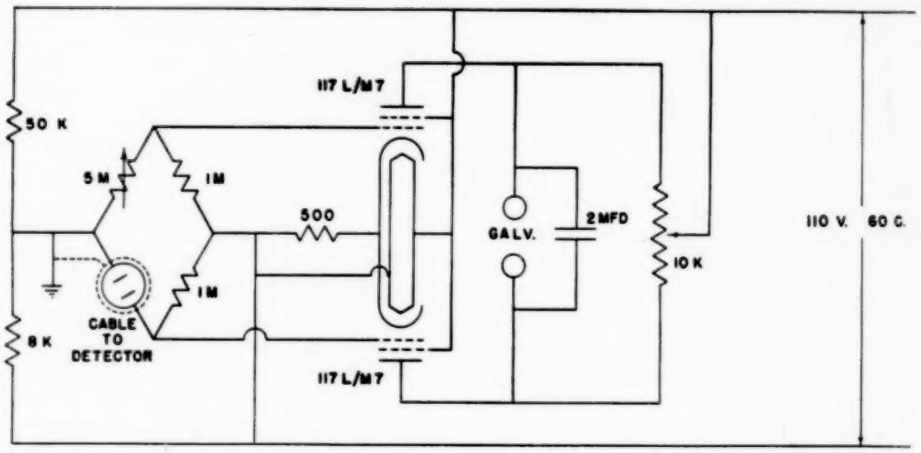

FIGURE 10.—*Indicating circuit for water detector for 60 cycles, 110 v, alternating current.*

tions from the plates of the twin amplifier. Weston galvanometers Model 440 and microammeters model 801 have been used with equal satisfaction. The galvanometers have a resistance of about 123 ohms and a range of 15 microamperes divided into 60 scale divisions. The microammeters have a range of 50 microamperes with 50 scale divisions. The galvanometers with their thin needles backed by mirrors can be read with greater accuracy, but this is rarely required, and the microammeters cost less and are easier to read.

The characteristics of the electrical indicator as a whole (they are about the same for all four circuits) are shown for the circuit of figure 9 by the calibration curves of figure 11. The galvanometer used was a Weston model 440 and the variable resistance, R, was a plug—box of 10,000 ohms in steps of 0.1 ohm. The three curves in the figure, with their corresponding scales, show resistances of the detector and corresponding values of the variable resistance, R, required to bring the galvanometer to balance. The calibration was made by replacing the detector with successive measured fixed resistances. The entire range of possible resistances from short circuit to open circuit is covered. The higher resistances are plotted on a reciprocal scale.

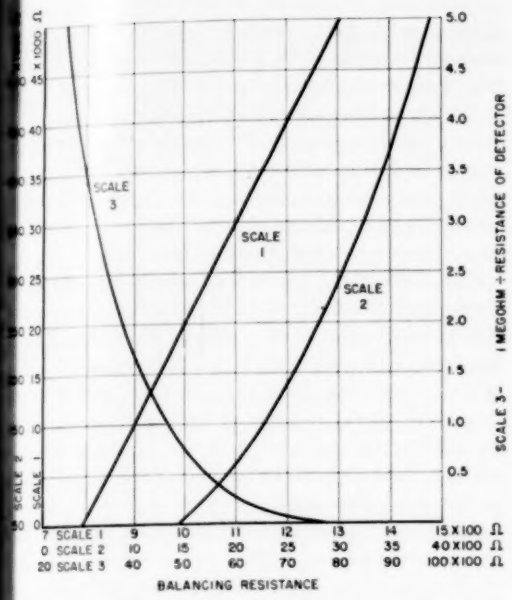
SCALE 3
SCALE 1
SCALE 2
SCALE 3 — 1 MEGOHM ÷ RESISTANCE OF DETECTOR
BALANCING RESISTANCE
SCALE 1 9 10 11 12 13 14 15 X 100 Ω
SCALE 2 10 15 20 25 30 35 40 X 100 Ω
SCALE 3 40 50 60 70 80 90 100 X 100 Ω

FIGURE 11.—*Calibration of measuring circuit in terms of resistance of detector.*

The amount of current available from the electronic amplifier is never sufficient to damage the galvanometer, hence at any time any resistance can be connected in the place of the detector with impunity. In view of the very great range of resistances to be encountered and the suddenness with which they sometimes change on going from one atmosphere to another, this is a great advantage.

4. Saturator

The saturator pictured in figure 12 has been generally used. Saturators with more elaborate packing have not worked as well. Saturators more simply packed have worked better. The saturator filling illustrated consists of about 4 in. of fragments of pumice stone the size of a finger nail and 1 inch of glass wool. The entering gas bubbles through about an inch of water. The filling was designed with the idea that the bubbles would break and most of the spray would be entrapped within the pumice, the porous nature of which would keep the surfaces wet but would tend to prevent bridging between solid fragments. The glass wool was intended as a filter for spray from the breaking bubbles. In practice the glass wool usually became water-logged and either left only

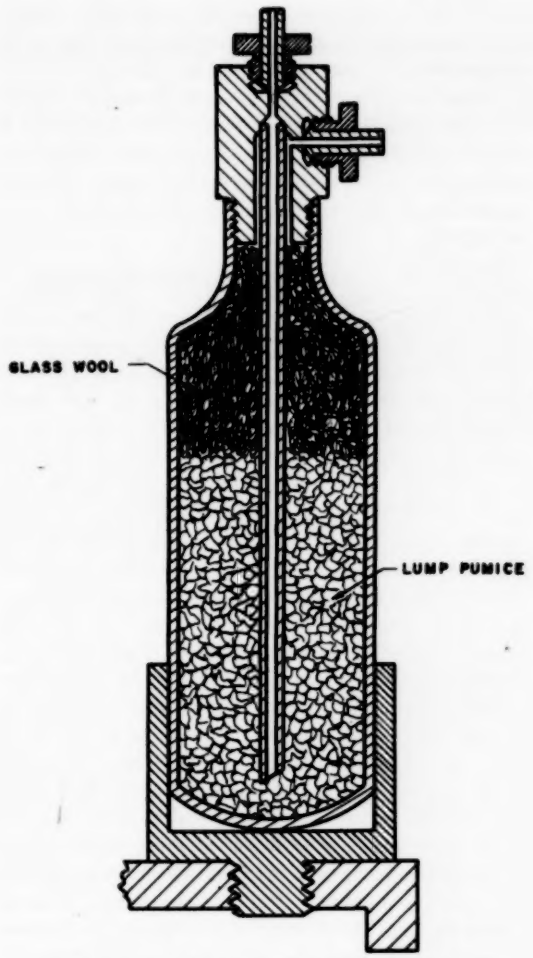

FIGURE 12.—*Section of saturator first used.*

narrow passages through which bubbles worked and broke near the outlet of the saturator, or gas entering below the pad squeezed it like a sponge and caused the water to overflow in a mass.

Unfortunately the first packing of this type worked well, and a large number of other saturators were packed in the same way. More recently the saturator has simply been filled with stream-washed gravel screened to pass a sieve of 5 meshes and be retained by one of 10 meshes per inch. If there is 3 in. of gravel above the water level, no trouble has been encountered with spray from cylinders filled in this way, even when the rate of flow of gas was much greater than necessary. The saturator leaves much to be desired. The

gravel has a high heat capacity, and with cooling from evaporation at the bottom and changing temperature in the surroundings, the actual temperature of saturation is uncertain. For highly accurate results the whole should be placed in a thermostat, of course. What it is hoped will prove to be a better saturator has been designed for use in further study but has not yet actually been employed.

5. Valves, Connections, Gages, Regulators

Accurately made needle valves of the simple construction shown in figure 3 have been mostly used. Valves of other types that have been tried have been no more satisfactory, at the best. Valves *B* and *D*, shown in the figure, have been used without packing, but this is now considered a mistake. Although packing is not needed in these valves for tightness, it helps to hold the stem steady when the valve is open and facilitates the adjustment of pressure. It is accordingly recommended that all valves be made like valve *A*.

The construction of the valve and the method of packing follow rather closely the design of H. F. Stimson of this Bureau. The packing of the valve is important. It should permit the stem to be turned easily and smoothly but never permit it to wobble. It should also resist the penetration of water, as the holding of liquid water in any place from which it can evaporate slowly into the cell or its connection is perhaps the most troublesome of all the sources of error to which this method is subject. A packing that can be dried without injury by heating above the boiling point of water is much to be desired. The packing indicated in the drawing is the plastic Saran, a vinylidene chloride polymer selected because it is less permeable to water than any other plastic known to us, can be dried by careful heating, and does not burn readily even in pure oxygen. It can be molded in place to an exact fit by compressing while heated above its softening temperature. This packing is good but makes the valves a little hard to turn. A packing most satisfactory in this respect, but a little harder to make or to dry out if it gets wet, consisted of the following in order along the valve stem. A brass washer about 1 mm thick, a cellulose acetate washer, 0.5 mm thick, a sole-leather washer impregnated with paraffin about 2 mm thick, a cellulose acetate washer and a brass washer like the first ones. The metal washers are turned to make a close but not a tight fit with valve stem and barrel. The plastic washers have the hole a little smaller and the outside diameter a little greater than the parts they are to fit, so that a little flow is involved when they are forced into place. The leather washer should fit a little less snugly than the plastic. This packing is tight against the highest pressures of commercial gas cylinders but offers a minimum of resistance to the operation of the valve.

The body of the valve that screws into the valve block and the detector are shown seated against offsets within the block. Alternatively, both have been made to seat against the outer surface of the block. Machining is a little simpler in the second case, but there is more chance to trap water in capillary spaces, more torque must be used to make a tight fit, and brass parts of the dimensions shown are rather easily twisted off.

Each connection between the valve-block and the cell consists of a foot or two of $\frac{1}{16}$-in. copper tubing, more or less coiled to act as a heat exchanger. The apparatus should be easy to take apart completely for drying and to reassemble. The connecting fittings shown have been particularly satisfactory; they are simple, rugged, and easy to make tight. Only metal-to-metal joints should be considered. Threads, tapered or otherwise, cannot be made tight without a vast amount of trouble; fiber washers and other forms of packing are as bad or worse, chiefly because they retain water.

In making up the assembly of valves and connections, every precaution must be taken to eliminate places where water can be stored by such things as hydroscopic salts, rubber, or rust (which is a good adsorbent and acts much like a little silica gel). Soldering flux is particularly bad, and capillary spaces such as screw threads can be troublesome. It is good practice before final assembly of the equipment to wash the parts with a solvent for grease and then to boil them for several hours with several changes of water to remove hydroscopic salts. Finally, the parts are dried in an oven.

Gages of the Bourdon type have been used exclusively for work involving pressures above atmospheric. In some work below atmospheric pressure, mercury manometers were used. If sufficient care is taken with other things, the accuracy of the pressure gages is at least one of the

limiting factors in the accuracy with which the method can be applied to various problems. Hence the gages used should be as good as it is practicable to obtain unless a lower degree of accuracy in the final result is considered sufficient. In the testing of oxygen, it is frequently desirable to apply the full pressure of the cylinder to the cell. Even when this is not the case, there is always the chance that the full pressure, sometimes as high as 2,640 psi, will be applied accidentally. Consequently, a gage reading to 3,000 psi should be used on the cell. There is generally less trouble from obscure sources of water if the standard gas is not too dry, hence the saturator is seldom kept at a pressure higher than 500 psi, and a gage reading to 500 or at most 1,000 psi is all that is required at this point. If only high concentrations of water, say above 1 percent relative humidity, are of interest, gages reading to 200 psi will afford greater accuracy than those of higher range.

Although lack of a high-pressure regulator does not preclude saturating the gas at a high pressure, such as 500 or 1,000 psi, by attaching directly to the cylinder at that pressure, a regulator is a great convenience. Regulators with upper limits of 500 and 1,000 psi have been used. The latter works slightly better at 500 psi than the former and is probably the more desirable for general use.

6. Systems Operating Below Atmospheric Pressure

The apparatus previously described has been designed for use only above atmospheric pressure. The employment of pressures less than atmospheric offers some inducements. The practicability of using glass apparatus of moderate strength is one. No supply of compressed gas is needed for saturation. If the usual comparison pressure, P_c, of eq 2 is reduced to 0.1 atmosphere instead of 1 atmosphere, that of P_s and P_x or both can be reduced to change their product in the same ratio, and the uncertainty of deviations from the ideal gas laws can be largely eliminated. These advantages are offset for most purposes by the fact that we lack suitable glass valves for controlling pressure, that low-pressure manometres have a lower percentage accuracy than high-pressure gages of equal convenience and cost, and that for gases of the same composition, sensitivity is lost by going to lower pressures. The use of metal needle valves with apparatus otherwise built of glass has been tried and may be desirable for work involving not too low or too extended ranges of humidity, especially the testing of reagents. We employed a mass of crushed ice, through which air was drawn, as the saturator in this apparatus. The greatest difficulty encountered with it was the certain prevention of leakage. Because an apparatus of this kind is immersed in an atmosphere usually containing 10,000 to 20,000 times the concentration of water vapor, easily detectable, a very small leakage is fatal to accuracy, and there is no easy way of detecting its occurrence. The temperature of saturation also gave trouble. Although the saturator was imbedded in as well as filled with crushed ice, droplets of water sometimes appeared so near the outlet that their temperature was in doubt.

If a vacuum system is to be employed, it is suggested that room air be used as the standard gas without attempting to saturate it, and that its moisture content be determined as often as necessary by separate tests. In this way, the uncertainties, both of leakage and temperature, can be eliminated from the main series of experiments, though not, of course, from the calibration.

III. Conducting Films

1. Phosphoric and Sulfuric Acids

(a) Range and Permanence

The electrolytic film preferred by the authors for most purposes is plain phosphoric aicd. At ordinary laboratory temperatures it changes resistance steadily and adequately between a concentration of water vapor of about 8 micrograms per liter and one of about 20 mg per liter (or relative humidities from about 0.03 percent to about 90 percent). Below 8 micrograms per liter, the resistance is likely to increase suddenly, particularly under high pressure, probably because of the crystallization of a solid phase. Phosphoric acid films have served for measurements as low as 3 micrograms per liter and are usually all right for 5 micrograms. The variation probably represents failure to crystallize under some conditions because of impurities or lack of a seed nucleus. In fact, the behavior of the resistance of a film under these conditions is fairly typical of crystallization in general; a film has worked well at about 3 micrograms per liter and a few minutes

later has been completely insensitive at 5 micrograms per liter. A film containing sodium chloride as the electrolyte behaves in much the same way, except that the humidity at which crystallization is likely to occur is about 2,000 times higher.[3]

Sulfuric acid has no lower limit of sensitivity that we have discovered, and it can be used successfully to indicate humidities of a fraction of a microgram per liter. The application of the method in this low range appears to be limited only by difficulties other than the sensitivity of the indicating electrolyte. One of these is the rapid disappearance of the sulfuric acid itself, probably by evaporation but possibly by reaction with the materials of the detector.

Phosphoric acid is much superior to sulfuric acid in this respect, but a phosphoric acid film also shows an increasing resistance on long exposure to a constant humidity. The rate is slow enough not to interfere with the usefulness of the film when calibrations are made to determine the significance of each reading. The change that takes place through loss of acid between a test and a prompt calibration is nearly always negligible.

It is a little hard to specify the magnitude of the losses of electrolyte in general terms, particularly because changes of temperature or other conditions cause the resistance of a detector coated with phosphoric acid to drift toward lower almost as frequently as toward higher values. The following observations will indicate something of the magnitude of the effects to be expected. A simple phosphoric acid film of 600,000 ohms in gas containing 0.06 mg of water per liter lost about three-fourths of its conductance in 24 hours. A film of sulfuric acid in metyl methacrylate, which had a resistance of about 1 megohm in an atmosphere containing 1 mg of water per liter, lost about 20 percent of its conductance in 3 hours. A roughly corresponding film of phosphoric acid lost about 30 percent of its conductance in 2 weeks. A film of phosphoric acid in gelatin prepared in 1919 and kept in a desk drawer in the laboratory was still usable 3 years later [1]. However, as will be shown, it is best to renew the film at least daily except when the detector must be undisturbed for longer periods.

In the range of humidities below about 8 micrograms per liter, it is advantageous to use mixtures of phosphoric and sulfuric acids. They do not crystallize as readily as the first nor change as rapidly as the second.

(b) Application of the Film

In the beginning it was considered necessary to apply the thin films in the form of dilute solutions of the electrolytes, to be left behind by the evaporation of the solvent. It was soon found that films of a salt or sulfuric acid when exposed to even moderately high concentrations of moisture seldom returned to even approximately the same value, and the tentative explanation that the changes resulted from physical displacement of the mobile solutions was confirmed when it was found that the trouble diminished if a binding agent such as gelatin was added to the solution. However, it was discovered by F. A. Smith that phosphoric acid is viscous enough and adheres well enough to glass to be used without a binder except possibly at humidities above 90 percent, and that the sticky concentrated acid can be applied to the smooth surface of a detector and wiped off to leave a film of almost any conductivity desired. The usual reagent phosphoric acid (85 percent) may be used, or a small quantity of phosphorus pentoxide may be exposed to the air until it becomes fluid enough for use. The detector is coated simply by touching a toothpick or the point of a lead pencil to the phosphoric acid and then to the surface of the insulator and wiping off the excess with a bit of cotton. Less than a minute is usually required. One soon learns about how much to rub off. Wiping with a moderate pressure on three successive clean portions of the cotton is one rule of thumb. Another is to wipe until the finely ground glass surface appears dull but not quite dry. If greater accuracy is desired the adjustable resistances of the indicator can be set to approximately the desired reading in room air and the coating wiped off with one light touch of the cotton after another until the swing of the galvanometer needle shows that the resistance has become higher than corresponds to electrical balance.

[3] One set of observations with a sodium chloride film, for example, showed no conductivity with increasing relative humidities until about 65 percent was reached, when the film suddenly became strongly conducting. On drying out, the film remained sensitive down to a relative humidity of about 40 percent, when it became suddenly nonconducting. Under increasing humidity, conductivity did not reappear until 65 percent was again reached.

Fortunately, the thickness of the film is not at all critical. One film may have five times the resistance of another, but their difference be hardly noticeable in use. In some ranges of humidity, it is quite possible to use interchangeably films having a ratio of resistances of 50:1. In general, a thicker film permits greater sensitivity, and a thinner one reaches equilibrium more rapidly. The rule is, therefore, to use as thin a film as will have the desired sensitivity, but the thinner the film the more rapid is the drift caused by loss of the reagent and the greater is the effect of leakage in the insulation of the detector and the measuring circuit. These may be the deciding factors in some cases.

Sulfuric acid is always applied in a solution containing a binder. Gelatin [1] and Crystalite (methyl methacrylate) have been used. The latter is preferred. The best method of applying the coating has not been studied, but the following will give a good result. Half a gram of the plastic is dissolved in 100 ml of acetone. To a 50-percent solution of sulfuric acid in water, an equal volume of acetone is added. Equal portions of the two solutions are mixed. If the plastic precipitates, enough acetone is added to redissolve it. The solution is painted on the detector with a camel-hair brush. It dries almost instantly and is ready for use.

(c) Sensitivity

The actual resistance of a single phosphoric acid film, film *A*, over almost the whole range of humidities was measured with the circuit of figure 8. The observed data are given in table 1 and represented by curve 1 of figure 13. The concentration of water in micrograms per liter is plotted on a logarithmic scale with respect to the balancing resistance (resistance *R* of fig. 8) on a linear scale. The approximate resistance of the film itself is plotted on a logarithmic scale with respect to the same ordinate in curve 2, the data for which were taken from curve 1 and the calibration of figure 11. Film *A* was such as would ordinarily be used in the lower part of the range accessible to phosphoric acid. For humidities in the higher range, a thinner film is preferable because it reaches equilibrium with the atmosphere more quickly and does not begin to flow at so low a humidity. A typical application of phosphoric acid for this purpose, film *B* is represented by curve 3, drawn on the same scale as curve 1. One film has about 20 times the resistance of the other, but both are readily usable over most of the range of humidities. In figure 14, the balancing resistances are plotted with respect to relative humidity. The two films were used at different temperatures of 83.6° F and 81° F, hence the ratios of weights per unit volume and of relative humidities are not the same. The resistance of film *B* reached a minimum before a relative humidity of 100 percent was reached, and the hook on the upper end of curve 3 of figure 13 represents a real effect. During exposure to the highest humidity observed with film *A*, its resistance passed through a minimum (which was the resistance recorded) and was increasing when the experiment was discontinued. In both cases the effects noted were probably caused by flow of the too mobile solutions formed as saturation was approached.

TABLE 1.—*Resistance of a film of phosphoric acid (A) at various concentrations of water vapor*

Balancing resistance	Resistance of detector	Concentration of water				
		Micrograms per liter [a]	Relative humidity at 83.6° F	Partial pressure	Approximate dew point	
Ohms	*Ohms*		*Percent*	*mm Hg*	*° C*	*° F*
5,730	$2,870\times10^3$	11.3	0.039	0.011	−74	−101
5,664	2,700	22.0	.076	.021	−53	−63
5,541	2,390	35.2	.12	.034	−49	−56
5,540	2,050	56.4	.19	.055	−45	−47
5,167	1,600	86.9	.30	.084	−41	−42
4,913	1,280	138	.48	.13	−38	−36
4,700	1,040	171	.59	.17	−35	−31
4,320	720	263	.91	.26	−30	−22
3,836	528	411	1.4	.40	−26.7	−16.2
3,420	394	563	1.9	.55	−23.5	−10.3
3,195	337	655	2.3	.64	−22.0	−7.6
3,174	332	655	2.3	.64	−22.0	−7.6
2,955	280	790	2.7	.77	−20.0	−4.0
2,830	253	879	3.0	.85	−19.0	−2.2
2,304	154	1,520	5.2	1.48	−13.1	+9.4
1,980	106	2,170	7.5	2.11	−9.1	15.6
1,825	88	2,600	9.0	2.53	−7.0	19.4
1,420	50	4,510	15.6	4.38	−0.5	31.1
1,177	37	7,220	24.9	7.01	+6.0	42.8
973	17	13,200	45.5	12.8	15.0	59.0
886	8	20,800	71.7	20.2	22.3	72.2
790	0	[b]	.....	.....	.....	.....
7,814	∞	[c]	.....	.....	.....	.....

[a] To obtain parts per million by volume, multiply micrograms per liter by 0.804. To obtain parts per million of air by weight, multiply by 0.62.
[b] Short circuit.
[c] Open circuit.

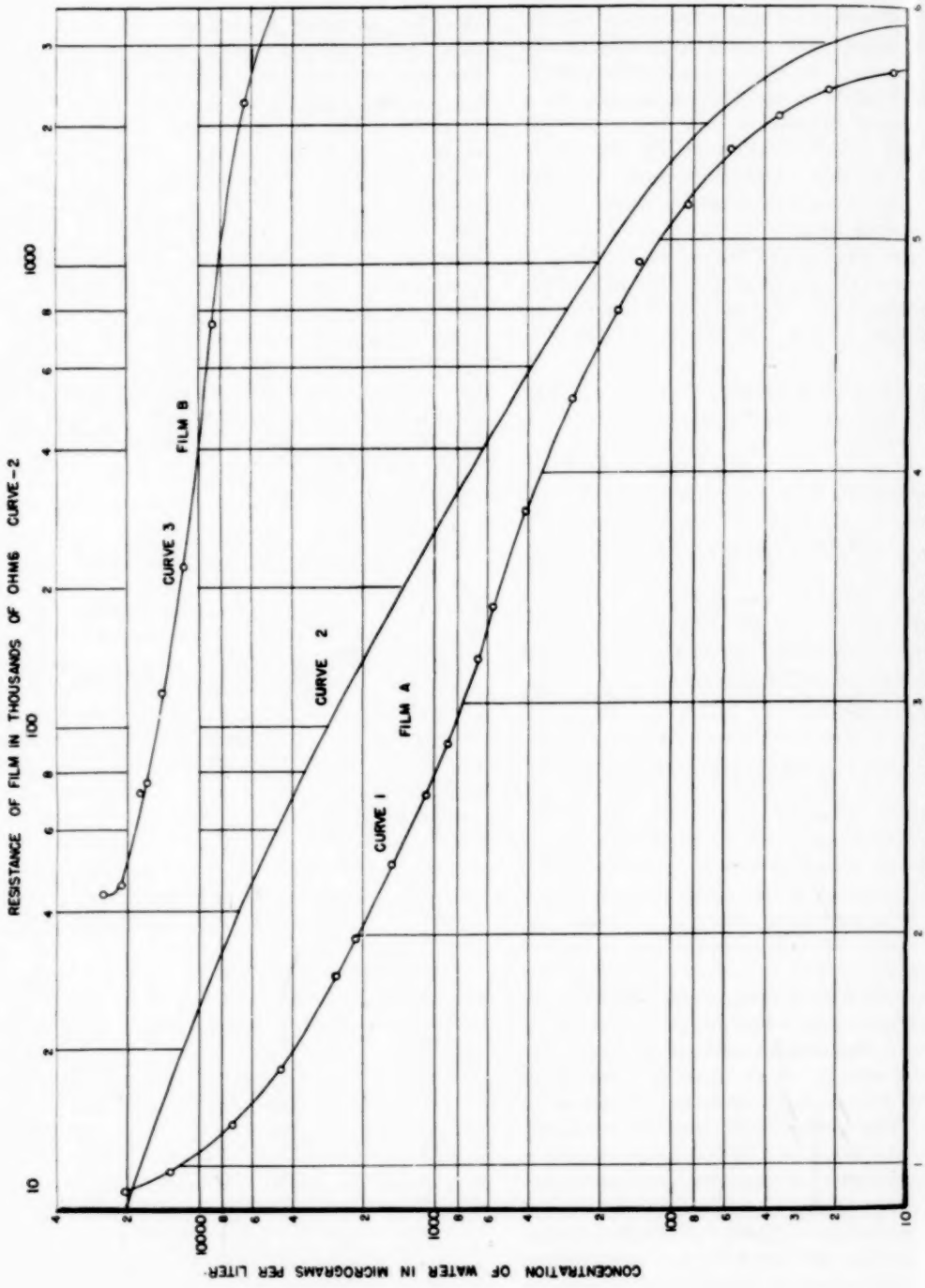
RESISTANCE OF FILM IN THOUSANDS OF OHMS CURVE-2
BALANCING RESISTANCE IN THOUSANDS OF OHMS CURVES 1 AND 3
CONCENTRATION OF WATER IN MICROGRAMS PER LITER
CURVE 1
CURVE 2
CURVE 3
FILM A
FILM B

FIGURE 13.—*Calibration of two conducting films in terms of concentration of water.*

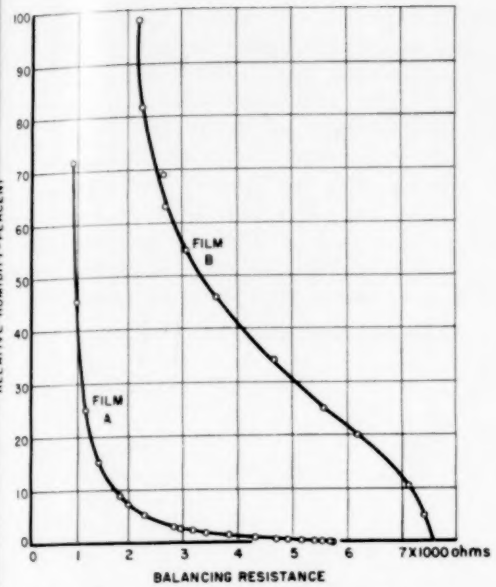

FIGURE 14.—*Calibration of two conducting films in terms of relative humidity.*

The sensitivity of the electrical indicator of figure 8 with film *A* is shown by figure 15. The curves were derived as follows. It was assumed that the balancing resistance could be read to 0.05 percent of its magnitude at any point. This corresponds to about 0.8 scale division of the galvanometer. The sensitivity, by which is meant the change in concentration of water that could be observed with the instrument, was assumed to have the same ratio to the difference between two observed humidities as the 0.05 percent of the mean balancing resistance had to the difference between balancing resistances, and this sensitivity was plotted with respect to the average of the two observed humidities. It is apparent at once that the sensitivity approaches about 0.3 microgram per liter or 0.1 percent of the water present, whichever is greater.

Figure 15 indicates instrumental sensitivity only. It must not be supposed that an absolute accuracy as great as this is usually or ever obtainable. The effects of all other sources of uncertainty remain to be accounted for. Actually, sensitivities, in the lower range of humidities at least, can be considerably increased by using thicker films or by examining gases under pressure, but at present there is usually no object in doing so because the overall accuracy would not be improved.

It is to be remembered, of course, that the differences of water content that can be detected are smaller than the minimum amount that can be detected with phosphoric acid because of the formation of a solid phase already mentioned.

(d) Speed of Approach to Equilibrium

The speed with which phosphoric acid films approach equilibrium with the atmosphere in which they are placed is shown for four different films by figure 16. The observations were all made by the use of the circuit of figure 8 in the following manner. The detector, with its film, was exposed at atmospheric pressure to gas containing 1.4 mg per liter until a steady condition was obtained and the resistance, R of figure 8, required to balance the galvanometer was recorded. The flow of the first gas was stopped; a different (higher) resistance R was set, leaving the galvanometer off balance; then as nearly simultaneously as possible a stopwatch was started and the valve of a cylinder containing 0.0114 mg of water per liter of gas was opened. When the galvanometer needle passed through zero, the stopwatch was read. The observed interval of time is plotted with respect to the difference between the initial and the preset resistance expressed as a percentage of the difference between the initial balancing resistance and that reached after 15 minutes of exposure to the second gas.

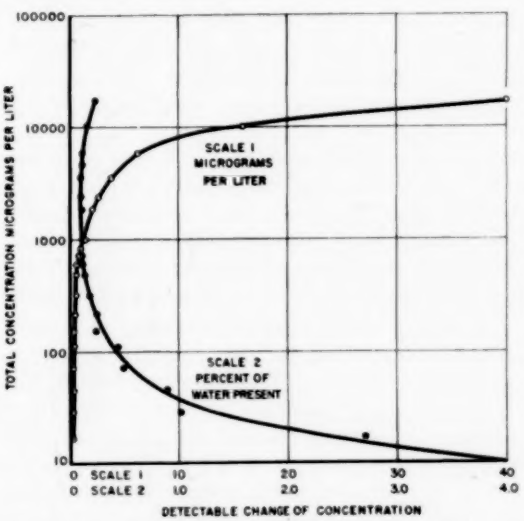
TOTAL CONCENTRATION MICROGRAMS PER LITER
SCALE 1 MICROGRAMS PER LITER
SCALE 2 PERCENT OF WATER PRESENT
DETECTABLE CHANGE OF CONCENTRATION
SCALE 1
SCALE 2

FIGURE 15.—*Sensitivity of a typical phosphoric-acid film.*

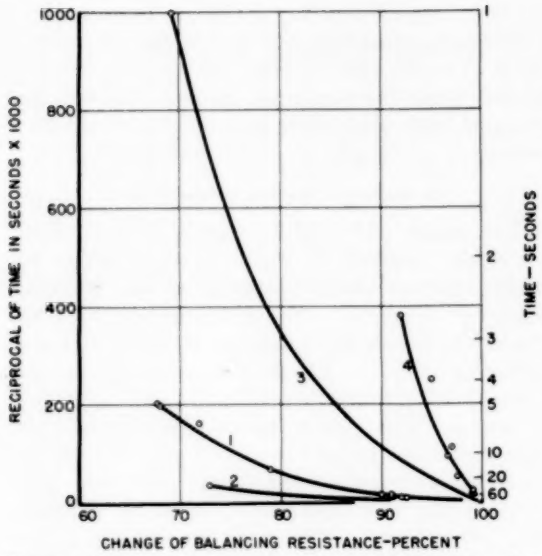

FIGURE 16.—*Speed of approach to equilibrium of typical films.*

In figure 16, the smallest change of resistance of each film for which a time was recorded is shown by the circle at the upper end of the curve. Other observed points are shown for only films 1 and 4. No interval of time longer than about 2 minutes is indicated because the reciprocal time-scale is too crowded. The many readings of longer intervals were consistent with the shorter intervals shown. It was impossible to read the time from a single start for more than one interval as short as a few seconds, hence several starts are represented by each of the curves. Specifically, curve 1 was plotted from three starts and curve 4 from seven starts.

Until these tests were made it had been assumed, somewhat carelessly, that the disappearance of a phosphoric acid film from the detector was the result of evaporation rather than reaction. If that were the case, an old coating of phosphoric acid should have the same speed as a fresh coating of the same resistance, and the coating of highest resistance should show the greatest speed in reaching equilibrium. These are not true at all.

The balancing resistance of the several films and their approximate actual resistances as read from the calibration curves of figure 11 are shown in table 2. Films 1 and 2 had the highest resistance, and for that reason might have been expected to react most rapidly. But film 1 was several days old and film 2 about 18 hr old. Films 3 and 4 were freshly applied. Films 1 and 2 are in the right relative order of speed to correspond to their resistances and so are 3 and 4. But the two pairs are definitely reversed. The probable explanation is that the phosphoric acid attacks the glass and forms a layer of salts and silicic acid roughly equivalent to a highly contaminated silica gel. This coating has comparatively little conductivity and reaches equilibrium much more slowly than pure phosphoric acid.

TABLE 2.—*Resistances of films used in speed tests*

Film	Concentration of water, mg/liter				Ratio, D:C
	1.4	0.011	1.4	0.01	
	Balancing resistance		Film resistance		
	A	B	C	D	
	Ohms	*Ohms*	*Megohms*	*Megohms*	
1	6,840	7,720	11.0	104	9.4
2	5,500	7,550	2.26	50	22.1
3	3,930	7,000	0.562	14.1	25.1
4	5,100	7,474	1.50	38.5	26.6

The numbers in the last column suggest also that old films do not change resistances in the same ratio as fresh ones, but the question is complicated by the fact that there is some conduction of current in the detector other than through the film, and there is room for considerable error in reading the higher resistances from figure 11.

2. Films Containing Salts as the Electrolyte

It would be obviously desirable to prepare films that always have the same resistances at the same humidities and could be given permanent calibration. Inorganic salts, in general, are not expected to evaporate or react with glass or the usual constituents of the atmosphere, hence they were the first electrolytes tried [1], and several attempts have since been made by the authors to use them, with indifferent success even in the limited upper range of humidities in which they form liquid solutions.

Dunmore's study of combinations of electrolytes and supporting materials in the development of his successful electrical hygrometer for meteorological work disclosed the source of at least a part of the difficulties. These are so great that "no limit was found which would maintain a satisfactory calibration when exposed to varying

humidities for long periods." He distinguished long-period and short-period aging and later [3] developed means for eliminating some of the causes of both, among them the corrosion of glass by water. In the end, however, the hygrometers "must go through an aging period of at least 10 to 14 days before they are ready for use." [3]

Some of the authors' experiences with films of the high conductivity needed for successful application with the detector designed for use in pressure-tight cells may help in the more complete understanding of the problem.

Figure 17 shows the results of observations made

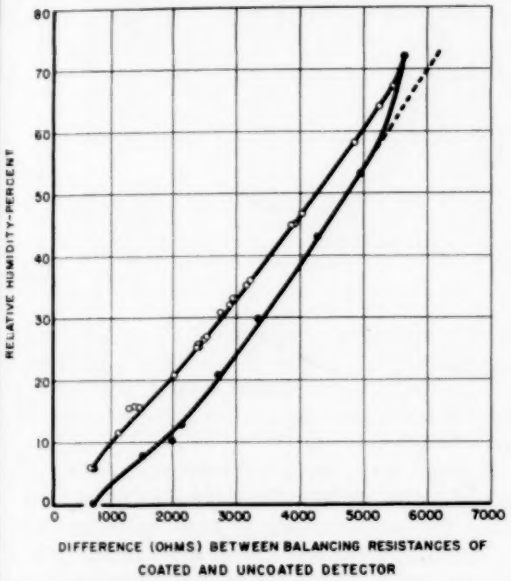

FIGURE 17. *Observations with a film containing lithium chloride in glycerol.*

with a coating of lithium chloride in glycerol. Equal volumes of glycerol and of a 5-percent solution of lithium chloride in water were mixed and applied to the detector like phosphoric acid. The detector was dried quickly by exposing it to air of about 0.1-percent relative humidity; then its resistance was measured at each of several humidities in increasing order. The results are represented as the difference between the balancing resistance (R of fig. 8) of the coated detector and that of the detector before coating. Hence the plotted values, shown by black circles, increase as the resistance of the detector decreases. At the highest humidity the resistance of the film decreased as water was absorbed, then began to increase. The point plotted represents the minimum resistance of the film at this humidity. The point is out of line with the observations at lower humidities, just as is the highest point of curve 3 of figure 13, representing a film of phosphoric acid, probably for the same reason—because the solution began to flow. Had there been no movement of the coating, it is probable that the change of resistance would have followed approximately the broken line drawn as an extension of the lower curve.

A series of observations at lower humidities followed immediately. They are represented by open circles and by the left-hand curve in the figure, which was drawn to approximate their average. Readings were made up and down this curve, but care was taken not to reach a relative humidity at which flow was expected to begin. The humidity corresponding to each of the observed resistances was then read from the average curve and compared with the observed humidity. The results are given in table 3 in the order in

TABLE 3.—*Relative humidities measured with a film of lithium chloride in glycerol made in the sequence given in the first column*

Test	Relative humidity	
	From electrical measurement [a]	From gage readings
	Percent	*Percent*
1	67.0	67.1
2	63.8	63.9
3	58.2	58.1
4	32.5	33.1
5	25.6	25.5
6	21.1	20.6
7	11.4	11.6
8	6.4	5.9
9	27.1	26.9
10	35.3	35.3
11	46.6	46.7
12	31.9	32.2
13	26.7	26.5
14	15.0	15.7
15	6.1	5.9
16	36.0	35.9
17	25.7	25.5
18	45.2	45.1
19	14.0	15.7
20	5.9	5.9
21	44.8	44.9
22	30.0	30.8
23	13.1	15.5
24	25.7	25.7

[a] Values read from average curve.

which the observations were made. The table shows that there was no important change in the calibration of the film during a short period of use if too high humidities were avoided. Not all the irregularities, perhaps none of them, are to be attributed to changes in the film. They are no greater than the probable errors of calibration of a constant film. Unfortunately, the calibration did change appreciably in a day or two, probably because the glycerol evaporated.

The solution of lithium chloride in glycerol, of which several films were made, was found to be amply sensitive down to a relative humidity of about 1 percent, and almost as fast as phosphoric acid itself. It has little or no advantage in permanence or in the upper range possible without flow. It may be useful in atmospheres that would react with an acid.

Figure 18 represents observations made with a film obtained by applying a solution of lithium chloride and polymerized methyl-methacrylate (Crystalite) in acetone. Again the series of exposures of the film made immediately after coating

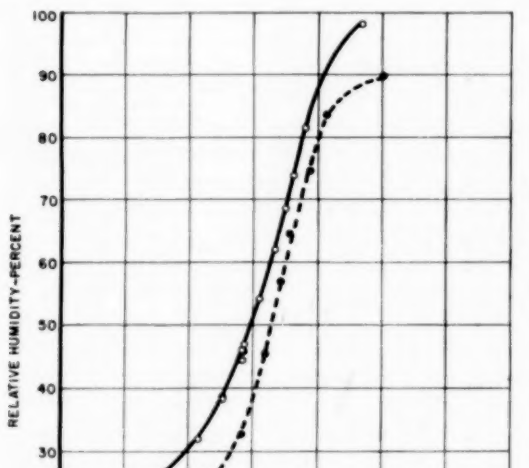

FIGURE 18. *Observations with a film containing lithium chloride in methyl methacrylate.*

TABLE 4.—*Relative humidities measured with a film of lithium chloride in Crystalite*

Test	Relative humidity	
	From electrical measurement	From gage readings
	Percent	*Percent*
1	6.0	6.0
2	9.0	8.8
3	15.3	15.0
4	19.9	17.6
5	24.4	24.0
6	31.8	32.0
7	38.5	38.8
8	46.2	46.0
9	54.2	54.2
10	68.7	68.8
11	46.1	44.6
12	25.4	25.8
13	14.8	16.0
14	38.9	38.4
15	47.0	46.2
16	62.0	61.8
17	81.7	81.6
18	98.2	98.2
19	47.0	47.0
20	19.5	22.8

is represented by black circles and later results by open ones. The second series was run about 5 hr after the first. Table 4 shows data for this film of the same kind as does table 3 for the solution in glycerol.

Figure 19 represents observations with films made of lithium chloride in several different binders. To avoid confusion, only the readings obtained in the first series of tests with each detector, corresponding to the black circles of figures 17 and 18, are represented.

In these tests, which were made before those of figures 17 and 18, the balancing resistance of the detector before coating was not measured, only that of open circuit. It is believed, however, that had the conductance of the uncoated detector been taken into account, it would have been found that none of the films with the exception of the glycerol had any significant conductance at less than 5-percent relative humidity. The glycerol film (which was not the one represented in fig. 17) gave reproducible readings without regard to previous exposure within the range of humidities tried; all the others shifted to new curves every time the films were exposed to very high or very low humidities.

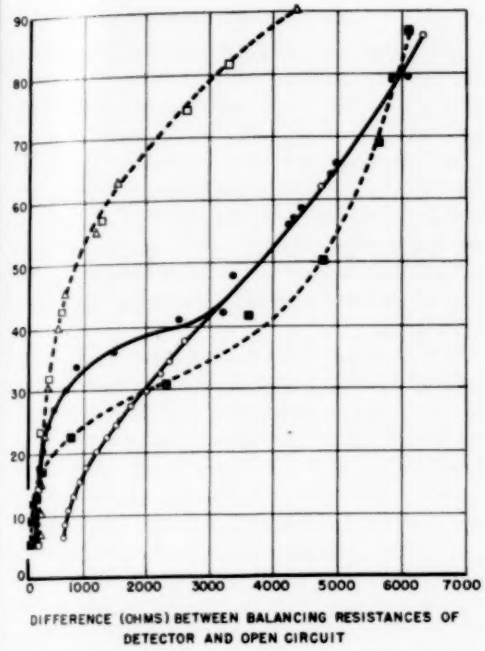

FIGURE 19. *Observations with several films containing lithium chloride.*

○, Lithium chloride in glycerol; ●, lithium chloride in polyvinyl acetate; ■, lithium chloride in gelatin hardened with formaldehyde; □, lithium chloride in soft gelatin; △, lithium chloride in gelatin and glycerol.

In addition to the films represented in figures 17 to 19, several other salts were tried with some of the plastics, and cellulose acetate was tried as a binder. Lithium chlorate, whose saturated solution should have the lowest vapor pressure of any known salt, appeared to be quite as good as lithium chloride, but not noticeably better; and none of the other salts seemed to be as good for general use. Less soluble salts may be useful in simple alarms.[4] Cellulose acetate films aged slowly and were particularly slow in reaching equilibrium after a change of humidity.

Several points of interest may be noted in connection with figures 17 to 19. The resistance at a given humidity of a salt solution in glycerol is independent of the past history of the film provided it has not lost material and not been diluted enough to flow by exposure to very high humidities. When subjected to a very dry atmosphere, the conductance of the film does not approach zero, and it responds to changes of humidity as low as 1 percent, far below the vapo pressure of a saturated solution of the salt. These observations seem to indicate that the salt is in true solution in the glycerol and that the latter acts to some slight extent as an ionizing solvent. As a true solution, the properties depend only on composition.

Films in which colloidal binders are used behave differently. Their conductances approach zero, not at zero humidity but at relative humidities as high as 20 percent. With the exception of solutions containing soft gelatin, the calibration curves have pronounced knees in the neighborhood of the vapor pressure of the saturated solution of the unmixed salt, but the position and magnitude of the knee-like bend depends on the colloid used. If the gelatin in a film is made tougher and less soluble in water (or less of a solvent for water) by the use of formaldehyde, a knee develops. But if the gelatin is made into a rubberlike jelly (printers' roll) by adding glycerin, its properties as a supporting material for an electrolyte are changed very little. The resistances of all the plastic films appear to depend on their past exposures to different humidities, particularly to strong drying, and when first formed they change more or less rapidly for a considerable time. Calibration curves retain their general form, including the knee but not their position on the resistance scale. Of the plastics tried by the authors, methyl methacrylate seems to reach a condition of stability most rapidly.

None of the plastic films respond to changes of humidity with the speed of phosphoric acid or of a salt in glycerol, but the methyl methacrylate films are fast enough for the purpose for which they are likely to be used. The readings of the film represented in figure 17 required about 3 minutes each, with the exception of those at the two or three highest humidities, which became substantially steady only after a much longer time. Unfortunately the methyl methacrylate films do not adhere well to the detector. Three days after the tests represented by figure 18, for example, the resistance of the film was infinite, probably because it had detached itself from one or both electrodes. We have had other experiences of the same sort.

[4] Such an alarm, consisting of a relay energized through a circuit that includes a salt film, will be actuated only when the vapor pressure of water in the atmosphere reaches the vapor pressure of a saturated solution of the salt. The choice of the salt will determine the relative humidity that will cause a signal.

IV. Procedures, Corrections, and Sources of Error

1. Operation of the Instrument

(a) Procedure in Testing Compressed Gas

The method of operating the instrument when testing oxygen has already been given but is so simple that it will be repeated here for convenience in the more detailed discussion of points of interest. Referring to figure 1, gas from the nitrogen cylinder is maintained in the saturator at a pressure of about 500 psi by means of the regulator. The cylinder of gas to be tested is connected to valve C. Valve B is opened widely and valve A is opened a little to permit a slight flow of gas from the saturator through the cell. The indicating circuit is adjusted, usually by changing resistance R (but sometimes V) of figure 7 to produce any convenient scale reading of the galvanometer, and as soon as this reading is sufficiently constant, it is noted. This reading will be referred to as the balance-point. Valves A and B are closed in that order and valve D opened widely. Valve C is then opened to permit a moderately brisk flow of the gas to be tested through the cell. As soon as this gas reaches the cell, the galvanometer needle goes off-scale on the dry side, corresponding to a high resistance of the detector. Valve D is now closed gradually, and the pressure built up in the cell until the galvanometer needle swings back to or past the balance-point. If, as usually happens, the first adjustment carries the needle past the balance-point, valve D is opened a little, carefully; if the new adjustment overshoots the balance-point in the opposite direction, the valve is closed a little, still more carefully. This series of approximations is continued until a satisfactory adjustment to the balance point is obtained. It is something of a game of skill, the object of which is to make the galvanometer reading come to the balance-point as quickly as possible and stop there. When this is substantially accomplished, the pressure in the cell, P_x, is read. If there is any doubt that the pressure reading is sufficiently accurate, valve C or D is changed and another adjustment of the galvanometer to balance is made. When the observer is satisfied as to the balancing pressure, the thermometer is read and the concentration of water vapor is computed.

(b) Control of Standard Gas

Details of the measurement will now be discussed. A saturator pressure, P_s, of 500 psi is selected for this particular purpose, because at ordinary room temperature, oxygen that meets Army-Navy specification for aviator's oxygen will have a substantially equal balancing pressure, P_x. If there is the same probable error in reading the two gages, the probable error of the comparison and the correction for deviation from the ideal gas laws are both minimized by making the two pressures equal.

The principal source of error is, without doubt, some uncertainty regarding the water content of the gas from the saturator, and this is affected by the condition of the apparatus and the rates of flow employed. To begin with, the regulator rarely controls perfectly the pressure in the saturator. When flow is stopped, the pressure builds up a little; when flow is resumed the pressure falls, and this change tends to produce an increase in the water content of the gas as flow is increased. On the other hand, the evaporation of water within the cylinder tends to cool the gas and cause the water content to decrease during the test. If the rate of flow is too high, there may not be time for complete saturation. Expansion at the valve causes a sharp drop in temperature of the gas with a tendency to precipitate the water as liquid. Fortunately most of the cooling takes place after the gas passes the narrowest passage in the valve, and any mist that is formed reevaporates. The massive block is intended to supply heat rapidly to the valve seat and prevent, as far as practicable without auxiliary heating, the chilling of the inlet to the valve and the condensation of water from the gas before expansion. This is never completely accomplished unless the valve-block as a whole is warmer than the saturator, and from time to time a little condensed water comes through the valve and produces a momentary movement of the galvanometer needle toward the wet side. In practice these brief deflections of the galvanometer are disregarded. They are comparatively rare, and the amount of water indicated would not affect the reading of the instrument much if it were distributed throughout the gas stream. The slower the flow, the less effect there is from this source of difficulty.

In practice it is assumed that the gas flowing through the cell is at atmospheric pressure. Of

course it is not, or it would not flow. Consequently, the detector is exposed to a little higher concentration of water than would otherwise be the case. The gas cooled by expansion may not reach room temperature by the time it arrives at the detector. This affects the reading in two ways; the lower temperature tends to condense more water in the film and thus cause a decrease of resistance, but a film containing a given quantity of water has a high temperature coefficient in the opposite direction. Available data seem to indicate that under some conditions of temperature and pressure the net effect is in one direction, under other conditions in the opposite direction. This is still somewhat uncertain, but the needed study of temperature effects has been deferred until a more elaborate set of controls is made available.

The discussion thus far would indicate that accuracy is promoted by making the flow of gas from the saturator very slow. We should add that at a very high rate of flow there is danger that liquid water will be carried over from the saturator mechanically and that there is even the possibility that a sudden blast of gas over the detector will displace the film (this not infrequently happens with the gas to be tested if valves are manipulated carelessly).

Another factor of importance enters, however. The dry side of the instrument is rarely completely dry. Even though the parts of the apparatus are made, dried, and assembled with care, they seem to have the property of sorbing water from moist gas in sufficient quantity to be readily detected and giving it up later to a drier atmosphere. Gages are the worst parts of the apparatus in this respect; valve packings probably next. This exchange of moisture with surfaces and pockets within the apparatus generally affects the resistance of the detector when there is no flow of gas. A very small flow is affected to some extent, a large flow is not affected appreciably. For this reason we do not want gas from the saturator to flow too slowly; there is also a saving of time in reaching equilibrium if the rate is increased. A rate of 250 ml/min from the saturator is probably usually about right. It is not necessary to measure it, however; the observer soon learns to control it satisfactorily by other means. In a quiet room the gas escaping from the saturator at 500 psig should be barely audible to a normal ear, or silent but on the verge of audibility. The stream issuing from the small outlet of valve *B* should not be perceptible to the hand unless the outlet is blocked momentarily with a finger or thumb. The little spurt of gas when the pressure is relieved should be noticeable. Momentarily blocking the flow should also cause the galvanometer to respond decisively and at once. If the apparatus is thoroughly dry, the galvanometer reading should be the same for any rate of flow of gas sufficient to prevent diffusion upstream from the outlet valve and not great enough to build up appreciable pressure in the cell. To save time, it is better to adjust near the latter limit than the former one. The American Instrument Co. puts an adjustable stop on valve *A*, which permits it to be opened the right amount without uncertainty or delay, and this is a distinct convenience.

(c) Troubleshooting

The condition of the apparatus can usually be judged by the quick and simple tests that follow. Set the rate of flow (with valve *A*) at what is considered a little more than is desirable, to produce a slight pressure in the cell, then close the valve half way. A prompt but slight deflection toward the dry side (higher resistance) is the normal reaction if the system is dry, because the pressure in the cell diminishes. An immediate and permanent deflection toward the wet side indicates that water is entering the gas stream steadily as it evaporates from a packing, screw thread, or other source near the main channel of gas flow. A strong momentary deflection followed by the return to a steady reading, which is equal to or on the dry side of the reading obtained before the change of flow, indicates a nearly isolated pocket in which wet gas can accumulate and from which it is released only by a change of pressure. This pocket is usually the gage. If no deflection occurs when the rate of flow is changed it may be because the rate was initially too low to produce appreciable pressure in the cell, because the detector or indicator is insensitive, or because there is so much water in the cell or its connections that the gas is nearly saturated regardless of rate of flow.

The conditions may be further explored by checking and releasing the flow with a thumb at the outlet of valve *B*. Usually the galvanometer deflects sharply to the wet side when flow is

stopped, and returns to the original reading when it is released. Sometimes a sequence of deflections will follow the release in such a way as to disclose a source of water, but this is less likely than with the less violent changes of flow produced by valve *A*.

If stopping and starting the flow at the outlet does not produce normal deflections of the galvanometer, the detector should be taken out of the cell and its response to the ever-changing humidity of room air noted, particularly the effect of bringing the detecting film near the operator's hand. If the indicator responds normally to this by promptly indicating a much lowered resistance. and particularly if the resistance of the detector in the cell was low, the apparatus is probably flooded. If exposing the detector to the atmosphere near the skin does not cause a sharp decrease of resistance, the system is inherently insensitive. If touching the electrodes with the finger does not produce a quick off-scale deflection, the trouble is in the electrical indicator and may be caused by a run-down battery, a broken connection, shunting by a low resistance, or the like. If the response to touching the electrodes is normal the trouble is in the film, which must be renewed.

The troubleshooting procedure is not as cumbersome as its description suggests. It should not require more than 2 or 3 minutes including the renewal of the sensitive film, if that is needed. Correcting faults in the electrical system and drying out the apparatus, when this is necessary, take longer.

If liquid water in quantity has gotten into the dry side of the apparatus, it is all but impossible to dry it out completely except by disassembling the apparatus and baking the individual parts. If the moisture has come only from exposure to gases of fairly high humidity, it can usually be removed sufficiently by attaching a cylinder of dry gas and alternately building up and discharging a pressure of several atmospheres in the system. The cycle can be repeated every 2 or 3 seconds. If 500 or 1,000 cycles are not effective, more thorough means of drying should be resorted to. This treatment is usually needed and usually successful after the apparatus has been out of use for a considerable period of time.

(d) Selecting and Matching a Balance Point

It has been remarked by one of the users of the instrument that the galvanometer reading is always drifting, and this is substantially true. There are numerous possible causes for drifting, especially when gas is coming from the saturator. To those causes that will be evident from the preceding discussion must be added changing battery voltage and the effect of changing temperature and humidity on the measuring circuit, including the resistance of the insulation of leads and detector. That these are real effects is clearly shown by the different balancing resistances required from time to time with an open circuit. Probably, however, the major cause of drifting is the slow approach to equilibrium within the glass insulator. The glass is, after all, an extremely viscous liquid that never possesses infinite resistance. In time, the electrolyte with which it is in contact probably diffuses into the glass to a considerable depth, making it more conducting. The subsurface electrolyte reaches equilibrium with water only very slowly, probably only at a rate comparable to that at which the electrolyte penetrated originally. When not in use, the detector is usually exposed to the relatively high concentration of water in normal air and tends to reach equilibrium with it. Then when the detector is used with gases of far lower water content, the freshly applied surface film follows closely the momentary changes of water vapor in the atmosphere, but the resistance of the underlying glass drifts slowly and without much reference to the surface changes, usually toward a higher value. Usually we cannot afford to wait for the reading in the standard gas to become constant, and we have to wait only for it to become so slow that we are not concerned with the change that takes place in a minute or two, for it will take no longer than that to complete the comparison with the unknown gas. Neither are we concerned with the temperature coefficient of the film, the condition of the batteries, or the electrical connections, provided these do not change appreciably during the measurement and that the measuring instrument is still sensitive enough. All these effects are cancelled out by the fact that they influence the reading with the standard gas to the same extent that they influence the unknown.

Usually it is a waste of time to set the electrical distance with the first gas involved in the comparison so that no current passes through the galvanometer or that any other predetermined reading is indicated. It is more convenient merely to bring the reading well onto the scale so that later the approach to it can be observed, and to make a mental note of it. The observer may forget the balance-point occasionally, but will take less time to recompare the gases in the few cases of doubt than to adjust to preselected points or to jot down the balance-point in all cases. When following conditions that cannot be reproduced at will, it is safest to record each balance-point, of course.

As the galvanometer is expected to drift, there is virtue in completing the test as quickly as possible. Just as anything dries more quickly in a wind than in still air, the completion of the test is hastened by a rapid flow of the unknown gas. Too strong a gust, however, wastes gas, tends to displace the film, and fails to warm up through between the valve and the detector and introduces an uncompensated thermal effect. In testing compressed oxygen, the initial rate of flow through valve C with D wide open is probably best made at about 1 to 1.5 liters per minute. This will be considerably reduced as D is closed down.

When tests are being made only to determine whether gas does or does not meet a specification, one takes account of the temperature and the setting of the regulator and computes the pressure at which gas that just meets the specification would balance. Thereafter until test conditions are changed, it is necessary only to run the pressure of the gas to be tested up to the predetermined value and note whether the galvanometer reading is to the right or left of that made with the standard gas. A setting with the standard gas is made with each cylinder, but this is easily done by an observer while someone else changes the test cylinder. It has been found practicable for one observer, with a sufficient crew of laborers to shift cylinders, to make tests by this method at the rate of 100 cylinders an hour. If it is to be determined how much water is present, not merely whether it is above or below a certain limit, more time is required. A test does not often require more than 2 minutes exclusive of the time required to move and connect the cylinder.

(e) Use of Compressed Gas as Standard

Actually it is not practicable to measure the water content of most of the aviators' oxygen now made by direct comparison with gas from a saturator, even if the saturation pressure is 1,000 psi instead of the recommended 500 psi. If, for example, gas saturated at 1,000 psi and 25° C (77° F) and expanded to 1 atmosphere matches gas at the usual charging pressure for storage cylinders, 2,000 psi, the water content of the stored gas is 4 micrograms per liter (after expansion to 1 atmosphere). If the saturation pressure is 500 psi, the minimum measurable water content of the stored gas is 7 micrograms per liter. Most of the aviator's oxygen tested at the Bureau of Standards, after the oxygen manufacturers began trying to comply with the specified maximum of 20 micrograms, has contained less than 4 micrograms per liter. To determine the water content actually present in such dry compressed gas, or to measure conveniently the water content below 0.2 or 0.3 mg per liter of gas not initially under pressure, it is best to use a cylinder of fairly dry compressed gas as a secondary standard. Even for gases within range of direct comparison with the saturator, the cylinder is a convenience because less care is required than in the control of the saturator, and the composition of the standard gas is less dependent on temperature.

The gas to be used as the secondary standard must be compared frequently with gas from the saturator, for the water content of gas discharged from a cylinder invariably increases as the pressure falls, because the gas in the cylinder is always in near equilibrium with water adsorbed on the walls. This equilibrium is somewhat affected by temperature, but changes in the gas are slow.

A cylinder of gas to be used as a secondary standard in testing other cylinders can usually be selected from the lot. Otherwise it can be conveniently prepared in a laboratory in which compressed air and a vacuum pump are available by thoroughly drying an evacuated cylinder, admitting as much air from the room as is desired, and filling with compressed air, dried with a good desiccant after compression. An an example, assume that a water content of about 25 micrograms per liter is desired in the secondary standard, that compressed air is available at 1,800 psi,

and that the laboratory air is 50 percent saturated at 25° C. The room air contains about 11,500 micrograms of water per liter. At 1,800 psi, the cylinder will contain about 125 volumes (at 1 atmosphere) of air. Hence we want about $(25\times125)/11{,}500=0.27$ atm $=210$ mm Hg of room air in the cylinder. As a secondary standard this gas can be used, while still at the initial pressure, to measure gas at 1 atmosphere containing from about 25 to about 3,000 micrograms per liter, or gas compressed at 1,800 psi at about 0.2 microgram per liter after expansion. It will measure the quantity corresponding to saturation with liquid water in the cylinder of any gas above about 4 atmospheres. As the gas in the standard cylinder is used up, the usable range becomes narrower. The upper limit decreases because only lower comparison pressures (P_c of eq 2) are available; the lower limit increases because some water evaporates from the cylinder walls.

The actual use of standard gas from cylinders differs from the use of a saturator in only one important respect. It is more often advantageous to use the secondary standard at other than a pressure of 1 atmosphere; unless advantage is taken of the fact that the barometric pressure is known more accurately than any small pressure can be measured on the gage attached to the instrument, accuracy is favored by making the pressures of standard and unknown gas as high as practicable. There is less reason than with the saturator to avoid excessive flows, and the observer may wish to gain speed by increasing somewhat the flow used. On the other hand, he may wish to conserve the supply because of the trouble of renewing it.

(f) Operations Other Than Testing Compressed Gases

In most of the numerous possible applications of the method other than testing compressed gases, the gas to be tested is at atmospheric pressure. Instead of varying the pressure of the unknown gas to obtain a balance corresponding to an observation already made of the standard gas, the first galvanometer setting is made with the unknown gas, and the pressure of the standard, whether from saturator or calibrated cylinder, is varied to obtain a balance. The details of the procedure are so like those already given that they probably require no further description. Because we lack the ability to change the pressure of the unknown sample the range of concentrations that can be measured with a single standard is narrower than in testing compressed gas, and we may need two secondary standards in addition to the saturator, whereas we rarely need more than one in work with compressed gases.

One source of error should be emphasized in connection with miscellaneous uses of the instrument. No rubber whatever can be used in any connection through which a gas to be tested flows. Exposing the gas to contact with any rubber surface is almost equivalent to exposing it to contact with an equal free surface of water.

2. Deviation from the Ideal Gas Laws and Computation of Results

(a) Oxygen, Nitrogen, and Air

The equations given in the introduction would serve to compute correctly the results of experiments provided all the gases involved, including water vapor, behaved as ideal gases. This statement is meant to include as a part of the behavior of ideal gases the commonly assumed rule that the mass of water vapor per unit volume in equilibrium with liquid water is independent of the presence of other gases. The rule is not strictly true, and the deviation from it is to be attributed to forces between the molecules of water vapor and other gases, which are the same forces that cause the deviations from Boyle's and Dalton's laws. Hence it is correct as well as convenient to include the rule of constant vapor pressure among those defining relations for ideal gases.

In the initial use of the pressure-balancing method for water in oxygen, the amount of water found was always lower than that found by gravimetric determinations. C. E. Earle, of the U. S. Navy Department, suggested deviation from ideality as the explanation. The results of pressure determinations were studied statistically by the junior author, and simplified eq 2

$$W=\frac{SP_cP_w}{P_sP_x}$$

was replaced by the empirical equation,

$$W=\frac{SP_c(1-KP_c)P_w(1-KP_w)}{P_s(1-KP_s)P_x(1-KP_x)},$$

d a tentative value of 0.00015 was assigned to e constant K when pressures are expressed in unds per square inch. If pressures are expressed in atmospheres, this amounts to $K=$ 0022.

Entirely independently an attempt was made evaluate K from data in the literature on the ncentration of water vapor in compressed gas in uilibrium with the liquid and the deviation of ygen from Boyle's law. The available data ere not entirely adequate; they involved some certain extrapolations, but they led to the value =0.002. An additional decimal place was not stified by the accuracy of the data. This may considered a satisfactory agreement with the served results.

Figure 20 represents the results of one set of periments intended to determine the value of K. he equation in the figure is eq 5 with pressures pressed in pounds per square inch and P_c and each equal to 1 atmosphere. In the tests the essure of saturation was varied as much as acticable, and the determination completed by e usual method of comparison. When plotted th respect to the pressure of saturation the ater formed from the uncorrected eq 2 passed rough a maximum (this plot is not shown), oducing a substantially symmetrical curve. nce the product of P_s and P_x decreases when increases, the parts of the curve on opposite es of the maximum, which occurred at a value about 350 psi for both P_s and P_x, could be mbined in a more condensed figure by plotting e amount of water found with respect to the wer of P_s and P_x. This has been done in figure , in which four different plots have been made results calculated with four different values of from 0 to 0.00018. It is at once apparent that results are low and in poor agreement with each her if K is given a value of 0 or 0.00010. If the lue assigned to K is 0.00015, the average of e results by the electrical method is in agreement th the average of the gravimetric tests, but the otted results still show a definite slope. If we sign the slightly higher value $K=0.00018$, there no longer a distinct slope to the plot, but it ows a higher average than the gravimetric tests. owever, of the three gravimetric tests two were ose together and the third about 10 percent low. a case of this kind, there is probably as much ason to accept the two closely agreeing results as the average of the three. If this is done, all observations agree with the gravimetric result within 2 micrograms per liter.

It is to be noted that the factor K can apparently be determined almost as well from the agreement of results at different pressures of saturation as from agreement with gravimetric tests. There was some question as to whether the same value should be used for the Ks affecting P_s and P_x, i. e. whether a high pressure in the saturator and a low matching pressure was exactly equivalent to a reversal of the two. Both from the results shown in figure 20 and from much more numerous tests with other cylinders, it was decided that any error introduced by using the same value of K in connection with all observed pressures was outside the limit of error of the current observations.

There was also a question whether the same value of K should be used for nitrogen and oxygen. This was tested directly several times by substituting air and oxygen for nitrogen in the saturator for testing the same cylinders of gases. Although we should expect a slightly lower factor for nitrogen than for oxygen, the difference again seemed to be outside the limit of error. Hence the same constant, 0.00015, has been used for air, oxygen, and nitrogen. The value 0.00017 may be better.

Without doubt the exact value of the constant changes with temperature; but again the effect is not noticeable in comparison with other variations within the usual range of laboratory temperatures, hence the same constant is used at all ordinary temperatures. The true value may be expected to decrease with increasing temperature.

(b) Computer and Its Use for Compressed Gas

The solution of eq 5 involves ascertaining the value of S, the saturation pressure of water at the temperature of test, and reducing four pressures from gage to the absolute scale in addition to the subtractions and multiplications indicated by the formula. The time involved in doing this by longhand is greatly in excess of that involved in making the tests themselves. Accordingly, a simple computer was designed by the authors to do most of the work. It is in principle a circular slide rule with three pressure scales on two rotating disks above a base-plate. The base has two scales. The computer is made of either metal or plastic. Computers of both types are shown in

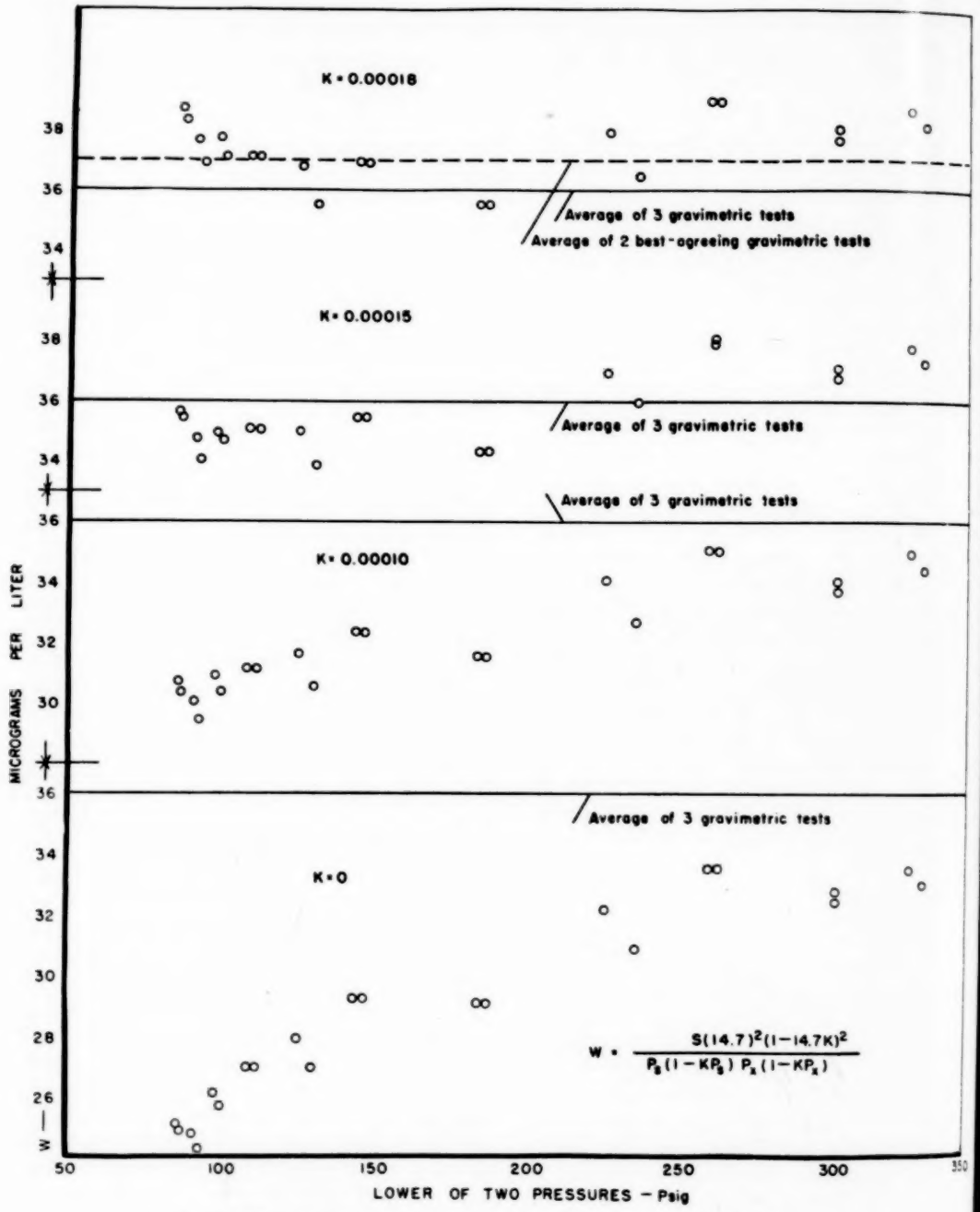

FIGURE 20.—*Correction for deviation of water vapor in oxygen from ideal vapor.*

igures 21 and 22. The computer is designed to ive numerical results from eq 5 when pressures re expressed in pounds per square inch gage, arometric pressure is 14.7 psi, and $K=0.00015$. he scale for the vapor pressure S is engraved on he base plate by laying off angles proportional to he logarithms of the vapor pressures at definite emperatures and marking the temperature in egrees Fahrenheit to which each angle corre-ponds. On the scales for saturation pressure, P_s, r test gas pressure, P_x, and for comparison pres-ure, P_c, angles are proportional to the logarithms f absolute pressures, but marked with the corre-ponding gage pressures when the barometric ressure is 14.7 psi. Values of W are on an ordi-ary (slide rule) logarithmic scale and are marked fractions of a milligram per liter from 0.001 to 0. The computer is designed for a constant alue of P_w of 14.7 psi, which is represented by he angular spacing on the base plate of the cales for S and W.

Further understanding of the operation of the rule will be best conveyed by a description of some actual computations. In figure 21 the computer is set to show the concentration of water in gas discharged from a cylinder at atmospheric pressure if the standard gas, saturated at 500 psig and 70° F and expanded to 0 psig (14.7 psi), is matched by gas from the cylinder at a pressure of 400 psig. The number 500 on the saturation pressure is set opposite 70° F on the temperature scale. The zero of the comparison pressure scale is set opposite 400 of the test gas pressure scale, and the desired answer, 0.0215 mg/liter, is read opposite the zero of the comparison pressure scale. Since both P_c and P_w are equal to 1 atmosphere in the example given, the value of W is just opposite that of P_x, and any line drawn from the center across the scales would serve as well as the zero of the comparison pressure scale to connect the two points. The Air-Force designer of the plastic computer thought it more convenient to use a line on the handle of one of the disks for this purpose than to use the end of the comparison pressure

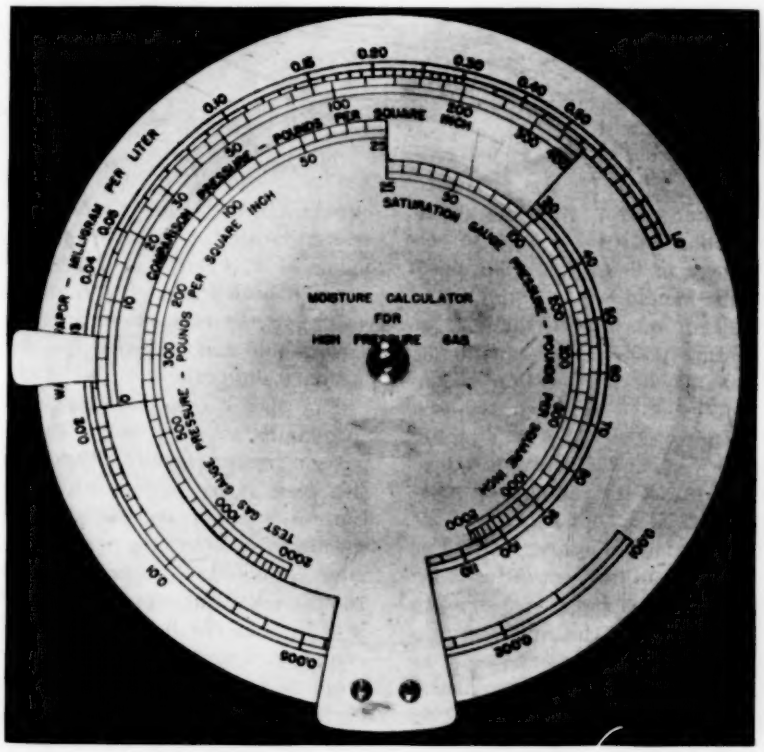
MOISTURE CALCULATOR
FOR
HIGH PRESSURE GAS
SATURATION GAUGE PRESSURE - POUNDS PER SQUARE INCH
COMPARISON PRESSURE - POUNDS PER SQUARE INCH
TEST GAS GAUGE PRESSURE - POUNDS PER SQUARE INCH
VAPOR - MILLIGRAM PER LITER

FIGURE 21.—*Metal computer.*

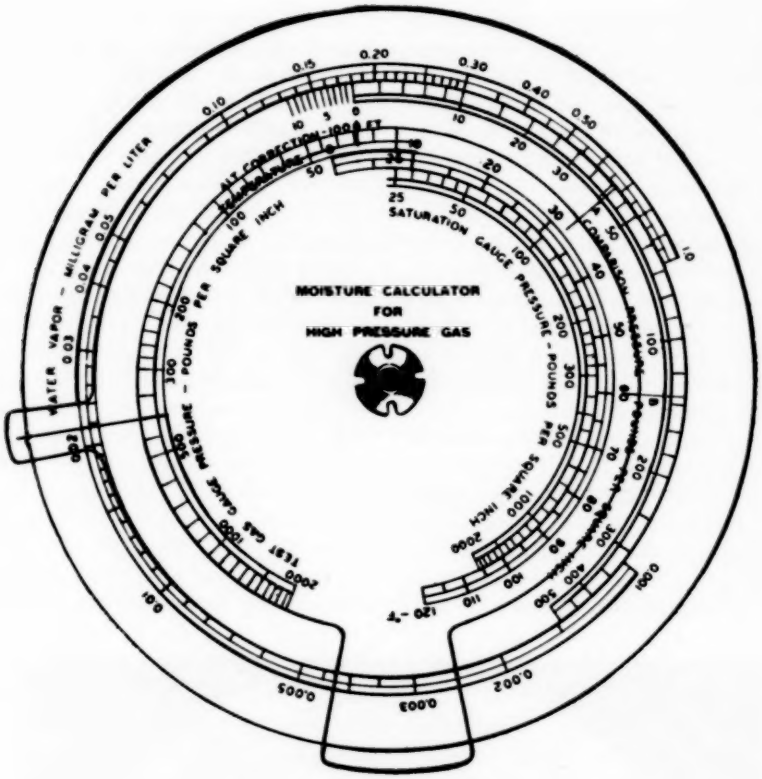
MOISTURE CALCULATOR
FOR
HIGH PRESSURE GAS
WATER VAPOR - MILLIGRAM PER LITER
SATURATION GAUGE PRESSURE - POUNDS PER SQUARE INCH
TEST GAS GAUGE PRESSURE - POUNDS PER SQUARE INCH
COMPARISON PRESSURE - POUNDS PER SQUARE INCH
ALT. CORRECTION - 1000 FT.
0.10
0.15
0.20
0.30
0.40
0.50
1.0
0.03
0.04
0.05
0.002
0.003
0.005
0.01
0.02
0.1
0.2
0.3
0.4
0.5
1.0
2.0
3.0
4.0
5.0
10.0
20.0
30.0
40.0
50.0
100
200
300
400
500
1000
2000
3000
4000
5000
10000
20000
30000
40000
50000
100000
200000
300000
400000
500000
1000000
2000000
3000000
4000000
5000000
10000000
20000000
30000000
40000000
50000000
100000000
200000000
300000000
400000000
500000000
1000000000
2000000000
3000000000
4000000000
5000000000
10000000000
20000000000
30000000000
40000000000
50000000000
100000000000
200000000000
300000000000
400000000000
500000000000
1000000000000
2000000000000
3000000000000
4000000000000
5000000000000
10000000000000
20000000000000
30000000000000
40000000000000
50000000000000
100000000000000
200000000000000
300000000000000
400000000000000
500000000000000
1000000000000000
2000000000000000
3000000000000000
4000000000000000
5000000000000000
10000000000000000
20000000000000000
30000000000000000
40000000000000000
50000000000000000
100000000000000000
200000000000000000
300000000000000000
400000000000000000
500000000000000000
1000000000000000000
2000000000000000000
3000000000000000000
4000000000000000000
5000000000000000000
10000000000000000000
20000000000000000000
30000000000000000000
40000000000000000000
50000000000000000000
100000000000000000000
200000000000000000000
300000000000000000000
400000000000000000000
500000000000000000000
1000000000000000000000
2000000000000000000000
3000000000000000000000
4000000000000000000000
5000000000000000000000
10000000000000000000000
20000000000000000000000
30000000000000000000000
40000000000000000000000
50000000000000000000000
100000000000000000000000
200000000000000000000000
300000000000000000000000
400000000000000000000000
500000000000000000000000
1000000000000000000000000
2000000000000000000000000
3000000000000000000000000
4000000000000000000000000
5000000000000000000000000
10000000000000000000000000
20000000000000000000000000
30000000000000000000000000
40000000000000000000000000
50000000000000000000000000
100000000000000000000000000
200000000000000000000000000
300000000000000000000000000
400000000000000000000000000
500000000000000000000000000
1000000000000000000000000000
2000000000000000000000000000
3000000000000000000000000000
4000000000000000000000000000
5000000000000000000000000000
10000000000000000000000000000
20000000000000000000000000000
30000000000000000000000000000
40000000000000000000000000000
50000000000000000000000000000
100000000000000000000000000000
200000000000000000000000000000
300000000000000000000000000000
400000000000000000000000000000
500000000000000000000000000000
1000000000000000000000000000000
2000000000000000000000000000000
3000000000000000000000000000000
4000000000000000000000000000000
5000000000000000000000000000000
10000000000000000000000000000000
20000000000000000000000000000000
30000000000000000000000000000000
40000000000000000000000000000000
50000000000000000000000000000000
100000000000000000000000000000000
200000000000000000000000000000000
300000000000000000000000000000000
400000000000000000000000000000000
500000000000000000000000000000000
1000000000000000000000000000000000
2000000000000000000000000000000000
3000000000000000000000000000000000
4000000000000000000000000000000000
5000000000000000000000000000000000
10000000000000000000000000000000000
20000000000000000000000000000000000
30000000000000000000000000000000000
40000000000000000000000000000000000
50000000000000000000000000000000000
100000000000000000000000000000000000
200000000000000000000000000000000000
300000000000000000000000000000000000
400000000000000000000000000000000000
500000000000000000000000000000000000
1000000000000000000000000000000000000
2000000000000000000000000000000000000
3000000000000000000000000000000000000
4000000000000000000000000000000000000
5000000000000000000000000000000000000
10000000000000000000000000000000000000
20000000000000000000000000000000000000
30000000000000000000000000000000000000
40000000000000000000000000000000000000
50000000000000000000000000000000000000
100000000000000000000000000000000000000
200000000000000000000000000000000000000
300000000000000000000000000000000000000
400000000000000000000000000000000000000
500000000000000000000000000000000000000
1000000000000000000000000000000000000000
2000000000000000000000000000000000000000
3000000000000000000000000000000000000000
4000000000000000000000000000000000000000
5000000000000000000000000000000000000000
10000000000000000000000000000000000000000
20000000000000000000000000000000000000000
30000000000000000000000000000000000000000
40000000000000000000000000000000000000000
50000000000000000000000000000000000000000
100000000000000000000000000000000000000000
200000000000000000000000000000000000000000
300000000000000000000000000000000000000000
400000000000000000000000000000000000000000
500000000000000000000000000000000000000000
1000000000000000000000000000000000000000000
2000000000000000000000000000000000000000000
3000000000000000000000000000000000000000000
4000000000000000000000000000000000000000000
5000000000000000000000000000000000000000000
10000000000000000000000000000000000000000000
20000000000000000000000000000000000000000000
30000000000000000000000000000000000000000000
40000000000000000000000000000000000000000000
50000000000000000000000000000000000000000000
100000000000000000000000000000000000000000000
200000000000000000000000000000000000000000000
300000000000000000000000000000000000000000000
400000000000000000000000000000000000000000000
500000000000000000000000000000000000000000000
1000000000000000000000000000000000000000000000
2000000000000000000000000000000000000000000000
3000000000000000000000000000000000000000000000
4000000000000000000000000000000000000000000000
5000000000000000000000000000000000000000000000
10000000000000000000000000000000000000000000000
20000000000000000000000000000000000000000000000
30000000000000000000000000000000000000000000000
40000000000000000000000000000000000000000000000
50000000000000000000000000000000000000000000000
100000000000000000000000000000000000000000000000
200000000000000000000000000000000000000000000000
300000000000000000000000000000000000000000000000
400000000000000000000000000000000000000000000000
500000000000000000000000000000000000000000000000
1000000000000000000000000000000000000000000000000
2000000000000000000000000000000000000000000000000
3000000000000000000000000000000000000000000000000
4000000000000000000000000000000000000000000000000
5000000000000000000000000000000000000000000000000
10000000000000000000000000000000000000000000000000
20000000000000000000000000000000000000000000000000
30000000000000000000000000000000000000000000000000
40000000000000000000000000000000000000000000000000
50000000000000000000000000000000000000000000000000
100000000000000000000000000000000000000000000000000
200000000000000000000000000000000000000000000000000
300000000000000000000000000000000000000000000000000
400000000000000000000000000000000000000000000000000
500000000000000000000000000000000000000000000000000
1000000000000000000000000000000000000000000000000000
2000000000000000000000000000000000000000000000000000
3000000000000000000000000000000000000000000000000000
4000000000000000000000000000000000000000000000000000
5000000000000000000000000000000000000000000000000000
10000000000000000000000000000000000000000000000000000
20000000000000000000000000000000000000000000000000000
30000000000000000000000000000000000000000000000000000
40000000000000000000000000000000000000000000000000000
50000000000000000000000000000000000000000000000000000
100000000000000000000000000000000000000000000000000000
200000000000000000000000000000000000000000000000000000
300000000000000000000000000000000000000000000000000000
400000000000000000000000000000000000000000000000000000
500000000000000000000000000000000000000000000000000000
1000000000000000000000000000000000000000000000000000000
2000000000000000000000000000000000000000000000000000000
3000000000000000000000000000000000000000000000000000000
4000000000000000000000000000000000000000000000000000000
5000000000000000000000000000000000000000000000000000000
10000000000000000000000000000000000000000000000000000000
20000000000000000000000000000000000000000000000000000000
30000000000000000000000000000000000000000000000000000000
40000000000000000000000000000000000000000000000000000000
50000000000000000000000000000000000000000000000000000000
100000000000000000000000000000000000000000000000000000000
200000000000000000000000000000000000000000000000000000000
300000000000000000000000000000000000000000000000000000000
400000000000000000000000000000000000000000000000000000000
500000000000000000000000000000000000000000000000000000000
1000000000000000000000000000000000000000000000000000000000
2000000000000000000000000000000000000000000000000000000000
3000000000000000000000000000000000000000000000000000000000
4000000000000000000000000000000000000000000000000000000000
5000000000000000000000000000000000000000000000000000000000
10000000000000000000000000000000000000000000000000000000000
20000000000000000000000000000000000000000000000000000000000
30000000000000000000000000000000000000000000000000000000000
40000000000000000000000000000000000000000000000000000000000
50000000000000000000000000000000000000000000000000000000000
100000000000000000000000000000000000000000000000000000000000
200000000000000000000000000000000000000000000000000000000000
300000000000000000000000000000000000000000000000000000000000
400000000000000000000000000000000000000000000000000000000000
500000000000000000000000000000000000000000000000000000000000
1000000000000000000000000000000000000000000000000000000000000
2000000000000000000000000000000000000000000000000000000000000
3000000000000000000000000000000000000000000000000000000000000
4000000000000000000000000000000000000000000000000000000000000
5000000000000000000000000000000000000000000000000000000000000
10000000000000000000000000000000000000000000000000000000000000
20000000000000000000000000000000000000000000000000000000000000
30000000000000000000000000000000000000000000000000000000000000
40000000000000000000000000000000000000000000000000000000000000
50000000000000000000000000000000000000000000000000000000000000
100000000000000000000000000000000000000000000000000000000000000
200000000000000000000000000000000000000000000000000000000000000
300000000000000000000000000000000000000000000000000000000000000
400000000000000000000000000000000000000000000000000000000000000
500000000000000000000000000000000000000000000000000000000000000
1000000000000000000000000000000000000000000000000000000000000000
2000000000000000000000000000000000000000000000000000000000000000
3000000000000000000000000000000000000000000000000000000000000000
4000000000000000000000000000000000000000000000000000000000000000
5000000000000000000000000000000000000000000000000000000000000000
10000000000000000000000000000000000000000000000000000000000000000
20000000000000000000000000000000000000000000000000000000000000000
30000000000000000000000000000000000000000000000000000000000000000
40000000000000000000000000000000000000000000000000000000000000000
50000000000000000000000000000000000000000000000000000000000000000
100000000000000000000000000000000000000000000000000000000000000000
200000000000000000000000000000000000000000000000000000000000000000
300000000000000000000000000000000000000000000000000000000000000000
400000000000000000000000000000000000000000000000000000000000000000
500000000000000000000000000000000000000000000000000000000000000000
1000000000000000000000000000000000000000000000000000000000000000000
2000000000000000000000000000000000000000000000000000000000000000000
3000000000000000000000000000000000000000000000000000000000000000000
4000000000000000000000000000000000000000000000000000000000000000000
5000000000000000000000000000000000000000000000000000000000000000000
10000000000000000000000000000000000000000000000000000000000000000000
20000000000000000000000000000000000000000000000000000000000000000000
30000000000000000000000000000000000000000000000000000000000000000000
40000000000000000000000000000000000000000000000000000000000000000000
50000000000000000000000000000000000000000000000000000000000000000000
100000000000000000000000000000000000000000000000000000000000000000000
200000000000000000000000000000000000000000000000000000000000000000000
300000000000000000000000000000000000000000000000000000000000000000000
400000000000000000000000000000000000000000000000000000000000000000000
500000000000000000000000000000000000000000000000000000000000000000000
1000000000000000000000000000000000000000000000000000000000000000000000
2000000000000000000000000000000000000000000000000000000000000000000000
3000000000000000000000000000000000000000000000000000000000000000000000
4000000000000000000000000000000000000000000000000000000000000000000000
5000000000000000000000000000000000000000000000000000000000000000000000
10000000000000000000000000000000000000000000000000000000000000000000000
20000000000000000000000000000000000000000000000000000000000000000000000
30000000000000000000000000000000000000000000000000000000000000000000000
40000000000000000000000000000000000000000000000000000000000000000000000
50000000000000000000000000000000000000000000000000000000000000000000000
100000000000000000000000000000000000000000000000000000000000000000000000
200000000000000000000000000000000000000000000000000000000000000000000000
300000000000000000000000000000000000000000000000000000000000000000000000
400000000000000000000000000000000000000000000000000000000000000000000000
500000000000000000000000000000000000000000000000000000000000000000000000
1000000000000000000000000000000000000000000000000000000000000000000000000
2000000000000000000000000000000000000000000000000000000000000000000000000
3000000000000000000000000000000000000000000000000000000000000000000000000
4000000000000000000000000000000000000000000000000000000000000000000000000
5000000000000000000000000000000000000000000000000000000000000000000000000
10000000000000000000000000000000000000000000000000000000000000000000000000
20000000000000000000000000000000000000000000000000000000000000000000000000
30000000000000000000000000000000000000000000000000000000000000000000000000
40000000000000000000000000000000000000000000000000000000000000000000000000
50000000000000000000000000000000000000000000000000000000000000000000000000
100000000000000000000000000000000000000000000000000000000000000000000000000
200000000000000000000000000000000000000000000000000000000000000000000000000
300000000000000000000000000000000000000000000000000000000000000000000000000
400000000000000000000000000000000000000000000000000000000000000000000000000
500000000000000000000000000000000000000000000000000000000000000000000000000
1000000000000000000000000000000000000000000000000000000000000000000000000000
2000000000000000000000000000000000000000000000000000000000000000000000000000
3000000000000000000000000000000000000000000000000000000000000000000000000000
4000000000000000000000000000000000000000000000000000000000000000000000000000
5000000000000000000000000000000000000000000000000000000000000000000000000000
10000000000000000000000000000000000000000000000000000000000000000000000000000
20000000000000000000000000000000000000000000000000000000000000000000000000000
30000000000000000000000000000000000000000000000000000000000000000000000000000
40000000000000000000000000000000000000000000000000000000000000000000000000000
50000000000000000000000000000000000000000000000000000000000000000000000000000
100000000000000000000000000000000000000000000000000000000000000000000000000000
200000000000000000000000000000000000000000000000000000000000000000000000000000
300000000000000000000000000000000000000000000000000000000000000000000000000000
400000000000000000000000000000000000000000000000000000000000000000000000000000
500000000000000000000000000000000000000000000000000000000000000000000000000000
1000000000000000000000000000000000000000000000000000000000000000000000000000000
2000000000000000000000000000000000000000000000000000000000000000000000000000000
3000000000000000000000000000000000000000000000000000000000000000000000000000000
4000000000000000000000000000000000000000000000000000000000000000000000000000000
5000000000000000000000000000000000000000000000000000000000000000000000000000000
10000000000000000000000000000000000000000000000000000000000000000000000000000000
20000000000000000000000000000000000000000000000000000000000000000000000000000000
30000000000000000000000000000000000000000000000000000000000000000000000000000000
40000000000000000000000000000000000000000000000000000000000000000000000000000000
50000000000000000000000000000000000000000000000000000000000000000000000000000000
100000000000000000000000000000000000000000000000000000000000000000000000000000000
200000000000000000000000000000000000000000000000000000000000000000000000000000000
300000000000000000000000000000000000000000000000000000000000000000000000000000000
400000000000000000000000000000000000000000000000000000000000000000000000000000000
500000000000000000000000000000000000000000000000000000000000000000000000000000000
1000000000000000000000000000000000000000000000000000000000000000000000000000000000
2000000000000000000000000000000000000000000000000000000000000000000000000000000000
3000000000000000000000000000000000000000000000000000000000000000000000000000000000
4000000000000000000000000000000000000000000000000000000000000000000000000000000000
5000000000000000000000000000000000000000000000000000000000000000000000000000000000
10000000000000000000000000000000000000000000000000000000000000000000000000000000000
20000000000000000000000000000000000000000000000000000000000000000000000000000000000
30000000000000000000000000000000000000000000000000000000000000000000000000000000000
40000000000000000000000000000000000000000000000000000000000000000000000000000000000
50000000000000000000000000000000000000000000000000000000000000000000000000000000000
100000000000000000000000000000000000000000000000000000000000000000000000000000000000
200000000000000000000000000000000000000000000000000000000000000000000000000000000000
300000000000000000000000000000000000000000000000000000000000000000000000000000000000
400000000000000000000000000000000000000000000000000000000000000000000000000000000000
500000000000000000000000000000000000000000000000000000000000000000000000000000000000
1000000000000000000000000000000000000000000000000000000000000000000000000000000000000
2000000000000000000000000000000000000000000000000000000000000000000000000000000000000
3000000000000000000000000000000000000000000000000000000000000000000000000000000000000
4000000000000000000000000000000000000000000000000000000000000000000000000000000000000
5000000000000000000000000000000000000000000000000000000000000000000000000000000000000
10000000000000000000000000000000000000000000000000000000000000000000000000000000000000
20000000000000000000000000000000000000000000000000000000000000000000000000000000000000
30000000000000000000000000000000000000000000000000000000000000000000000000000000000000
40000000000000000000000000000000000000000000000000000000000000000000000000000000000000
50000000000000000000000000000000000000000000000000000000000000000000000000000000000000
100000000000000000000000000000000000000000000000000000000000000000000000000000000000000
200000000000000000000000000000000000000000000000000000000000000000000000000000000000000
300000000000000000000000000000000000000000000000000000000000000000000000000000000000000
400000000000000000000000000000000000000000000000000000000000000000000000000000000000000
500000000000000000000000000000000000000000000000000000000000000000000000000000000000000
1000000000000000000000000000000000000000000000000000000000000000000000000000000000000000
2000000000000000000000000000000000000000000000000000000000000000000000000000000000000000
3000000000000000000000000000000000000000000000000000000000000000000000000000000000000000
4000000000000000000000000000000000000000000000000000000000000000000000000000000000000000
5000000000000000000000000000000000000000000000000000000000000000000000000000000000000000
10000000000000000000000000000000000000000000000000000000000000000000000000000000000000000
20000000000000000000000000000000000000000000000000000000000000000000000000000000000000000
30000000000000000000000000000000000000000000000000000000000000000000000000000000000000000
40000000000000000000000000000000000000000000000000000000000000000000000000000000000000000
50000000000000000000000000000000000000000000000000000000000000000000000000000000000000000
100000000000000000000000000000000000000000000000000000000000000000000000000000000000000000
200000000000000000000000000000000000000000000000000000000000000000000000000000000000000000
300000000000000000000000000000000000000000000000000000000000000000000000000000000000000000
400000000000000000000000000000000000000000000000000000000000000000000000000000000000000000
500000000000000000000000000000000000000000000000000000000000000000000000000000000000000000
1000000000000000000000000000000000000000000000000000000000000000000000000000000000000000000
2000000000000000000000000000000000000000000000000000000000000000000000000000000000000000000
3000000000000000000000000000000000000000000000000000000000000000000000000000000000000000000
4000000000000000000000000000000000000000000000000000000000000000000000000000000000000000000
5000000000000000000000000000000000000000000000000000000000000000000000000000000000000000000
10000000000000000000000000000000000000000000000000000000000000000000000000000000000000000000
20000000000000000000000000000000000000000000000000000000000000000000000000000000000000000000
30000000000000000000000000000000000000000000000000000000000000000000000000000000000000000000
40000000000000000000000000000000000000000000000000000000000000000000000000000000000000000000
50000000000000000000000000000000000000000000000000000000000000000000000000000000000000000000
100000000000000000000000000000000000000000000000000000000000000000000000000000000000000000000
200000000000000000000000000000000000000000000000000000000000000000000000000000000000000000000
300000000000000000000000000000000000000000000000000000000000000000000000000000000000000000000
400000000000000000000000000000000000000000000000000000000000000000000000000000000000000000000
500000000000000000000000000000000000000000000000000000000000000000000000000000000000000000000
1000000000000000000000000000000000000000000000000000000000000000000000000000000000000000000000
2000000000000000000000000000000000000000000000000000000000000000000000000000000000000000000000
3000000000000000000000000000000000000000000000000000000000000000000000000000000000000000000000
4000000000000000000000000000000000000000000000000000000000000000000000000000000000000000000000
5000000000000000000000000000000000000000000000000000000000000000000000000000000000000000000000
10000000000000000000000000000000000000000000000000000000000000000000000000000000000000000000000
20000000000000000000000000000000000000000000000000000000000000000000000000000000000000000000000
30000000000000000000000000000000000000000000000000000000000000000000000000000000000000000000000
40000000000000000000000000000000000000000000000000000000000000000000000000000000000000000000000
50000000000000000000000000000000000000000000000000000000000000000000000000000000000000000000000
100000000000000000000000000000000000000000000000000000000000000000000000000000000000000000000000
200000000000000000000000000000000000000000000000000000000000000000000000000000000000000000000000
300000000000000000000000000000000000000000000000000000000000000000000000000000000000000000000000
400000000000000000000000000000000000000000000000000000000000000000000000000000000000000000000000
500000000000000000000000000000000000000000000000000000000000000000000000000000000000000000000000
1000000000000000000000000000000000000000000000000000000000000000000000000000000000000000000000000
2000000000000000000000000000000000000000000000000000000000000000000000000000000000000000000000000
3000000000000000000000000000000000000000000000000000000000000000000000000000000000000000000000000
4000000000000000000000000000000000000000000000000000000000000000000000000000000000000000000000000
5000000000000000000000000000000000000000000000000000000000000000000000000000000000000000000000000
10000000000000000000000000000000000000000000000000000000000000000000000000000000000000000000000000
20000000000000000000000000000000000000000000000000000000000000000000000000000000000000000000000000
30000000000000000000000000000000000000000000000000000000000000000000000000000000000000000000000000
40000000000000000000000000000000000000000000000000000000000000000000000000000000000000000000000000
50000000000000000000000000000000000000000000000000000000000000000000000000000000000000000000000000
100000000000000000000000000000000000000000000000000000000000000000000000000000000000000000000000000
200000000000000000000000000000000000000000000000000000000000000000000000000000000000000000000000000
300000000000000000000000000000000000000000000000000000000000000000000000000000000000000000000000000
400000000000000000000000000000000000000000000000000000000000000000000000000000000000000000000000000
500000000000000000000000000000000000000000000000000000000000000000000000000000000000000000000000000
1000000000000000000000000000000000000000000000000000000000000000000000000000000000000000000000000000
2000000000000000000000000000000000000000000000000000000000000000000000000000000000000000000000000000
3000000000000000000000000000000000000000000000000000000000000000000000000000000000000000000000000000
4000000000000000000000000000000000000000000000000000000000000000000000000000000000000000000000000000
5000000000000000000000000000000000000000000000000000000000000000000000000000000000000000000000000000
10000000000000000000000000000000000000000000000000000000000000000000000000000000000000000000000000000
20000000000000000000000000000000000000000000000000000000000000000000000000000000000000000000000000000
30000000000000000000000000000000000000000000000000000000000000000000000000000000000000000000000000000
40000000000000000000000000000000000000000000000000000000000000000000000000000000000000000000000000000
50000000000000000000000000000000000000000000000000000000000000000000000000000000000000000000000000000
100000000000000000000000000000000000000000000000000000000000000000000000000000000000000000000000000000
200000000000000000000000000000000000000000000000000000000000000000000000000000000000000000000000000000
300000000000000000000000000000000000000000000000000000000000000000000000000000000000000000000000000000
400000000000000000000000000000000000000000000000000000000000000000000000000000000000000000000000000000
500000000000000000000000000000000000000000000000000000000000000000000000000000000000000000000000000000
1000000000000000000000000000000000000000000000000000000000000000000000000000000000000000000000000000000
2000000000000000000000000000000000000000000000000000000000000000000000000000000000000000000000000000000
3000000000000000000000000000000000000000000000000000000000000000000000000000000000000000000000000000000
4000000000000000000000000000000000000000000000000000000000000000000000000000000000000000000000000000000
5000000000000000000000000000000000000000000000000000000000000000000000000000000000000000000000000000000
10000000000000000000000000000000000000000000000000000000000000000000000000000000000000000000000000000000
20000000000000000000000000000000000000000000000000000000000000000000000000000000000000000000000000000000
30000000000000000000000000000000000000000000000000000000000000000000000000000000000000000000000000000000
40000000000000000000000000000000000000000000000000000000000000000000000000000000000000000000000000000000
50000000000000000000000000000000000000000000000000000000000000000000000000000000000000000000000000000000
100000000000000000000000000000000000000000000000000000000000000000000000000000000000000000000000000000000
200000000000000000000000000000000000000000000000000000000000000000000000000000000000000000000000000000000
300000000000000000000000000000000000000000000000000000000000000000000000000000000000000000000000000000000
400000000000000000000000000000000000000000000000000000000000000000000000000000000000000000000000000000000
500000000000000000000000000000000000000000000000000000000000000000000000000000000000000000000000000000000
1000000000000000000000000000000000000000000000000000000000000000000000000000000000000000000000000000000000
2000000000000000000000000000000000000000000000000000000000000000000000000000000000000000000000000000000000
3000000000000000000000000000000000000000000000000000000000000000000000000000000000000000000000000000000000
4000000000000000000000000000000000000000000000000000000000000000000000000000000000000000000000000000000000
5000000000000000000000000000000000000000000000000000000000000000000000000000000000000000000000000000000000
10000000000000000000000000000000000000000000000000000000000000000000000000000000000000000000000000000000000
20000000000000000000000000000000000000000000000000000000000000000000000000000000000000000000000000000000000
30000000000000000000000000000000000000000000000000000000000000000000000000000000000000000000000000000000000
40000000000000000000000000000000000000000000000000000000000000000000000000000000000000000000000000000000000
50000000000000000000000000000000000000000000000000000000000000000000000000000000000000000000000000000000000
100000000000000000000000000000000000000000000000000000000000000000000000000000000000000000000000000000000000
200000000000000000000000000000000000000000000000000000000000000000000000000000000000000000000000000000000000
300000000000000000000000000000000000000000000000000000000000000000000000000000000000000000000000000000000000
400000000000000000000000000000000000000000000000000000000000000000000000000000000000000000000000000000000000
500000000000000000000000000000000000000000000000000000000000000000000000000000000000000000000000000000000000
1000000000000000000000000000000000000000000000000000000000000000000000000000000000000000000000000000000000000
2000000000000000000000000000000000000000000000000000000000000000000000000000000000000000000000000000000000000
3000000000000000000000000000000000000000000000000000000000000000000000000000000000000000000000000000000000000
4000000000000000000000000000000000000000000000000000000000000000000000000000000000000000000000000000000000000
5000000000000000000000000000000000000000000000000000000000000000000000000000000000000000000000000000000000000
10000000000000000000000000000000000000000000000000000000000000000000000000000000000000000000000000000000000000
20000000000000000000000000000000000000000000000000000000000000000000000000000000000000000000000000000000000000
30000000000000000000000000000000000000000000000000000000000000000000000000000000000000000000000000000000000000
40000000000000000000000000000000000000000000000000000000000000000000000000000000000000000000000000000000000000
50000000000000000000000000000000000000000000000000000000000000000000000000000000000000000000000000000000000000
100000000000000000000000000000000000000000000000000000000000000000000000000000000000000000000000000000000000000
200000000000000000000000000000000000000000000000000000000000000000000000000000000000000000000000000000000000000
300000000000000000000000000000000000000000000000000000000000000000000000000000000000000000000000000000000000000
400000000000000000000000000000000000000000000000000000000000000000000000000000000000000000000000000000000000000
500000000000000000000000000000000000000000000000000000000000000000000000000000000000000000000000000000000000000
1000000000000000000000000000000000000000000000000000000000000000000000000000000000000000000000000000000000000000
2000000000000000000000000000000000000000000000000000000000000000000000000000000000000000000000000000000000000000
3000000000000000000000000000000000000000000000000000000000000000000000000000000000000000000000000000000000000000
4000000000000000000000000000000000000000000000000000000000000000000000000000000000000000000000000000000000000000
5000000000000000000000000000000000000000000000000000000000000000000000000000000000000000000000000000000000000000
10000000000000000000000000000000000000000000000000000000000000000000000000000000000000000000000000000000000000000
20000000000000000000000000000000000000000000000000000000000000000000000000000000000000000000000000000000000000000
30000000000000000000000000000000000000000000000000000000000000000000000000000000000000000000000000000000000000000
40000000000000000000000000000000000000000000000000000000000000000000000000000000000000000000000000000000000000000
50000000000000000000000000000000000000000000000000000000000000000000000000000000000000000000000000000000000000000
100000000000000000000000000000000000000000000000000000000000000000000000000000000000000000000000000000000000000000
200000000000000000000000000000000000000000000000000000000000000000000000000000000000000000000000000000000000000000
300000000000000000000000000000000000000000000000000000000000000000000000000000000000000000000000000000000000000000
400000000000000000000000000000000000000000000000000000000000000000000000000000000000000000000000000000000000000000
500000000000000000000000000000000000000000000000000000000000000000000000000000000000000000000000000000000000000000
1000000000000000000000000000000000000000000000000000000000000000000000000000000000000000000000000000000000000000000
2000000000000000000000000000000000000000000000000000000000000000000000000000000000000000000000000000000000000000000
3000000000000000000000000000000000000000000000000000000000000000000000000000000000000000000000000000000000000000000
4000000000000000000000000000000000000000000000000000000000000000000000000000000000000000000000000000000000000000000
5000000000000000000000000000000000000000000000000000000000000000000000000000000000000000000000000000000000000000000
10000000000000000000000000000000000000000000000000000000000000000000000000000000000000000000000000000000000000000000
20000000000000000000000000000000000000000000000000000000000000000000000000000000000000000000000000000000000000000000
30000000000000000000000000000000000000000000000000000000000000000000000000000000000000000000000000000000000000000000
40000000000000000000000000000000000000000000000000000000000000000000000000000000000000000000000000000000000000000000
50000000000000000000000000000000000000000000000000000000000000000000000000000000000000000000000000000000000000000000
100000000000000000000000000000000000000000000000000000000000000000000000000000000000000000000000000000000000000000000
200000000000000000000000000000000000000000000000000000000000000000000000000000000000000000000000000000000000000000000
300000000000000000000000000000000000000000000000000000000000000000000000000000000000000000000000000000000000000000000
400000000000000000000000000000000000000000000000000000000000000000000000000000000000000000000000000000000000000000000
500000000000000000000000000000000000000000000000000000000000000000000000000000000000000000000000000000000000000000000
1000000000000000000000000000000000000000000000000000000000000000000000000000000000000000000000000000000000000000000000
2000000000000000000000000000000000000000000000000000000000000000000000000000000000000000000000000000000000000000000000
3000000000000000000000000000000000000000000000000000000000000000000000000000000000000000000000000000000000000000000000
4000000000000000000000000000000000000000000000000000000000000000000000000000000000000000000000000000000000000000000000
5000000000000000000000000000000000000000000000000000000000000000000000000000000000000000000000000000000000000000000000
10000000000000000000000000000000000000000000000000000000000000000000000000000000000000000000000000000000000000000000000
20000000000000000000000000000000000000000000000000000000000000000000000000000000000000000000000000000000000000000000000
30000000000000000000000000000000000000000000000000000000000000000000000000000000000000000000000000000000000000000000000
40000000000000000000000000000000000000000000000000000000000000000000000000000000000000000000000000000000000000000000000
50000000000000000000000000000000000000000000000000000000000000000000000000000000000000000000000000000000000000000000000
100000000000000000000000000000000000000000000000000000000000000000000000000000000000000000000000000000000000000000000000
200000000000000000000000000000000000000000000000000000000000000000000000000000000000000000000000000000000000000000000000
300000000000000000000000000000000000000000000000000000000000000000000000000000000000000000000000000000000000000000000000
400000000000000000000000000000000000000000000000000000000000000000000000000000000000000000000000000000000000000000000000
500000000000000000000000000000000000000000000000000000000000000000000000000000000000000000000000000000000000000000000000
1000000000000000000000000000000000000000000000000000000000000000000000000000000000000000000000000000000000000000000000000
2000000000000000000000000000000000000000000000000000000000000000000000000000000000000000000000000000000000000000000000000
3000000000000000000000000000000000000000000000000000000000000000000000000000000000000000000000000000000000000000000000000
4000000000000000000000000000000000000000000000000000000000000000000000000000000000000000000000000000000000000000000000000
5000000000000000000000000000000000000000000000000000000000000000000000000000000000000000000000000000000000000000000000000
10000000000000000000000000000000000000000000000000000000000000000000000000000000000000000000000000000000000000000000000000
20000000000000000000000000000000000000000000000000000000000000000000000000000000000000000000000000000000000000000000000000
30000000000000000000000000000000000000000000000000000000000000000000000000000000000000000000000000000000000000000000000000
40000000000000000000000000000000000000000000000000000000000000000000000000000000000000000000000000000000000000000000000000
50000000000000000000000000000000000000000000000000000000000000000000000000000000000000000000000000000000000000000000000000
100000000000000000000000000000000000000000000000000000000000000000000000000000000000000000000000000000000000000000000000000
200000000000000000000000000000000000000000000000000000000000000000000000000000000000000000000000000000000000000000000000000
300000000000000000000000000000000000000000000000000000000000000000000000000000000000000000000000000000000000000000000000000
400000000000000000000000000000000000000000000000000000000000000000000000000000000000000000000000000000000000000000000000000
500000000000000000000000000000000000000000000000000000000000000000000000000000000000000000000000000000000000000000000000000
1000000000000000000000000000000000000000000000000000000000000000000000000000000000000000000000000000000000000000000000000000
2000000000000000000000000000000000000000000000000000000000000000000000000000000000000000000000000000000000000000000000000000
3000000000000000000000000000000000000000000000000000000000000000000000000000000000000000000000000000000000000000000000000000
4000000000000000000000000000000000000000000000000000000000000000000000000000000000000000000000000000000000000000000000000000
5000000000000000000000000000000000000000000000000000000000000000000000000000000000000000000000000000000000000000000000000000
10000000000000000000000000000000000000000000000000000000000000000000000000000000000000000000000000000000000000000000000000000
20000000000000000000000000000000000000000000000000000000000000000000000000000000000000000000000000000000000000000000000000000
30000000000000000000000000000000000000000000000000000000000000000000000000000000000000000000000000000000000000000000000000000
40000000000000000000000000000000000000000000000000000000000000000000000000000000000000000000000000000000000000000000000000000
50000000000000000000000000000000000000000000000000000000000000000000000000000000000000000000000000000000000000000000000000000
100000000000000000000000000000000000000000000000000000000000000000000000000000000000000000000000000000000000000000000000000000
200000000000000000000000000000000000000000000000000000000000000000000000000000000000000000000000000000000000000000000000000000
300000000000000000000000000000000000000000000000000000000000000000000000000000000000000000000000000000000000000000000000000000
400000000000000000000000000000000000000000000000000000000000000000000000000000000000000000000000000000000000000000000000000000
500000000000000000000000000000000000000000000000000000000000000000000000000000000000000000000000000000000000000000000000000000
1000000000000000000000000000000000000000000000000000000000000000000000000000000000000000000000000000000000000000000000000000000
2000000000000000000000000000000000000000000000000000000000000000000000000000000000000000000000000000000000000000000000000000000
3000000000000000000000000000000000000000000000000000000000000000000000000000000000000000000000000000000000000000000000000000000
4000000000000000000000000000000000000000000000000000000000000000000000000000000000000000000000000000000000000000000000000000000
5000000000000000000000000000000000000000000000000000000000000000000000000000000000000000000000000000000000000000000000000000000
10000000000000000000000000000000000000000000000000000000000000000000000000000000000000000000000000000000000000000000000000000000
20000000000000000000000000000000000000000000000000000000000000000000000000000000000000000000000000000000000000000000000000000000
30000000000000000000000000000000000000000000000000000000000000000000000000000000000000000000000000000000000000000000000000000000
40000000000000000000000000000000000000000000000000000000000000000000000000000000000000000000000000000000000000000000000000000000
50000000000000000000000000000000000000000000000000000000000000000000000000000000000000000000000000000000000000000000000000000000
100000000000000000000000000000000000000000000000000000000000000000000000000000000000000000000000000000000000000000000000000000000
200000000000000000000000000000000000000000000000000000000000000000000000000000000000000000000000000000000000000000000000000000000
300000000000000000000000000000000000000000000000000000000000000000000000000000000000000000000000000000000000000000000000000000000
400000000000000000000000000000000000000000000000000000000000000000000000000000000000000000000000000000000000000000000000000000000
500000000000000000000000000000000000000000000000000000000000000000000000000000000000000000000000000000000000000000000000000000000
1000000000000000000000000000000000000000000000000000000000000000000000000000000000000000000000000000000000000000000000000000000000
2000000000000000000000000000000000000000000000000000000000000000000000000000000000000000000000000000000000000000000000000000000000
3000000000000000000000000000000000000000000000000000000000000000000000000000000000000000000000000000000000000000000000000000000000
4000000000000000000000000000000000000000000000000000000000000000000000000000000000000000000000000000000000000000000000000000000000
5000000000000000000000000000000000000000000000000000000000000000000000000000000000000000000000000000000000000000000000000000000000
10000000000000000000000000000000000000000000000000000000000000000000000000000000000000000000000000000000000000000000000000000000000
20000000000000000000000000000000000000000000000000000000000000000000000000000000000000000000000000000000000000000000000000000000000
30000000000000000000000000000000000000000000000000000000000000000000000000000000000000000000000000000000000000000000000000000000000
40000000000000000000000000000000000000000000000000000000000000000000000000000000000000000000000000000000000000000000000000000000000
50000000000000000000000000000000000000000000000000000000000000000000000000000000000000000000000000000000000000000000000000000000000
100000000000000000000000000000000000000000000000000000000000000000000000000000000000000000000000000000000000000000000000000000000000
200000000000000000000000000000000000000000000000000000000000000000000000000000000000000000000000000000000000000000000000000000000000
300000000000000000000000000000000000000000000000000000000000000000000000000000000000000000000000000000000000000000000000000000000000
400000000000000000000000000000000000000000000000000000000000000000000000000000000000000000000000000000000000000000000000000000000000
500000000000000000000000000000000000000000000000000000000000000000000000000000000000000000000000000000000000000000000000000000000000
1000000000000000000000000000000000000000000000000000000000000000000000000000000000000000000000000000000000000000000000000000000000000
2000000000000000000000000000000000000000000000000000000000000000000000000000000000000000000000000000000000000000000000000000000000000
3000000000000000000000000000000000000000000000000000000000000000000000000000000000000000000000000000000000000000000000000000000000000
4000000000000000000000000000000000000000000000000000000000000000000000000000000

rather small fractions of the probable values of these pressures. Since the humidity with which we are most concerned is 0.02 mg per liter, and this is usually obtained with scale readings of about 500 psig on both the saturation and test gas pressure scales, the altitude correction was computed for the values 0, 500, and 500 psig of the three significant pressures and marked on the computer. When making a test of oxygen by the usual routine at the altitude of Denver, the saturation gage pressure is set opposite the temperature of saturation and the zero of the comparison pressure scale is set opposite the test gas gage pressure, as usual, but the water content of the gas discharged from the cylinder is read opposite 5.3 thousand feet, the altitude of the city. A setting that would result for a gas that just meets the specification is shown by figure 23. If the correction for altitude were not applied, the determination would be in error by about 0.0035 mg per liter.

(c) Computing Relative Humidities

As the scale marked water vapor is an ordinary logarithmic scale, its use is no more confined to that one quantity than is the scale of an ordinary slide rule. In computing relative humidities, it is convenient to use it to represent ratios. In combination with the comparison pressure scale it is possible to work a large variety of problems involving ratios and gage pressures just as a slide rule would be used. One edge of the handle of the upper disk can be used as a marker in place of the glass slide of the conventional rule.

Three examples will be given:

1. Room air at atmospheric pressure is matched with air from the saturator, which is at room temperature, by adjusting the comparison pressure at which it flows over the detector in the cell. If the pressure in the saturator is 300 psig and the comparison pressure at which matching occurs is 100 psig, what is the relative humidity in the room?

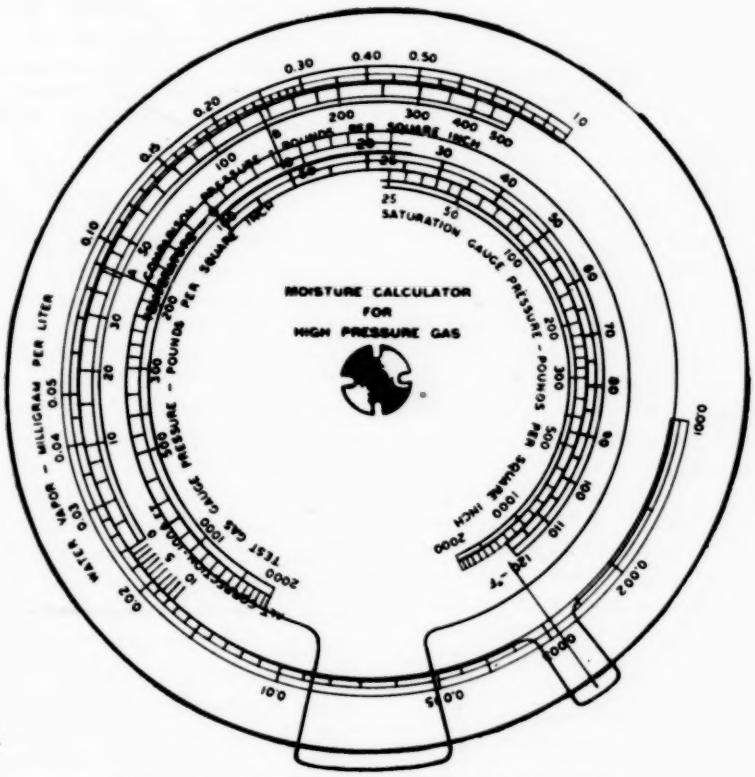
MOISTURE CALCULATOR
FOR
HIGH PRESSURE GAS
SATURATION GAUGE PRESSURE - POUNDS PER SQUARE INCH
TEST GAS GAUGE PRESSURE - POUNDS PER SQUARE INCH
WATER VAPOR - MILLIGRAM PER LITER

FIGURE 23.—*Plastic computer set for altitude of Denver.*

Solution: Set *300* of the comparison pressure scale under *1.0* of the water vapor scale. Opposite *100* of the comparison pressure scale, read *37.5* percent, the relative humidity measured.

2. A cylinder containing 300 psig of oxygen is compared with gas delivered at a comparison pressure of 35 psig from a saturator in which the pressure is 400 psig. Matching occurs at a test gas pressure of 25 psig; cylinder and saturator are at the same temperatures. It there liquid water in the oxygen cylinder?

Solution: Set *400* of the comparison pressure scale opposite *1.0* of the water vapor scale. Mark the position of 35 on the comparison pressure scale. (It indicates a relative humidity of about 12.5 percent in the cell when the comparison was made.) Bring *25* under the mark. Then *300* on the comparison pressure scale is found opposite *0.97*. This is too close to 1.0 (which would definitely indicate the presence of liquid) to be considered safe, and the cylinder should be baked out before it is refilled.

3. It should be apparent that all the scales of the computer can be used in adding and subtracting the logarithms of the numbers represented. The last problem will be a long one to illustrate the use of several scales.

Problem: A test chamber is maintained at 32° F and atmospheric pressure. Air drawn from it (and warmed in the process) is compared at atmospheric pressure with gas from a saturator at 75° F. The pressure in the saturator is 1,000 psig, and the comparison pressure at which matching occurs is 70 psig. What is the relative humidity in the test-chamber? If it is cooled further, at what temperature will the dew point be reached?

Solution: Since the comparison pressure scale ends at 400 psig, it must be supplemented with one of the other scales, most conveniently that for saturation pressure. To do this, the upper end of the comparison pressure scale is used as a marker, and *1,000* of the saturation pressure scale is brought under *1.0* of the water vapor scale. The end (400) of the comparison pressure scale is now set opposite the *400* of the saturation pressure scale and is now in the position it would be in had it been extended and its *1.000* mark made to coincide with 1.0 of the water vapor scale (fig. 24, a). The position of the actual comparison-pressure, 70 psig, is now marked with the handle of the upper disk. It is found to be at about 0.097. As gas from the test chamber matches that from the saturator at the test pressure, it would have a relative humidity of 9.7 percent if heated to 75° F (fig. 24, b). The end of the comparison pressure scale is now placed on this point as a marker, and the upper disk is rotated to bring the edge of its handle over 32° F of the temperature scale (fig. 24, c). The two disks are now rotated together until the handle-marker reaches 75° F. We have thereby rotated the other marker through the angle between the marks corresponding to these two temperatures and have thereby multiplied a relative humidity of 9.7 percent by the ratio between the vapor pressure of water at 75° F and that at 32° F. The result, read at the end of the comparison pressure scale, is 44 percent, the relative humidity in the test chamber (fig. 24, d). We now rotate the upper disk to bring its handle to *1.0* of the percentage scale (fig. 24, e). The angle between this marker and the other (the end of the comparison pressure scale) now represents the ratio of saturation pressures at the ends of the range of temperature through which the test chamber must be reduced to cause moisture to precipitate. Hence if we again rotate the two disks together until one marker is at 32° F, the other indicates the dew-point in the test chamber, 13° F (fig. 24, f).

(d) Measurement of Water in Carbon Dioxide

A somewhat hasty search failed to disclose published data regarding the density of water vapor in equilibrium with water in more than a very few gases, and the data that exist are not very concordant. So far as they go, they are consistent with the view that the increased density is the result of van der Waal forces and that the effect can be expected to increase with the van der Waal constant a. We then expect the value of k in eq 5 to be very small for hydrogen and helium, not far from that of air for methane, and considerably higher for the more readily condensable gases. An approximation can be made in any case of interest by comparing the gas at pressures as different as practicable with the same standard and introducing a value of k that will give the same result in the two comparisons. With the exception of nitrogen, oxygen, and air, the only gas for which we have done this carefully is carbon dioxide.

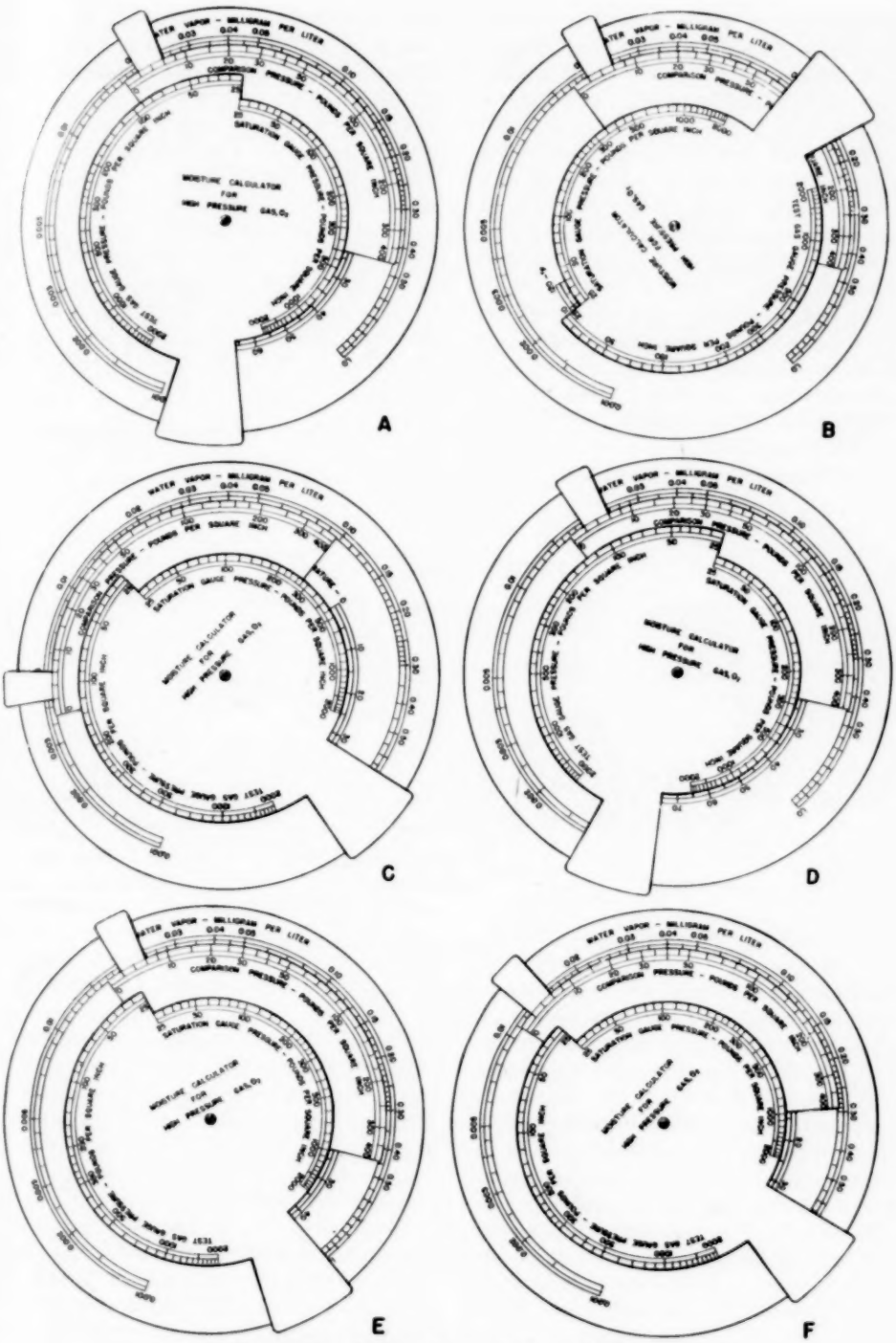

FIGURE 24.—*Settings of computer for problem 3.*

The measurement of water in carbon dioxide is second in importance only to its measurement in aviator's oxygen and for the same reason. The liquefied gas is widely used in emergencies for fire fighting, for the operation of mechanical equipment in aircraft, and for the inflation of life rafts. The discharge of carbon dioxide is accompanied by a strong refrigerating action, and freeze-ups are of frequent occurrence and of possibly disastrous consequences in all the applications mentioned.

In testing carbon dioxide with the electrical indicator it was soon found that the cooling effect of expansion through the valves of the oxygen-testing apparatus was too great to permit satisfactory operation. Accordingly an auxiliary heater was constructed, which is shown in section in figure 25. The sample for testing can be drawn

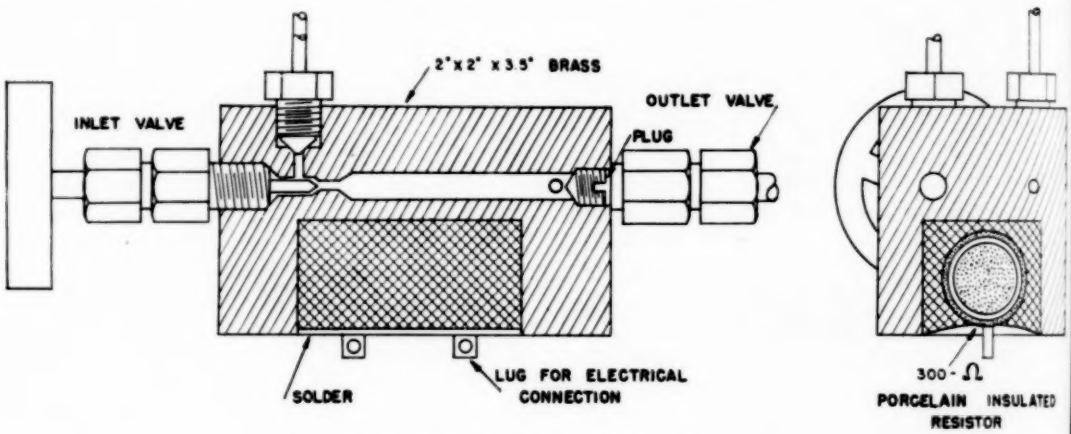

FIGURE 25.—*Vaporizer used for carbon dioxide.*

either as gas from the top of the cylinder or as liquid from the bottom. (The two methods of sampling should not and do not give the same results except at or above the critical temperature of carbon dioxide, 88° F). In the heater, the first needle valve is nearly closed, and complete vaporization of the liquid carbon dioxide is expected to take place there if it has not already taken place. The rate of flow is principally regulated by this valve. The vapor is warmed enough in the passages of the block to prevent it from reliquefying at the second valve, which serves chiefly to smooth out fluctuations of flow caused by irregular evaporation of the liquid at the first valve. The first valve (C) of the regular water-measuring apparatus serves as an auxiliary in smoothing the flow. Only a moderate change of pressure can take place here without cooling the detector enough to affect the reading.

The effect on water-vapor pressure of the deviation of carbon dioxide from an ideal gas is much greater than that of oxygen. The data of Wiebe and Gaddy [4] give the compositions of the phase rich in carbon dioxide for the system water–carbon dioxide. From the method of sampling, it is evident that the measurements at 25° C and 31.04° C, and at 1, 25, and 50 atmospheres were of the vapor phase in equilibrium with liquid water. The data reported may be represented for 25° C by the equation

$$W=S(1+0.0089P+0.000324P^2), \quad (6)$$

and for 31.04° C by

$$W=S(1+0.0136P+0.000144P^2), \quad (7)$$

in which P is the pressure in atmospheres; W is the reported quantity of water vapor in unit volume of expanded gas; S is the quantity per unit volume that would have been found in the *expanded* gas had (1) the quantity per unit volume in the *compressed* gas been the same as that in equilibrium with liquid water in an otherwise evacuated space, and had (2) the compressed gas expanded in exact accordance with Boyle's law. The quantities in parentheses in these equations will be referred to as the correction factors for carbon dioxide. If pressures are expressed in the usual gage readings, the factors are

For 25° C (77° F)	$1+0.000605P+0.00000150P^2$.
For 31.04° C (87.9° F)	$1+0.000925P+0.00000067P^2$.

It is probable that the correction factor to be applied to carbon dioxide containing the fairly small percentage of water vapor represented by saturation at 25° or 30° C will apply satisfactorily to still smaller percentages.

When we compare carbon dioxide with air containing a known quantity of water and make the calculations with the computer for use with oxygen, we automatically apply a correction for the pressure of carbon dioxide as though it were air. If we divide the total corrections to be made according to eq 6 and 7 by the correction introduced by the computer, we find the corrections to be applied to the results obtained with the aid of the computer. These corrections, for the two temperatures are as follows:

For 25° C:

$$W=W_1(1+0.0067P+0.000305P^2). \quad (8)$$

For 31.04° C:

$$W=W_1(1+0.0114P+0.000114P^2). \quad (9)$$

W_1 is the concentration of water found by using the computer only.

The accuracy of the data from which these equations were derived and the accuracy of the tests themselves probably do not justify the somewhat laborious application of these equations in routine work nor even the use of different correction factors for different temperatures within the ordinary range of temperature in the laboratory. Hence, the simpler correction factor

$$\frac{1}{1-0.0007P_x}$$

was selected empirically to be applied to results computed with the oxygen calculator. If this factor is used, the entire correction, including that inherent in the calculator is

$$\frac{1}{(1-0.0007P_x)(1-0.00015P_x)}.$$

In figure 26 are plotted this correction factor, curve C, and the correction factors from eq 6 and 7, curves A and B. It is evident that if eq 6 and 7 are correct and if measurements are made at any

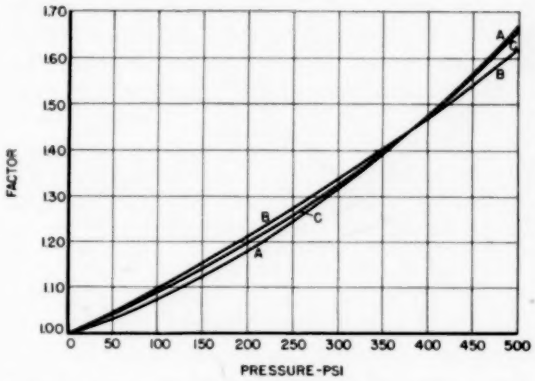

FIGURE 26.—*Correction factors for water vapor in carbon dioxide.*

Curve	Correction factor
A	$1+0.000605\ P+0.0000015\ P^2$
B	$1+0.000925\ P+0.00000067\ P^2$
C	$\frac{1}{(1-0.00015\ P)\ (1-0.00070\ P)}$

temperature between 25° and 31° C and at pressures of carbon dioxide less than 450 psi, no error greater than about 1 to 5 percent of the water present can result from using the computer and multiplying the results by

$$\frac{1}{1-0.0007P_x}.$$

Measurements were made of the water vapor in gas from a commercial cylinder of carbon dioxide, for the purpose of determining the applicability of this correction formula, by comparing it with a cylinder of compressed air in which the water vapor had been measured (0.183 mg per liter). First the water vapor was determined by a comparison made with the carbon dioxide at atmospheric pressure. The average of two determinations was 0.840 mg per liter. A curve was then plotted (fig. 27) showing the relation between pressures of air and carbon dioxide that would give this value if the results to be obtained in theory from the oxygen computer were multiplied by the factor

$$\frac{1}{1-0.0007P_x}.$$

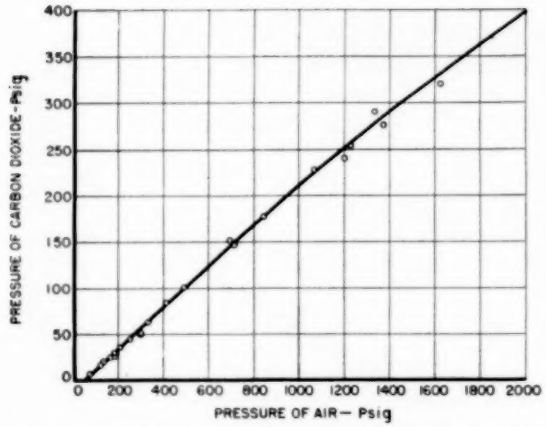

FIGURE 27.—*Effect of pressure of measurement on carbon-dioxide determination.*

Then a series of comparisons of air and carbon dioxide from the two cylinders was made at a temperature of 76° C and at different pressures. The points marked by circles on figure 27 show the results. The curve in this figure was plotted in advance, not drawn to represent the observations. The results of the series of observations are shown in detail in table 5. The last two columns were computed by the use of the correction factor C.

The trend of the results indicates an overcorrection for the carbon dioxide if anything, but they are too scattered to make this certain. The results would not be appreciably improved by using the theoretical correction factor A (represented by curve A of fig. 26) instead of C, which must be considered as satisfactory as anything available until a more accurate study is made.

V. Applications and Results

1. Compressed Gases

The application of the method to the measurement of compressed gases has been sufficiently described. Here will be reported briefly some results obtained. In effect, others have been given already in figures 20 and 27. Figure 28 shows the results of seven electrical and three gravimetric tests of the same cylinder of oxygen. The change of water content of the discharged gas as the pressure in the cylinder decreases is typical of many cylinders that have been tested and is attributed to water adsorbed on the cylinder

TABLE 5.—*Comparison of carbon dioxide and air at different pressures*

(Temperature, 76° F)

Carbon dioxide pressure	Air pressure	Ratio of water in CO_2 to water in air	Water found
psig	*psig*		*mg/liter*
0	50	4.42	0.809
7	74	4.11	.752
17	121	4.31	.789
25.5	165	4.26	.780
20	132.5	4.27	.781
29	181	4.51	.825
35	209	4.74	.867
44	250	4.56	.834
62	330	4.56	.834
100	486	4.48	.820
145	712	4.19	.767
177	826	4.56	.834
239	1,201	4.95	.906
252	1,236	4.88	.893
292	1,534	5.17	.946
321	1,622	5.08	.930
275	1,378	4.99	.913
236	1,071	4.57	.836
151	697	4.45	.814
83	418	4.51	.825
48	302	5.08	.930
36	190	4.09	.748
0	53	4.63	.847
Avg.....	.....	4.59	0.840

walls, mainly in the scale or rust that is always present to some extent. When the water vapor changes with pressure in this way, the large samples needed for a gravimetric test gives the average of a changing composition. A spot sample taken before a gravimetric sample nearly always shows less water, one taken afterward shows more water than the gravimetric test.

During 3 or 4 years, approximately 100 cylinders were tested by both gravimetric and electrical methods. In general the agreement was good, taking into account the changes of pressure during the gravimetric tests. Sometimes they were not good, and a part of the disagreements unquestionably resulted from errors in the electrical method. Sometimes the fault may have been in the gravimetric method, as shown by occasional irregular results of gravimetric tests of the same cylinder. Approximately half a dozen cylinders persistently showed differences between repeated gravimetric and electrical determinations that must have represented some real effect. In each of these

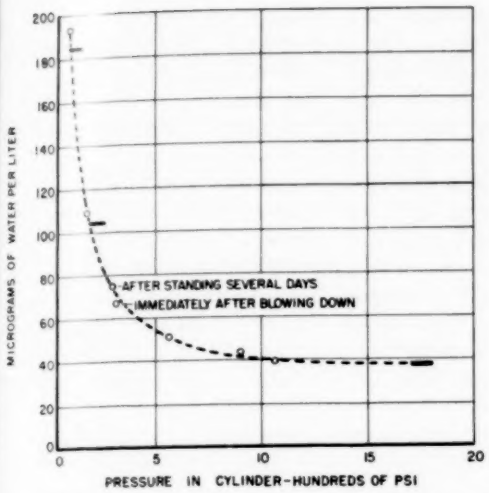

FIGURE 28.—*Water vapor in gas from a cylinder of compressed oxygen determined gravimetrically and electrically.*

———, Gravimetric test; ○, electrical test.

cases the electrical test was low. The best explanation seems to be that something was taken out by the phosphorus pentoxide used in the gravimetric method that affects the conductivity of phosphoric acid little or not at all. The source was probably the lute used to seal the threads of the cylinder valve. Sometimes this is shellac dissolved in alcohol, sometimes it is litharge and glycerin. Both glycerin and alcohol are held by phosphorus pentoxide, at least in part. The discrepancy between the results of different methods of test was never too great to be accounted for by saturation with the vapor of glycerin to say nothing of alcohol.

That the thread-sealing compound could be a troublesome source of vapor was disclosed by experience with the cylinders sent from one company by the Navy Department for checking, which repeatedly showed more than the amount of water permitted by specification, while those from other companies were generally under 20 percent of the limit specified. This seemed the more remarkable because the company having trouble apparently had the best practice in drying cylinders and filled them directly with oxygen from the liquid phase. After inquiry disclosed that cylinder valves were being sealed with a suspension of graphite in water, no cylinder from that company failed to pass the specification readily.

In table 6 are shown the results of measurements of water in four cylinders of oxygen with an electrical apparatus and four frost-point instruments, which it was the purpose of the observations to test. The table shows the agreement obtained between successive electrical tests of the same sample as well as the agreement with frost-point instruments.

TABLE 6.—*Comparative tests of compressed oxygen made with electrical and frost-point instruments*

(Tests made on different days are separated by a space)

Water found with—				
Electrical instrument	Frost-point instruments a number—			
	1	2	3	4
CYLINDER A				
mg/liter	*mg/liter*	*mg/liter*	*mg/liter*	*mg/liter*
.....	0.024	.....	.....	.....
0.022	.022	.....	.....	.....
.022	.020	.....	.....	.....
.020	.021	.....	.....	.....
.022	.022	.....	.....	.....
.022	.017	.....	.....	.....
.023	.024	.....	.....	.....
.020	.020	.....	.....	.....
.....	.018	.....	.....	.....
.....	.018	.....	.....	.....
.021	.024	.....	.....	.....
.021	.022	.....	.....	.....
.....	.021	.....	.....	.....
.022	.021	0.028	.....	.....
.022	.024	.028	.....	.....
.....	.016	.028	.....	.....
.....	.016	.028	.....	.....
.....	.016	.027	.....	.....
.....	.017	.025	.....	.....
.....	.016	.025	.....	.....
.....	.018	.025	.....	.....
.....	.024	.025	.....	.....
.....	.016	.025	.....	.....
.....	.018	.028	.....	.....
.....	.016	.028	.....	.....
.....	.018	.027	.....	.....
.....	.019	.026	.....	.....
.....	.017	.026	.....	.....
.....	.018	.027	.....	.....
.....	.018	.027	.....	.....
.....	.019	.025	.....	.....
.....	.....	025	.....	.....
.020	.023	.019	0.022	.....
.021	.019	.018	.022	.....
.022	.019	.018	.020	.....
.....	.019	.....	.021	.....
.....	.019	.....	.....	.....
.....	.019	.....	.....	.....
.022	.....	.....	.....	0.028
.....	.....	.....	.....	.023
.....	.....	.....	.....	.019
.....	.....	.....	.....	.025

TABLE 6.—*Comparative tests of compressed oxygen made with electrical and frost-point instruments*—Continued

Water found with—				
Electrical instrument	Frost-point instruments [a] number—			
	1	2	3	4
CYLINDER B				
0.045	0.046	0.065	0.051	.....
.048	.045	.063	.050	.....
.048	.045	.060	.048	.....
.049	.045	.061	.047	.....
.....	.047	.061	.046	.....
.....	.....	.061	.046	.....
.....	.....	.061	.046	.....
.....	.....	.055	.....	.....
.....	.....	.054	.....	.....
.....	.....	.054	.....	.....
CYLINDER C				
0.060	0.060	0.077	.....	.....
.....	.060	.078	.....	.....
.....	.060	.078	.....	.....
.060	.070	.085	.....	.....
.....	.065	.080	.....	.....
.....	.064	.082	.....	.....
.....	.....	.082	.....	.....
.....	.....	.080	.....	.....
CYLINDER D				
0.097	0.094	0.095	.....	.....
.100	.092	.094	.....	.....
.100	.090	.090	.....	.....
.....	.091	.089	.....	.....
.....	.091	.092	.....	.....
.....	.091	.092	.....	.....
.....	.....	.092	.....	.....

[a] In a frost-point apparatus, observations are always made with falling temperatures. If thermal distribution and measurement were always perfect, the results should be a little low because of the lag between the formation of the first frost and its observation.

2. Freon

The electrical method was used in a study of the distribution of water in a refrigerating system using Freon 12 (dichlorodifluoromethane) and of the action of driers within the system. The Freon used showed, in the original cylinder, a water content of about 0.008 mg per liter, much too low for direct comparison with gas from a saturator. Two cylinders of gas containing about 0.05 mg and 0.003 mg per liter were used as secondary standards.

The first question that arose was naturally the deviation from ideality of the water vapor in Freon. The moisture content and the pressure of the original material were much too low to determine this; but the use of the computer for water in oxygen gave results that were the same within the limit of error at all pressures. Later the same thing was found to be true in samples of high water content drawn from the refrigerating system at a time when the composition was changing very little if at all. It is not to be supposed that the deviation is the same for Freon as for oxygen, but for the comparatively low pressures possible without condensing Freon at ordinary temperatures the oxygen computer can be used with very little error.

In testing Freon, either gas or liquid was sampled at will (they did not have the same concentration of water, of course). In both cases it was necessary to make the expansion through a heated valve. The apparatus shown in figure 25 was used as for carbon dioxide.

The only difficulty encountered in the measurements was from the compressor oil, which is in solution in the Freon and came over as a fog that deposited on the detector, screening it from the gas and eventually washing off the phosphoric acid. Even this oil interfered with the tests much less than might have been expected. Apparently the first oil does not affect greatly the action of the detector.

No determination of water in the Freon was made by an independent method, hence there is nothing with which to compare the electrical measurements. However, the amount of water dissolved in the Freon when the expansion valve froze was always in rough agreement with the published solubility of ice in Freon at the temperature of the experiment.

Figure 29 shows two sets of measurements of water in the liquid freon in the pipe between the liquid receiver and the silica-gel dryer following the introduction of small quantities of water into the receiver. The regularity of the curves indicates that changes of one part by weight of water per million of Freon are readily followed at intervals of 1 minute or less. The step-like breaks in the descending portions of the curve were sufficiently reproducible in numerous tests to establish their reality, and they were satisfactorily explained by considering the mechanical system involved.

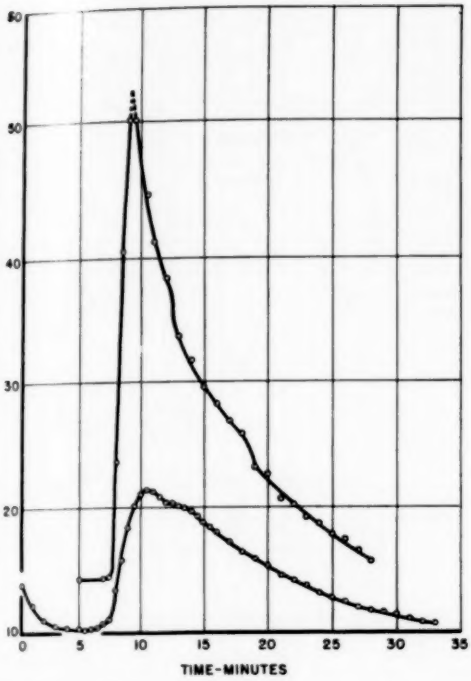

FIGURE 29.—*Typical series of measurements of water in Freon.*

3. Measurement of Relative Humidity

A detector in the air follows monetary changes of relative humidity with great rapidity. Ordinarily there are large and constantly changing local differences in the air of a laboratory. For one thing, we respire roughly once a second and deliver 100 to 200 ml of air saturated with moisture at 98° F, which becomes distributed at the rate and in the manner easily seen by watching a puff of tobacco smoke. Perspiration is an equally important source of moisture, distributed irregularly by our movements. The galvanometer needle indicates these changes by shifting like a flag in a breeze. Because of this irregular movement, it is usually a little hard to determine what galvanometer reading represents the average humidity of the room. Once this is decided, the detector is screwed into the cell, and gas from the saturator used to reproduce the previous galvanometer reading. Relative humidity is then computed as already described.

The sources of error in relative humidity determinations are almost exclusively those involved in uncertainty regarding the moisture content of gas from the saturator, which have already been discussed. An uncertainty of 1° C in the temperature of saturation amounts to an uncertainty of about 5 percent in relative humidity in the upper ranges.

Relative humidities taken approximately daily in the laboratory during 1 month gave the following average results in comparison with wet-and-dry bulb thermometers in the stream from an electric fan:

Number of tests	Saturator pressure	Relative humidity	
		Electrical	Wet-and-dry bulb
	psig		
5	460	31. 8	32. 1
21	230	31. 6	31. 4

Individual results were somewhat scattered but not more so than could be reasonably explained by uncertainties in the uncontrolled temperature of the saturator.

There is little doubt that with careful control of the conditions of measurement the method will give excellent results for relative humidity. However, the instrument is more elaborate than the psychrometers commonly employed, and would not give better results with the same attention.

The electrical method is not recommended for ordinary psychrometry for these reasons, but it does have advantages of speed of response, of range of humidity measurable, and from the fact that it can be located in and will measure the humidity of small spaces with relatively little effect on that humidity and without the necessity of blowing the air over it. It is much easier to arrange for its use in places that are accessible with difficulty than either dew-point or wet-and-dry bulb instruments. It has already found some applications in which these characteristics are important and should find others.

Figure 30 shows an arrangement that has been used at this Bureau for measuring water in small closed containers without disturbing their atmospheres. The detector is screwed into a flat disk, which forms one-half of a rotating slide valve. The other half is another disk through which a hole leads to the container. By rotating the upper disk, the detector is brought to the opening

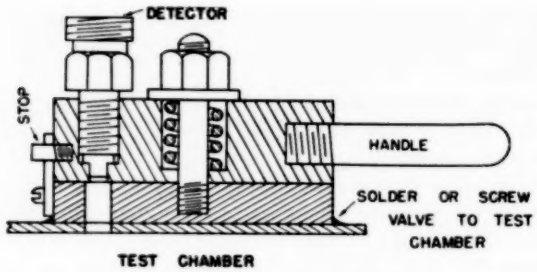

FIGURE 30.—*"Valve" used to connect detector to a test-chamber.*

of the container, where it can reach equilibrium with the confined atmosphere; or it can be turned away and the container left sealed. The detector is then unscrewed from its plate, inserted into the cell of a regular instrument, and the reading it had when in communication with the test chamber is matched in the usual way. One merit of this arrangement is that with the duplication of only the flat valve, a single detector and measuring apparatus can be used with a number of containers.

A somewhat more elaborate apparatus was designed for another Government Department and was built and used by it with reported satisfaction. It is shown in figure 31; it differs from the previously described arrangement only in the presence of channels in the base plate of the slide valve through which a standard gas can be brought to the detector when the valve has been rotated to the position for comparison. In other words, the comparison cell is built into the valve head. If a very wide range of humidities is expected in the test chamber, an auxiliary screw to tighten the detector support over the comparison cell is supplied as shown. A channel around the port for the standard gas leading to the outside prevents the possibility that high pressure under a large area will unseat the valve plate and contaminate the test chamber.

4. Estimating Moisture in Powdered Solids

By passing dry air at a steady rate through a powdered solid and thence through the measuring cell and recording at short intervals of time the electrical resistance of the detector, the amount of water removed from the solid can be estimated. Of course, any desired temperatures may be applied so long as the water driven off does not

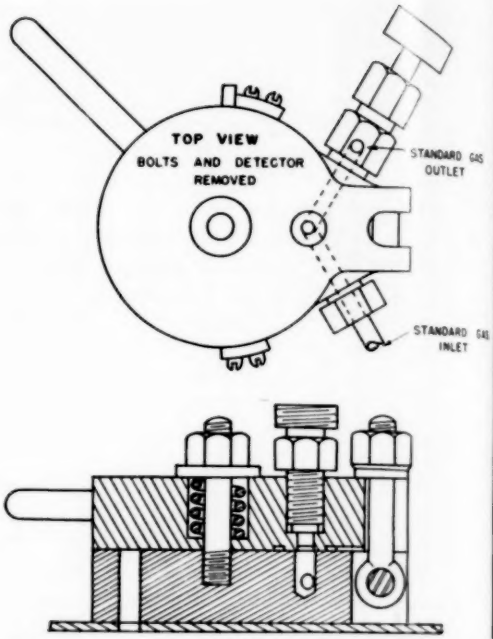

FIGURE 31.—*"Valve" used to connect detector alternately to test chamber and to built-in "cell" for calibration.*

condense on the way to the cell. The advantages of the procedure are those of the method in general, use of small samples, speed, sensitivity to very small quantities of water, independence of many (not all) other volatile substances that would be involved in a measurement of loss of weight, and ability to follow the course of the drying operation. The principal application made of this procedure has been in determining the relative dryness of samples of silica gel of a particle size corresponding to about a 30-mesh sieve. The apparatus used in shown in figure 32. The sample to be tested, usually about 1 g, was placed in the thin-walled tube in an atmosphere of steam above vigorously boiling water and several minutes were allowed for the solid to reach steam temperature. Then a brisk flow of dry air was started through the solid, and the resistance of the detector observed. The moist air in the connections always caused a momentary sharp drop of resistance of the detector, but a steady resistance was quickly attained and remained almost constant for several minutes, then quickly broke to nearly the resistance corresponding to the moisture content of the incoming gas. Experi-

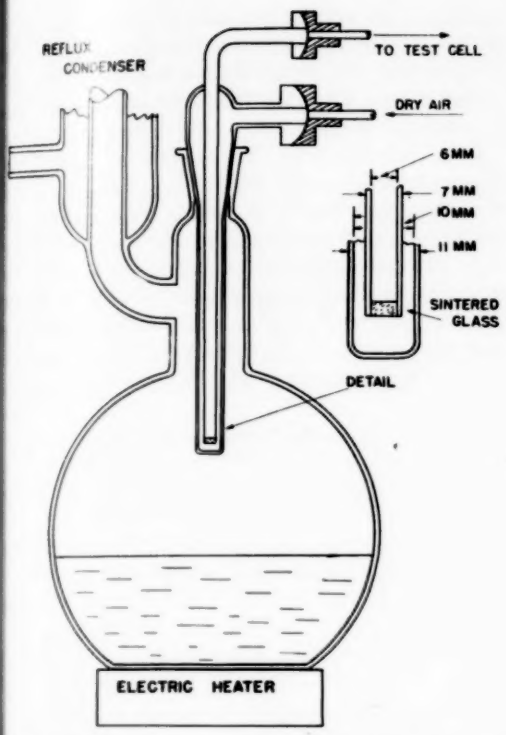

FIGURE 32.—*Arrangement used to test moisture content of powdered solids.*

ment showed that the moisture content of the gas leaving the gel during the period of constancy was nearly independent of the rate of flow, of the amount of solid, and of the moisture content of the entering gas, which could be either higher or lower than that of outflowing gas. In other words, the greater part of the gel had a characteristic water-vapor pressure, and the air entering came to equilibrium with this so rapidly that the system behaved almost as though a plug of air in equilibrium with the sample were pushed along between the initial and final portions of the flow. Different treatments of the gel resulted in products having vapor pressures at 100° C from about 0.1 to 20 mm of Hg. A few comparisons with gravimetric tests made by drying the gel at much higher temperatures showed fairly good correlation. The need for the test was ended before comparisons could be made between determinations of moisture by weighing and by integrating the product of rate of flow and moisture content of the air passed through the material. The work done on this subject therefore demonstrated merely that observations can be made in a few minutes that will show approximately the condition of such a drying material, once the observer has learned to interpret the results.

An alternative method for determining adsorbed or capillary moisture on solids, which should be a better one in many cases, is to shake up the solid with an organic liquid, and to determine the water in the resulting solution by the method described in the second section, V, 6.

5. Testing the Capacity of Drying Agents

On a larger scale, the drying capacity of several reagents at normal atmospheric pressure and at 1,650 psi were measured at various rates of flow by saturating the gas, passing it through about 2 feet of ½-in. iron pipe filled with the dryer, measuring the moisture at the outlet at the pressure of experiment, usually in a small flow through a by-pass, and finally measuring the volume of the whole stream at atmospheric pressure with a gas meter.

Figure 33 shows a typical curve, in this case for silica gel previously dried at 165° F when saturated air is passed into it at about 80° F (27° C) at the rate of 20 times the volume of the desiccant per minute. Under these conditions the desiccant dries the air to about 0.1 mg per liter (a relative humidity of about 0.03 percent) for approximately 1 hour. At the end of this time the weight of the

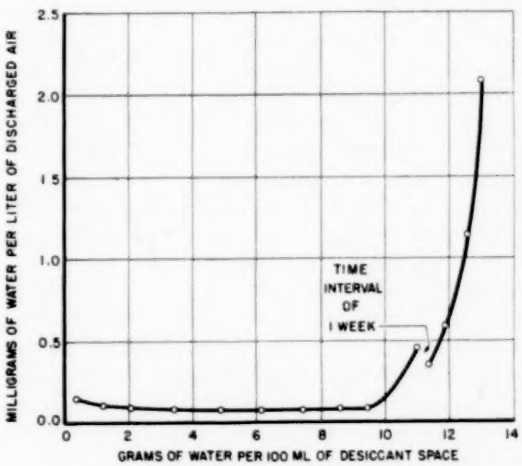

FIGURE 33.—*Adsorption of water by silica-gel.*

adsorbed water is about 10 percent of the weight of liquid water that would fill the space occupied by the desiccant. A point of interest is the interruption of the test after the break-point of the curve had been reached, and its continuance 1 week later. The purpose of this interruption was to see whether the drying power of the nearly exhausted desiccant would be significantly increased by permitting the water adsorbed by the surface layers of the pieces of solid (screen-size, 6 to 16 meshes per inch) to diffuse to the interior of the lumps.

6. Water Content of Organic Liquids

It is certain that at a definite temperature the water content of a liquid of otherwise constant composition will bear a definite relation to the water content of the air with which it will come to equilibrium. If we know from past experience what this relation is and have a means for quickly measuring the moisture content of the air, this can also be used to determine the amount of water in the liquid. With this certainty in view, some experiments were made to find whether it is practicable to determine water in organic liquids by exposing the electrical detector to the atmosphere above them.

The first tests were made by the simple procedure of removing the stopper from a reagent bottle, such as ether, and thrusting the detector on the end of its electrical connections nearly to the surface of the liquid. Irregular results were obtained that were made worse by shaking the bottle before the tests or swirling the liquid with the detector in place. The least possible disturbance of the atmosphere led to the best results. It appears that there is enough interchange of air between the inside and outside of the bottle to affect appreciably the moisture content of the air over the liquid, and it takes a surprisingly long time for saturation to be complete after fresh air has been introduced. This, no doubt, is because the atmospheres above the liquids tested contained enough of their own vapors to make them heavier than the unsaturated air in the top of the bottle, so that diffusion had to be relied on to restore equilibrium. If we try to hasten the result by producing convection, we merely introduce more air from the outside, unless the closure around the electrical leads is tight. It seems quite possible that in some cases the amount of outside air that gets into the bottle may change the amount of water in the surface layer of liquid enough to affect the result noticeably.

The device shown in figure 34 was constructed to minimize some of these difficulties. A spring clip was attached to the detector of such form that a glass tube could be quickly attached to cover the detector. This tube had a small opening in the bottom and made a snug but not airtight fit with the detector plug. When the detector with this attachment is dipped into a bottle of liquid to be tested, the glass cell fills with liquid from well below the surface at a rate that forces air from the cell past the detector under slight positive

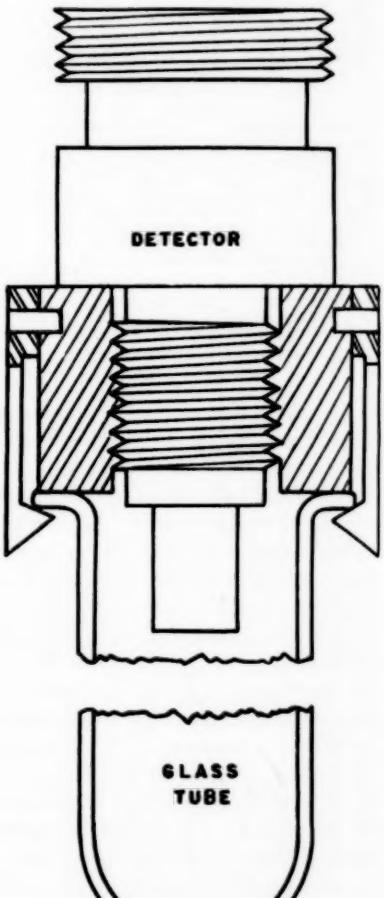

FIGURE 34.—*Arrangement used in testing water vapor in equilibrium with a liquid.*

pressure. The detector is lowered until the detecting surface is only a few millimeters above the liquid surface and left there; or it may be raised once to let the nearly saturated air in the bottle outside the cell sweep it out, then again lowered into place. The resistance of the detector is followed. It changes rapidly at first, but soon reaches practical constancy when the small volume of residual air becomes saturated. Since this volume is almost isolated from the surrounding atmosphere, which is itself fairly near to equilibrium with the liquid, there is very little disturbance by diffusion from the outside. Two or three minutes usually suffices to obtain a steady reading, and successive tests are reproducible.

As many clean, dry glass tubes as will be needed for all the tests to be made in rapid succession should be provided so that one liquid will not be contaminated with another and there will be no interchange of water between the liquid to be tested and any film on the wall of the tube. The method has been tried in a preliminary way with several liquids, including ether, petroleum hydrocarbons, carbon disulfide, carbon tetrachloride, and benzene, the vapors of which are believed not to affect the reading appreciably, and with alochol, the vapor of which does affect the apparent water content markedly. Only ether and alcohol will be discussed.

Figure 35 shows results obtained with ethyl ether, the water content of which had been determined by Stanley Clabaugh by an independent method. To this ether measured quantities of water were added. The data obtained are plotted both on a linear scale to show adequately the upper part of the humidity curve and on a logarithmic scale to show the lower part. The method should be capable of measuring with speed and precision very small amounts of water in such a liquid as ether. It can probably be used to determine the water in things that dissolve in ether, such as fats or cellulose derivatives, by testing their solutions.

Alcohol presents complications. In an atmosphere saturated with the vapor of alcohol, believed from other tests to be practical water-free, the detector had a conductivity equal to that in air of about 11-percent relative humidity. According to recorded data, alcohol in equilibrium with an atmosphere of 11-percent relative humidity should contain about 2 percent of water. Small additions

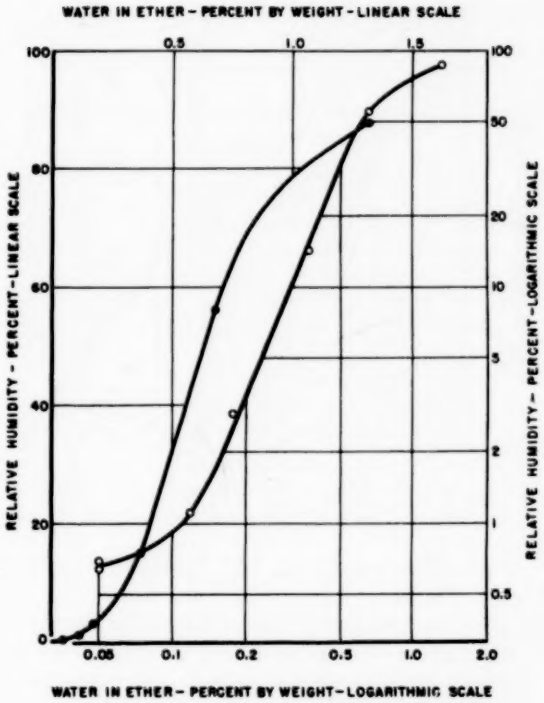

FIGURE 35.—*Relative humidity above ether.*

of water increase the conductivity of the gas above absolute alcohol by very nearly the amount they would be expected to increase that above 98 percent alcohol, if the alcohol vapor itself had no effect. The experiments made were of the sketchiest kind. Results are shown in figure 36, in which are represented the relative humidities of atmospheres in equilibrium with alcohol containing water at 20° and 40° C [5] and the apparent relative humidity of atmospheres above alcohol at 28° C. The points representing the observed data have been shifted to the left by 2 percent, where they are shown by the solid dots. This entire subject merits further investigation when better facilities, particularly a better saturator, are available. The electrical method will probably be of little use in determining the dryness of otherwise pure alcohol, because other methods that are quick and easy are available, but it gives promise of usefulness in the case of solutions of other things in alcohol that would interfere with the simple determination of water by other methods. It is desirable to express moisture content in terms of relative humidity in this case, because this ratio

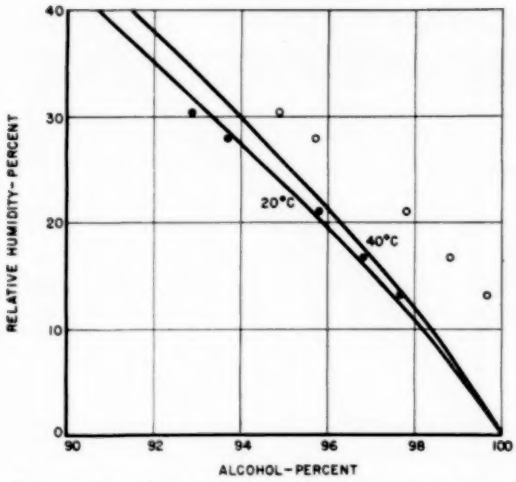

FIGURE 36.—*Apparent relative humidity above alcohol.*

○, Observed results at 28° C; ●, observed results minus 2 percent of alcohol.

changes relatively little with changing temperature. The method should have the merit of speed, applicability to small samples, and a fair degree of independence of the presence of other volatile substances, although the alcohols will cause some interference.

7. Permeability of Membranes to Water

The permeability to water vapor of protective films or membranes used in packaging materials for shipment and storage is a matter of considerable importance. For a closely related problem, the permeability of ballon fabrics to hydrogen and helium, the Shakespear Permeameter [6] has been extensively used. In the Permeameter, the fabric or membrane to be tested is clamped between the two halves of a permeability cell, one-half of which is suddenly swept out with the gas, e. g., hydrogen, for which permeability is to be determined. The rate at which hydrogen builds up in the other side of the cell is then measured by a physical method, in the Permeameter by thermal conductivity. A comparison of the time required for the concentration to change between two preselected values is taken as a measure of the permeability. Because of its speed and convenience, the use of the Permeameter has almost superseded in practical use methods that give more direct but more delayed results.

It seemed probable that a similar method of comparing intervals of relative humidity by timing would be applicable to measuring permeabilities to water vapor with the aid of the electrical detector. The arrangement used is shown in figure 37. The vapor barrier is clamped over the top of what is, in effect, a dish of water. Above the barrier is a space, arbitrarily chosen as 1 inch, at the top of which is the detector. This space is connected through valves to a supply of dry air and to the outer atmosphere. Before inserting the detector, its resistance is determined in the usual way at a relative humidity of 25 percent. It is then inserted in the space above the vapor barrier, and the space is swept out with a brisk stream of dried air for 1 minute. Then the valves are closed and the time is recorded until the resistance of the detector indicates a relative humidity in the space of just 25 percent. The definite duration of sweeping out with dry gas is for the purpose of producing reproducible though arbitrary conditions of the moisture gradient in the membrane itself.

Table 7 shows the results of testing 15 different membranes by this method. The observations were made by Jean Doyle. Tests in any horizontal row are duplicates on the same piece of membrane and show the agreement between tests that should have given the same result. The tests were only preliminary and were hastily made without temperature control. Probably a more important factor in the variability of results is the failure to establish a regular gradient of dissolved moisture through the barrier before beginning the timing. Probably because of this failure, thick films show excessively greater resistance to the passage of moisture than do thin films of the same material. Considering the probability that the method can be greatly improved with a little attention to details, it is apparent that a quick method for getting at least approximate results is available.

One characteristic of the method that may be of value in some cases is the possibility of applying

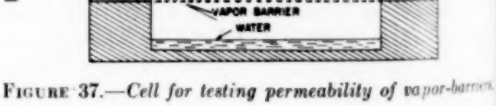

FIGURE 37.—*Cell for testing permeability of vapor-barriers.*

TABLE 7.—*Time required for 1 inch of gas space above water barrier to reach a relative humidity of 25 percent*

Material	Thickness	Test 1		Test 2		Test 3		Test 4		Test 5		Time divided by thickness
	mm	*min*	*sec*	*min*	*sec*	*min*	*sec*	*min*	*sec*	*min*	*sec*	*min*/0.01 *mm*
Cellulose acetate	0.03	0	46	0	50	0	34	0	32	0	43	0.23
Do	.13	3	55	5	02	4	47	4	28	5	21	.36
Cellophane	.03	0	47	0	50	0	49	0	51	0	34	.26
Polyvinyl alcohol	.05	1	39	1	33	1	45	1	50	1	05	.31
Nylon	.03	1	45	1	24	1	15	1	15	1	39	.49
Do	.04	3	40	3	36	3	32	3	38	3	19	.89
Vinylite plasticizer, a	.07	6	47	7	15	7	15	7	40	5	[a] 06	.97
Do	.13	22	40	22	28	30	16	29	30	31	09	2.09
Do	.23	225	34									9.67
Plasticizer b	.11	16	08	16	14	15	47	16	14	17	12	1.48
Plasticizer c	.08	18	54	23	47	20	15	23	38	22	30	2.73
Plasticizer d	.13	30	04	35	43	39	25	42	40	42	20	2.93
Plasticizer e	.10	12	[a] 44	17	01	15	57	17	51	17	51	1.63
Do	.15	81	00									5.40
Saran [b]	.05											

[a] Test made after membrane had been exposed to saturated atmosphere overnight.
[b] Did not reach 25-percent saturation in 4 hours.

it to very small samples. Although account would have to be taken of the water combined with the phosphoric acid on the detector, it seems entirely possible that a satisfactory test could be made on an area of membrane equal only to that of the end of the detector, a few square millimeters, and that it could be done with nearly the same speed and accuracy as the testing of a large sample.

The sample of Saran was so slow in responding to the previously used test that it was decided to vary the method by observing the relative humidity reached in a given time after sweeping out with dry air. The time chosen was 1 hour, and three tests were made. They showed close agreement at about 10-percent relative humidity.

For membranes of high permeability another method is available, which is to sweep dry air over the surface of the water barrier at a measured rate and to determine the amount of water in the stream in the usual way. This method is slower than the one experimented with, but the results should be easier to interpret in comparison with those obtained by the usual procedure of collecting and weighing the water in solid desiccants.

8. Gas Detection

One purpose for which the method has been used from time to time since its first description [1] is the detection of oxygen in a combustible gas or of a combustible gas in oxygen or air. The method is obvious: the gas is thoroughly dried then passed over a heated filament or catalyst and thence over a detector. Since almost all fuel gases, including the explosive gases of mines, contain either free or combined hydrogen, water is formed wherever combustion takes place, and it can be detected and measured if desired when the amount present is only a minute fraction of that which could cause explosion. The promptness of the reaction suggests its possible use as a leak detector. The sensitivity would be high; if combustion were complete methane, for example, would provide two volumes of water vapor per volume of gas and should be detectable without difficulty in a concentration of 0.001 percent even at atmospheric pressure. Oxygen in hydrogen also gives two volumes for one. In a hydrocarbon it will give less, because some of it will go to carbon monoxide, and for this reason the amount of oxygen present may be hard to determine

accurately. However, under any conditions of combustion enough water should be formed to make the method a sensitive one for detection.

The use of combustion in connection with that of a permeability cell offers so obvious a method for measuring permeability to oxygen, to hydrogen, or to a variety of hydrogen compounds, that it need be no more than mentioned.

VI. References

[1] E. R. Weaver and P. G. Ledig, Tech. Pap. BS **17,** 637 (1923) T242; Ind. Eng. Chem. **15,** 931 (1923).

[2] Francis W. Dunmore, J. Research NBS **20,** 723 (19 RP1102.

[3] Francis W. Dunmore, J. Research NBS **23,** 701 (19 RP1265.

[4] R. Wiebe and V. L. Gaddy, J. Am. Chem. Soc. 815 (1940).

[5] International Critical Tables **3,** 290 (1928).

[6] G. A. Shakespear, Tech. Repts. Adv. Comm. Ae (British) **2,** 579 (1916–17).

[7] H. A. Daynes, Gas analysis by measurement of ther conductivity, p. 266–77. (Cambridge Univ. Pr Cambridge, Mass., 1933).

WASHINGTON, June 19, 1947.

S. Department of Commerce
National Bureau of Standards

Research Paper RP1866
Volume 40, March, 1948

Part of the Journal of Research of the National Bureau of Standards

Electric Quadrupole Coupling of the Nuclear Spin With the Rotation of a Polar Diatomic Molecule in an External Electric Field[1]

By U. Fano

Formulas are given that serve to determine the hyperfine spectrum of a rotating molecule in various cases, depending on the external field strength and on the rotational quantum number. A complete calculation is carried out for a case in which only one of the nuclei has a quadrupole moment, the molecule is in a rotational state ($1: \pm 1$ or 0), and the interaction between the field and the molecular dipole is comparable to that between the dipole and the nuclear spin.

I. Introduction

The rotation of a polar diatomic molecule in an electric field has been discussed theoretically by various authors, particularly by Brouwer [1].[2] Experimentally, this problem is being investigated at Columbia University using a modification of the standard molecular beam radio-frequency resonance method [2], in which the beam is subjected to electric instead of magnetic fields [3]. The method permits the energy differences between rotational states of the molecule to be measured. Various spin-dependent interactions between the nuclei and the rest of the molecule may give rise to a hyperfine structure of the rotational spectrum. The electric quadrupole interaction between the nuclei and the molecular electrons, if present at all, is likely to be the major factor in this connection and is the subject of the present theoretical investigation.

Molecular rotation.—The qualitative aspects of molecular rotation in an electric field will be reviewed here, disregarding the effects that give rise to a hyperfine spectrum. The electronic system of the molecule is assumed to be in a $^1\Sigma$ state, so that it has no net angular momentum. The rotation of the molecule is then similar to that of a dumbbell whose two spheres (the two atoms) carry charges of opposite sign. Several cases may be considered:

(a) The electric field is so strong that the potential energy of the molecule, when oriented along the field, is much greater than its rotational kinetic energy. Then the molecule remains oriented along the field, except for minor oscillations about this position. This case is unrealistic, however, as no sufficiently strong field is currently available.

(b) The field is vanishingly weak, so that the molecule rotates freely about its center of mass with a constant, quantized, angular momentum. The component of this angular momentum along the field is then also constant and quantized. The positively charged part of the molecule points in the direction of the field about as frequently as in the opposite direction. Thus the molecular electric moment averages out, and the presence of the field has no effect on the rotational energy levels.

(c) The field is moderately weak. The rotation is now appreciably perturbed by the field, and the molecular electric moment no longer averages out; an electric polarization is thus induced and each rotational energy level is accordingly lowered by an amount equal to a polarization coefficient times the square of the electric field. When the rotation has primarily the character of a precession (clockwise or counterclockwise) around the direction of the field, the effect of the field is to force the positively charged part of the molecule to lean in

[1] Part of this work was performed at the Pupin Physics Laboratory, Columbia University, during the tenure of a Research Associateship of the Carnegie Institution of Washington in 1946.

[2] Figures in brackets indicate the literature references at the end of this paper.

774908—48——4

the direction of the field, and so induces a positive polarization. An opposite effect occurs, however, when the rotation brings the positively charged part alternately close to the direction of the field (downhill), and then away from it in the opposite direction (uphill); the positive charge moves rapidly while it is downhill and spends little time there, but it lags in the uphill position, and on the average it will spend more time uphill, giving rise to a negative polarization.

(d) The field is intermediate or moderately strong. The rotation is perturbed by the field to a greater and greater extent. As the field increases, the positively charged part of the molecule is forced to lean in the direction of the field, whatever the type of rotation may be, and the polarization is always positive.

The quantitative treatment of cases (a), (b), and (c) is simple, but in case (d), which obtains most frequently, the energy levels cannot be given in general as analytic functions of the electric field. In work as yet unpublished, W. E. Lamb, Jr., has developed a convenient method for the numerical computation of the terms for any value of the field strength. The rotational wave equation is

$$[-(\hbar^2/2A)\Delta - lE\cos\vartheta_{\boldsymbol{R}} - W]\psi(\vartheta_{\boldsymbol{R}}, \varphi_{\boldsymbol{R}}) = 0, \quad (1)$$

where the electric field, $\boldsymbol{E}$, is taken as a polar axis, $(\vartheta_{\boldsymbol{R}}, \varphi_{\boldsymbol{R}})$ are polar coordinates of a vector $\boldsymbol{R}$ joining the nuclei, l is the dipole moment of the molecule A its moment of inertia, Δ the two-dimensional Laplace operator (in the coordinates $\vartheta_{\boldsymbol{R}}$, $\varphi_{\boldsymbol{R}}$), and W the energy eigenvalue. The first term in brackets represents the kinetic energy of rotation; the second represents the potential energy of the dipole in the electric field. A dimensionless form is obtained by dividing the equation by $(-\hbar^2/2A)$:

$$(\Delta + \alpha\cos\vartheta_{\boldsymbol{R}} + w)\psi = 0, \quad (1a)$$

where $\alpha = lE/(\hbar^2/2A)$ is a numerical index of the field strength and $w = W/(\hbar^2/2A)$. The eigenfunctions can be labeled by means of two quantum numbers n and m; m is the magnetic quantum number, which indicates the rate and the direction of the precession of the molecule around the electric field; $n - |m|$ is the number of nodal lines, which characterizes the component of the motion along the meridians of the polar coordinates. The eigenvalues are functions of α. For all values of α, we have $w_{n,\,m} = w_{n,-m}$, as the energy does not depend on the direction of the precession. For $\alpha = 0$, the results are familiar, namely, $w_{n,\,m} = n(n+1)$, $\psi_{n,\,m}$ is a spherical harmonic, and n is an azimuthal quantum number that measures the total angular momentum. For $\alpha \ll 1$, case (c), a perturbation calculation gives $w_{nm} \sim n(n+1) + \alpha^2[(n+m)(n-m)/2n(2n-1)(2n+1) - (n+1+m)(n+1-m)/2(n+1)(2n+1)(2n+3)]$; as expected, the coefficient of α^2 is positive for $|m/n| \sim 1$ (fast precession), negative for $|m/n| \ll 1$.

Quadrupole interaction.—The electrical charge distribution of a nucleus having a quadrupole moment resembles an ellipsoid of rotation rather than a sphere (the direction of the nuclear spin being the axis of symmetry of the ellipsoid). The value and sign of the quadrupole moment indicate the elongation of the ellipsoid. As the charge distribution of a diatomic molecule is not spherically symmetrical about any of its nuclei, the electrostatic energy of the nucleus within the molecule will depend upon the orientation of the nuclear spin with respect to the axis of symmetry of the molecule (i. e., the line joining the nuclei). If the spin be directed along the axis and then swung into the opposite direction and back into the initial one, the interaction energy will go through *two* maxima and *two* minima.

In the absence of this quadrupole interaction and of magnetic interaction, the nuclear spins would maintain a constant orientation in space while the polar molecule rotates in an electric field, and the orientation of each nuclear spin with respect to the axis of the rotating molecule would undergo periodic variations. In the presence of a quadrupole moment there will then be periodic variations of the interaction, and hence torques that affect both the rotation of the molecule and the orientation of the nuclear spins. This effect will be particularly conspicuous in case (b) described above, as the orientation of the angular momentum of the molecular rotation can then be shifted by a torque without performing any work. This angular momentum will then precess freely together with the nuclear spins, and only the total angular momentum, i. e., the vector sum of the molecular momentum and of the nuclear spins, will remain constant. When, on the other hand, considerable work must be performed to upset the molecular rotation, the quadrupole interaction will have no significant effect on the motion of the

molecular constituents; the energy of the system will then simply include a contribution from the quadrupole interactions averaged over the varying orientation of the spins with respect to the molecular axis. This contribution will depend on the state of rotational motion of the molecule and on the (constant) orientation of the nuclear spins with respect to the electric field. This situation prevails generally in cases (a) and (d) described above, i. e., for moderately to very strong fields; from this standpoint, case (c) represents an intermediate situation.

It should still be considered that no work is ever required for the simple operation of reversing the direction of the precession of the molecule around the electric field, provided the speed of precession is unchanged. Owing to the quadrupole interaction, and for any electric field strength, the uniform precession might therefore conceivably be turned into a precession whose direction is periodically reversed; the conservation of angular momentum would be preserved by corresponding variations of the precession of the nuclear spins. Quantum mechanically, there would thus be "standing waves of precession," the number of nodes of the standing wave depending on the speed of precession. However, it will be shown further below that only the standing wave with *two* nodes actually arises in this way. This is a direct consequence of the particular dependence of the quadrupole interaction upon the mutual orientation of the molecule and of the nuclear spin; as already stated this interaction goes through *two* maxima and minima when a cyclic change of orientation is performed.

The quantitative treatment of our problem will accordingly proceed as follows. As shown by Casimir, [4], the interaction energy between a nuclear quadrupole moment and the electronic charge of an atom or molecule is of the order of $e^2qQ/4$ (q and Q are the usual symbols for a molecular and a nuclear constant whose product is $<1\ cm^{-1}$). Hence, taking into account the possible values of the pertinent constants, it seems safe to assume for the dimensionless parameter characterizing this interaction:

$$|\beta| = |e^2qQ/4(\hbar^2/2A)| \lesssim 10^{-2}. \qquad (2)$$

This value must be related to the fact that, *in general*, the separation of different unperturbed rotational levels of the molecule is[3] $|w_{n'm'} - w_{nm}| \gtrsim 1$. Therefore, in general, the quadrupole interaction can be treated as a small perturbation of each rotational term, and each term will preserve its quantum numbers n, m. This procedure will not be adequate in the cases discussed above, in which the quadrupole interaction has a great effect on the rotation of the molecule, namely, for states (n, m) which are directly coupled by the quadrupole interaction to other states (n', m') such that $|w_{n'm'} - w_{nm}| \lesssim |\beta|$. Direct quadrupole coupling means that the quadrupole interaction energy H_Q has a matrix element $(n'm'|H_Q|nm) \neq 0$; this occurs only when $|m - m'| \leq 2$, as it will be shown in the next section. These two conditions can be fulfilled simultaneously in two cases only:

(1) $n = n' > 0$, $m = -m' = \pm 1$ (all values of α), in which the molecule precesses back and forth, i. e., clock- and counterclockwise;

(2) $n = n' > 0$, $\alpha^2 \lesssim |\beta|$ ($|m - m'| \leq 2$), in which the field is weak and the rotation is strongly perturbed.

The latter case becomes simpler when $\alpha^2 \ll |\beta|$ or even $\alpha^2 = 0$. In fact, the zero-field case involves a simple vector coupling of the rotational angular momentum $\boldsymbol{J}$ ($J = n$) with the nuclear spins $\boldsymbol{I}_1$ and $\boldsymbol{I}_2$. In the case of near-zero-field, this vector coupling is preserved and the effect of the electric field can be treated as a small perturbation, somewhat analogous to the anomalous Zeeman effect produced by a weak magnetic field.

The general expression for the quadrupole interaction matrix is given in the next section; the application to the different cases will then follow.

II. Matrix Elements of Quadrupole Interaction Between Molecular Rotation and a Spinning Nucleus

(*a*) The electrostatic interaction $-e^2/|\boldsymbol{r} - \boldsymbol{p}|$, between a nuclear proton at a position $\boldsymbol{p}$ with respect to the center of the nucleus and a molecular electron at a position $\boldsymbol{r}$ with respect to the same center, can be expanded into a series of Legendre spherical functions of the angle $\gamma_{\boldsymbol{rp}}$ between the vectors $\boldsymbol{r}$ and $\boldsymbol{p}$. The first term of this series

[3] The magnetic spin-spin interaction between the nuclei and the interaction between the nuclear magnetic moments and the rotation-induced magnetic moment of the molecule are generally weaker than the electric quadrupole interaction; in our scale they may be characterized by a parameter $\eta \lesssim 10^{-4}$. These interactions will be disregarded in the following therefore we must assume

$$|\alpha| \ll |\beta| \lesssim 10^{-2},\ \beta^2 \sim 0.$$

represents the Coulomb attraction of the electron toward the center of the nucleus, the second term has no average effect, and the third, namely:

$$H_Q = -e^2(p^2/r^3)P_2(\cos\gamma_{pr}) = -e^2(p^2/r^3)\left(\frac{3}{2}\cos^2\gamma_{pr} - \frac{1}{2}\right), \quad (3)$$

is called the quadrupole component of the interaction. This component must be integrated over the density of protons throughout the nucleus and the density of electrons throughout the molecule. The integration over the electron density is carried out in polar coordinates having as axis a vector R from the center of the molecule to the center of the nucleus. Using the addition theorem of spherical harmonics and taking into account the fact that the Σ-type electronic state has axial symmetry, we find:

$$\langle(1/r^3)P_2(\cos\gamma_{pr})\rangle_r = \langle(1/r^3)P_2(\cos\gamma_{Rr})\rangle_r P_2(\cos\gamma_{Rp}),$$

where the symbol $\langle\rangle_r$ indicates integration with respect to the electron density. The first factor on the right-hand side is a molecular characteristic which is indicated [4] by $q/2$. Using again the addition theorem of spherical harmonics,

$$P_2(\cos\gamma_{Rp}) = (4\pi/5)\Sigma_\mu(-1)^\mu Y_{2,-\mu}(\vartheta_p, \varphi_p)Y_{2,\mu}(\vartheta_R, \varphi_R),$$

we have,

$$\langle H_Q\rangle_r = (-e^2q/2)\Sigma_\mu(-1)^\mu[p^2(4\pi/5)^{1/2}Y_{2,-\mu}(\vartheta_p, \varphi_p)] \times[(4\pi/5)^{1/2}Y_{2,\mu}(\vartheta_R, \varphi_R)]. \quad (3a)$$

(The normalization of the spherical harmonics is such that $\int\int|Y_{l,\mu}|^2\sin\vartheta d\vartheta d\varphi = 1, Y^*_{l,\mu} = (-1)^\mu Y_{l,-\mu}$.

(b) All the matrix elements of the *first factor in square brackets*, i. e., the integrals of this factor over the proton density, associated with pairs of nuclear states with the same spin I and magnetic quantum numbers m_I, m_I', can be given in terms of just one such matrix element. Thus:

$$(m_I'|p^2(4\pi/5)^{1/2}Y_{2,-\mu}(\vartheta_p, \varphi_p)|m_I) = (I|p^2(4\pi/5)^{1/2}Y_{2,0}(\vartheta_p, \varphi_p)|I)(D^{Im_I'}_{Im_I}/D^{II}_{II})\delta_{m_I', m_I-\mu}.$$

The first factor on the right-hand side is a nuclear characteristic which is indicated [4] as $Q/2$ (i. e., half of the quadrupole moment). In the formula $\delta_{i,k}=1$ or 0, depending on whether $i=k$ or $i\neq k$. The coefficients $D^{jm'}_{im}$ may be found by means of group theory,[4] and are given in table 1. As $D^{II}_{II} = -I(2I-1)/(2I-1)(2I+3)$ we take:

$$d(j)^{m'}_{m} = -(2j-1)(2j+3)D^{jm'}_{im};$$

the coefficients d are given in table 2. Thus:

$$(m_I-\mu|p^2(4\pi/5)^{1/2}Y_{2,\mu}(\vartheta_p, \varphi_p)|m_I) = Qd(I)^{m_I-\mu}_{m_I}/2I(2I-1). \quad (4)$$

TABLE 1.—*Coefficients* $D^{jm'}_{im}$ *for:* $j'-j=0, \pm2$; $m'-m=0, \pm1, \pm2$.[a]

$D^{j}_{i,m}$	$=-[3m^2-j(j+1)]/(2j-1)(2j+3)$
$D^{j,m+1}_{i,m}$	$=(2m+1)[(3/2)(j+m+1)(j-m)]^{1/2}$
$D^{j,m+2}_{i,m}$	$=-[(3/2)(j+m+2)(j+m+1)(j-m)(j-m-1)]^{1/2}/(2j-1)(2j+3)$
$D^{j+2,m}_{i,m}$	$=(3/2)[(j+m+2)(j+m+1)(j-m+2)(j-m+1)/(2j+1)(2j+3)^2(2j+5)]^{1/2}$
$D^{j+2,m+1}_{i,m}$	$=[(3/2)(j+m+3)(j+m+2)(j+m+1)(j-m+1)/(2j+1)(2j+3)^2(2j+5)]^{1/2}$
$D^{j+2,m+2}_{i,m}$	$=[(3/8)(j+m+4)(j+m+3)(j+m+2)(j+m+1)/(2j+1)(2j+3)^2(2j+5)]^{1/2}$

[a] All other coefficients are obtained by means of the formulas

$$D^{jm}_{i'm'} = (-1)^{m'-m}D^{jm'}_{im}, D^{j'-m'}_{i,-m} = D^{j'm'}_{im}$$

TABLE 2.—*Coefficients* $d(j)^{m'}_{m} = -(2j-1)(2j+3)D^{jm'}_{im}$

d^{m+2}_{m}	$=[(3/2)(j+m+2)(j+m+1)(j-m)(j-m-1)]^{1/2}$
d^{m+1}_{m}	$=-(2m+1)[(3/2)(j+m+1)(j-m)]^{1/2}$
d^{m}_{m}	$=3m^2-j(j+1)$
d^{m-1}_{m}	$=(2m-1)[(3/2)(j-m+1)(j+m)]^{1/2}=d^{-m+1}_{-m}$
d^{m-2}_{m}	$=[(3/2)(j-m+2)(j-m+1)(j+m)(j+m-1)]^{1/2}=d^{-m+2}_{-m}$

(c) The matrix elements of the *factor in the second bracket* of eq 3a, pertaining to the rotational states of the molecule (n, m) and (n', m') is the average of this factor over the probability distribution $\psi^*_{n',m'}\psi_{n,m}$ and can be indicated as

[4] These coefficients are closely related to those indicated by E. Wigner, Gruppentheorie (Vieweg, Braunschweig 1931), p. 206, as $S^{(2)}_{j'm'}$. For j and j' integer $D^{jm'}_{im} = (4\pi/5)^{1/2}\int\int Y^*_{j',-m'}(\vartheta\varphi)Y_{2,m-m}(\vartheta,\varphi)Y_{j,m}(\vartheta\varphi)\sin\vartheta d\vartheta d\varphi$. The formula given means essentially that the ratio of matrix elements for different values of (m_I, m_I') is the same as though the angular distribution of the proton density in each nuclear state (I, m_I) were described by the spherical harmonic Y_{I,m_I} (suitably generalized for half-integer I).

$$\langle n', m'|(4\pi/5)^{1/2}Y_{2\mu}(\theta_R, \varphi_R)|n, m\rangle = (4\pi/5)^{1/2}\int\int \psi^*_{n',m'}(\theta_k\varphi_k)Y_{2\mu}(\theta_R, \varphi_R)\psi_{n,m}(\theta_R, \varphi_R)\sin\theta_R d\theta_R d\varphi = R^{n',m'}_{n,m}\delta_{m',m+\mu}. \quad (5)$$

Expanding the rotational wave functions $\psi_{n,m}$ into spherical harmonics:

$$\psi_{n,m}(\theta, \varphi) = \Sigma_J C^{n,m}_J Y_{J,m}(\theta, \varphi),$$

where the coefficients $C^{n,m}_J$ depend on the parameter α, we have:

$$R^{n',n}_{m',m} = \Sigma_J (D^{J+2,m'}_{J,m} C^{n',m'}_{J+2} + D^{J,m'}_{J,m} C^{n',m'}_J + D^{J-2,m'}_{J,m} C^{n',m'}_{J-2}) C^{n,m}_J. \quad (5a)$$

For $n=n'$, $m=m'$ (which is the only case involved in a first-order perturbation), we have:

$$R^{n,n}_{m,m} = R(n, m) = (3/2)\langle\cos^2\theta\rangle_R - 1/2.$$

There is also a simpler form for

$$R^{n,n-1}_{m,1} = S(n) = (3/8)^{1/2}\langle\sin^2\theta\ \cos\varphi\rangle_R.$$

The coefficients R must be obtained by numerical computation except when α is very large or very small. For $\alpha \ll 1$:

$$C^{n,m}_J = \delta_{n,J} + \alpha\delta_{n\pm1,J} f(n, n\pm1) + \text{terms in } \alpha^2, \text{ etc., [1]}$$

where f is a function of n and $n\pm1$; hence eq 5a gives

$$R^{n,m'}_{n,m} = D^{n,m'}_{n,m} + \text{terms in } \alpha^2, \text{ etc.}$$

For $\alpha \gg 1$, $|\psi_{n,m}| \sim 0$, except for $\vartheta_R \ll 1$ (i. e., the molecule points approximately in the direction of the field). Hence, according to eq 5, $\lim_{\alpha=\infty} R^{n',m'}_{n,m} = \delta_{n,n'}\delta_{m,m'}$. However, the convergence to this limit is slow. For example, $R(n, m)$ can be expanded in powers of $\alpha^{-1/2}$ as follows:

$$R(n, m) = 1 - 3(2n - m + 1)(2\alpha)^{-1/2} + \text{terms in } \alpha^{-1}, \text{ etc.}$$

(*d*) Combining eq 3a, 4, and 5, the matrix element of H_Q, pertaining to states with the same total magnetic quantum number $M = m_I + m = m'_I + m'$, is found to be

$$\langle n', m'|H_Q|n, m\rangle = -(e^2qQ/4)(-1)^{m'-m}R^{n',m'}_{n,m}d(I)^{M-m'}_{M-m}/I(2I-1) = -(\hbar^2/2A)(-1)^{m-m'}\beta' R^{n',m'}_{n,m}d(I)^{M-m'}_{M-m}, \quad (6)$$

where

$$\beta' = \beta/I(2I-1) = [e^2qQ/4I(2I-1)]/(\hbar^2/2A).$$

III. The General Case: $\alpha^2 \gg |\beta|$, $|m| \neq 1$

Here it is sufficient to treat the quadrupole coupling as a first order perturbation of each rotational term.

Only one of the nuclei has a quadrupole moment.—Each term of the complete system is characterized by the three quantum numbers n, m, and $m_I = M - m$. The term energy is then given, to the first order in β, by the sum of the rotational term and of the matrix element (6) with $n=n'$ and $m=m'$:

$$W_{n,m,m_I} = (\hbar^2/2A)[w_{n,m} - \beta' d(I)^{m_I}_{m_I} R^{n,m}_{n,m}] = (\hbar^2/2A)\{w_{n,m} - \beta'[3m_I^2 - I(I+1)]R(n,m)\} =$$

$$W_{n,m,-m_I} = W_{n,-m,m_I} = W_{n,-m,-m_I}. \quad (7)$$

Each rotational energy level of energy $w_{n,|m|}$ splits thus, in this approximation, into $I+\frac{1}{2}$ levels if I is a half-integer, into $I+1$ levels if I is an integer. The absolute values of the intervals between the levels of such a multiplet are functions of the electric field (through R), but their ratios are independent of it.

Both nuclei have a quadrupole moment.—Each term is now characterized by four quantum numbers n, m, m_{I1}, m_{I2}. The term energy is, again to the first order in β:

$$W_{n,\pm m,\pm m_{I1},\pm m_{I2}} = (\hbar^2/2A)\{w_{n,m} - \beta'_1[3m_{I1}^2 - I_1(I_1+1)]R(n,m) - \beta'_2[3m_{I2}^2 - I_2(I_2+1)]R(n,m)\} \quad (8)$$

IV. The Special Case: $\alpha^2 \gg |\beta|$, $|m| = 1$

Only one of the nuclei has a quadrupole moment.—The energy of terms with $m=1$, $m_I=(I-1)$ or I, $M=I$ or $(I+1)$, or with $m=-1$, $m_I=-(I-1)$ or $-I$, $M=-I$ or $-(I+1)$, is still given by eq 7.

For other terms, with $|M|<I$, m is no longer a good quantum number, but $|m|$ is. The term energy $\epsilon(\hbar^2/2A)$ is then obtained, to the first order in β, by solving the secular equation,

$$\begin{vmatrix} w_{n1}+(n,1|H_Q|n,1)-\epsilon & (n,1|H_Q|n,-1) \\ (n,-1|H_Q|n,1) & w_{n,-1}+(n,-1)|H_Q|n,-1)-\epsilon \end{vmatrix}=0,$$

with $R(n,1)=R(n,-1)$, $w_{n,1}=w_{n,-1}$. Its solution is

$$\epsilon=W_{n,1,M}/(\hbar^2/2A)=W_{n,1,-M}/(\hbar^2/2A)=w_{n1}-\beta' R(n,1)\{3(M^2+1)-I(I+1)\pm$$
$$[(3/2)(I+M)(I+M+1)(I-M)(I-M+1)S(n)^2/R(n,1)^2+36M^2]^{1/2}\}. \quad (9)$$

The original w_{n1} rotational level is thus split into $2I+1$ different levels, if I a half integer, and into $2(I+1)$, if I is an integer.

Both nuclei have a quadrupole moment.—This case is similar to the preceding one, but more complicated. There are three levels with total magnetic quantum number $|M|=I_1+I_2$ or I_1+I_2+1, for which the energy can be calculated by means of eq 8. These energies are indicated by the following symbols:

$$W_{n,1,I_1,I_2}=W_{n,-1,-I_1,-I_2};$$
$$W_{n,1,I_1,I_2-1}=W_{n,-1,-I_1,-I_2+1};$$
$$W_{n,1,I_1-1,I_2}=W_{n,-1,-I_1+1,-I_2}.$$

For each group of terms with $|M|<I_1+I_2$ one must solve two secular equations that in general will have more than two rows and columns. The rows and columns correspond to zero-order states characterized by particular values of (m, m_{I1}, m_{I2}) with $|m|=1$, $m+m_{I1}+m_{I2}=M$. The zero-order states belonging to each secular equation can be arranged in a succession, which (for $M>0$, $I_2>I_1$) can be of either type:

$(1,I_1, M-I_1-1)$, $(-1,I_1, M-I_1+1)$,
$(1,I_1-2, M-I_1+1)$, $(-1, I_1-2, M-I_1+3)\ldots$

or

$(1,I_1-1, M-I_1)$, $(-1,I_1-1, M-I_1+2)$,
$(1,I_1-3, M-I_1+2)$, $(-1, I_1-3, M-I_1+4)\ldots$

The diagonal elements of the secular equation are of the type:

$$w_{n1}-R(n,1)[\beta'_1 d(I_1)^{m_{I1}}_{m_{I1}}+\beta'_2 d(I_2)^{m_{I2}}_{m_{I2}}]-\epsilon;$$

the elements next to the diagonal are of the type:

$$-S(n)\beta'_1 d(I_1)^{m_{I1}+2}_{m_{I1}} \text{ or } -S(n)\beta'_2 d(I_2)^{m_{I2}-2}_{m_{I2}}$$

as the case may be; all other elements vanish.

V. The Special Case: $\alpha\ll 1$, $n>0$[5]

Only one nucleus has a quadrupole moment.—For $\alpha\ll 1$, or, more accurately, for:

$$\alpha^2/2n(n+1)\sim[\alpha/(w_{n+1,m}-w_{n,m})]^2\lesssim|\beta|\ll 1$$

the difference $R^{nm'}_{nm}-D^{nm'}_{nm}\sim\alpha^2$ can be disregarded, since R is multiplied by β in the expression of the matrix elements of quadrupole interaction.

Replacing then R with D and using the approximate expression for $w_{n,m}$ valid for small α[6], the matrix element of the complete energy operator pertaining to states with the same values of n, I, and $M=m+m_I$ is

$$(m'|H|m)=(\hbar^2/2A)\{n(n+1)\delta_{m,m'}-$$
$$\beta(-1)^{m'-m}D^{nm'}_{nm}[d(I)^{M-m'}_{M-m}/I(2I-1)-\delta_{m,m'}\alpha^2/2n(n+1)\beta]+$$
$$\text{terms in } \alpha^4,\ \alpha^2\beta, \text{ or } \beta^2, \text{ etc.}$$

The term energy $\epsilon(\hbar^2/2A)$ is then obtained, to the first order in β, by solving the secular equation:

$$|(m'|H|m)-\epsilon(\hbar^2/2A)\delta_{m,m'}|=0.$$

The number of rows and columns in the determinant, and hence the degree of the equation, is $\leq(2n+1)$ or $\leq(2I+1)$, whichever is the smaller, since m and m' take all the values that do not exceed either $(M+I)$ or n and are not less than either $(M-I)$ or $-n$. The term energy can also be indicated as:

$$(\hbar^2/2A)[(n(n+1)+\beta'' y)], \quad (10)$$

where $\beta''=\beta/(2n-1)(2n+3)I(2I-1)$ and y is a solution of the secular equation

[5] For $\alpha\ll 1$, $n=0$ we have $R^{00}_{00}\approx\alpha^2$; hence the quadrupole interaction can be disregarded.

[6] This expression can be given in terms of the coefficient $D^{nm'}_{nm}$, provided $n>0$.

$$(-1)^{m-m'}d(n)_m^{m'}(d(I)_{M-m}^{M-m'}+\delta_{m',m}x)-\delta_{m',m}y|=0 \qquad (10a)$$

Here $x=-[I(2I-1)/2n(n+1)](\alpha^2/\beta)$. The coefficients d are given in table 2, hence the further steps in calculating y for any given value of x (i. e., of the field strength) are straightforward, even though they may be laborious. The particular case for $n=1$ is worked out in the appendix, which also contains some comments about the methods of solving the secular equation.

Both nuclei have quadrupole moments.—The calculation is similar to that of the preceding case but is more complicated. The energy of each term can be expressed as:

$$(\hbar^2/2A)[n(n+1)+y\overline{\beta}/(2n-1)(2n+3)]. \qquad (11)$$

Where y is a solution of the secular equation:

$$\left|\begin{matrix}(-1)^{m'-m}d(n)_m^{m'}\ [b_1d_1(I_1)_{m_{I1}}^{m'_{I1}}\delta_{m'_{I1},m_{I1}}+b_2d(I_2)_{m_{I2}}^{m'_{I2}}\delta_{m'_{I1},m_{I1}}+ \\ x\delta_{m'_{I1},m_{I1}}\delta_{m'_{I2},m_{I2}}]-y\delta_{m'_{I1},m_{I1}}\delta_{m'_{I2},m_{I2}}\end{matrix}\right|=0. \qquad (11a)$$

Here $x=-\alpha^2/\overline{\beta}2n(n+1)$ and $\overline{\beta}$, b_1 and b_2 are so chosen that:

$$\overline{\beta}b_1=\beta_1/I_1(2I_1-1),\ \overline{\beta}b_2=\beta_2/I_2(2I_2-1),\ b_1\sim b_2\sim 1.$$

Finally, $|m|,|m'|\leq n$; $|m_{I1}|,|m'_{I1}|\leq I_1$; $|m_{I2}|,|m'_{I2}|\leq I_2$; $m+m_{I1}+m_{I2}=m'+m'_{I1}+m'_{I2}=M$.

VI. The Special Case: $\alpha^2\ll|\beta|$

Zero field. Only one nucleus has a quadrupole moment.—In this case the total angular momentum $\boldsymbol{F}=\boldsymbol{J}+\boldsymbol{I}$ ($J=n$), i. e., the sum of the rotational angular momentum and of the spin of the nucleus having a quadrupole moment, is a constant of the motion of the system. $\boldsymbol{J}$ and $\boldsymbol{I}$ are not constant but precess freely around $\boldsymbol{F}$ on account of the quadrupole interaction. All the states having the same value of F and different values of the total magnetic quantum number $M=m+m_I$ have the same energy. As shown by Casimir [4] [7] the energy of each term is proportional to an eigenvalue of the quadrupole coupling operator:

$$\frac{3}{2}(\boldsymbol{J}\cdot\boldsymbol{I})(\boldsymbol{J}\cdot\boldsymbol{I})+\frac{3}{4}(\boldsymbol{J}\cdot\boldsymbol{I})-\frac{1}{2}(\boldsymbol{J}\cdot\boldsymbol{J})(\boldsymbol{I}\cdot\boldsymbol{I}).$$

The proportionality factor can be determined by comparison with the solution obtained in section V for the case $M=F=n+I$, $\alpha^2=0$, which is trivial.

The energy levels for $n+I\geq F\geq|n-I|$ are

$$(\hbar^2/2A\ \{n(n+1)+\beta[3C(C+1)-4n(n+1)I(I+1)] /2(2n-1)(2n+3)I(2I-1)\}, \qquad (12)$$

with

$$C=2(\boldsymbol{J}\cdot\boldsymbol{I})=F(F+1)-n(n+1)-I(I+1).$$

Near-zero field. Only one nucleus has a quadrupole moment.—The weak electric field has the effect of splitting the levels with equal F and different M. The energy is calculated by considering the term proportional to α^2 in eq 10, that is,

$$\alpha^2D_{nm}^{nm}/2n(n+1),$$

as a small perturbation. This means simply averaging the value of this term over the participation of each rotational state (n, m) in the complete state (n, F, M). The following term must therefore be added to eq 12:

$$(\hbar^2/2A)[\alpha^2/2n(n+1)]\Sigma_m(C_{F,m,M-m}^{(nI)})^2D_{nm}^{nm}=-\alpha^2(\hbar^2/2A)[3M^2-F(F+1)][3D(D-1)-4F(F+1)n(n+1)]/ 2n(n+1)(2n-1)(2n+3)2F(F+1)(2F-1)(2F+3), \qquad (13)$$

where $C_{F,m,M-m}^{(nI)}$ is the coefficient of the eigenfunction $(n, m; I, M-m)$ in the linear combination which constitutes the eigenfunction (n, F, M) [5], and

$$D=2(\boldsymbol{J}.\boldsymbol{F})=F(F+1)+n(n+1)-I(I+1).$$

In the theory of the anomalous Zeeman effect [6] for a case of (LS) coupling, which is somewhat analagous to the present calculation, one has to calculate the average value of the quantum numbers m_L and m_S, namely, $\Sigma_{m_L}(C_{J,m_L,M-m_L}^{(LS)})^2m_L$, etc. It is shown by direct methods, however, that the results are $M(\boldsymbol{L}\cdot\boldsymbol{J})/J(J+1)$ and $M(\boldsymbol{S}\cdot\boldsymbol{J})/J(J+1)$. In our case the quantity D_{nm}^{nm} is a matrix element of quadrupole interaction,

[7] H. B. G. Casimir, Archives du Mus'e Teyler [III] **VIII,** 291 (1936). The application to a molecule in zero-field has been made by B. T. Feld and W. E. Lamb, Jr. (Phys. Rev. **67,** 15 (1945)). The definition of q by Feld and Lamb is, however, different from that introduced in this paper; this entails a difference in the multiplicative factor of some formulas.

while m_L is a matrix element of dipole interaction. It might therefore be expected that eq 13 could be expressed directly by means of quadrupole matrix elements. In fact eq 13 involves the expression D^{FM}_{FM} and the matrix element of the operator:

$$\frac{3}{2}(\boldsymbol{J}\cdot\boldsymbol{F})(\boldsymbol{J}\cdot\boldsymbol{F})-\frac{3}{4}(\boldsymbol{J}\cdot\boldsymbol{F})-\frac{1}{2}(\boldsymbol{J}\cdot\boldsymbol{J})(\boldsymbol{F}\cdot\boldsymbol{F}),$$

but the latter differs from the usual quadrupole coupling operator by the sign of the second term.

Both nuclei have quadrupole moments.—This case is again similar to the preceding ones but more complicated. Equation 13 should be extended to include two terms, one involving the coupling of $\boldsymbol{J}$ and $\boldsymbol{I}_1$, and the other that of $\boldsymbol{J}$ and $\boldsymbol{I}_2$. However, neither $\boldsymbol{J}+\boldsymbol{I}_1$ nor $\boldsymbol{J}+\boldsymbol{I}_2$ is a constant of the motion, but only the sum $\boldsymbol{F}=\boldsymbol{J}+\boldsymbol{I}_1+\boldsymbol{I}_2$. In general, there will be more than one term with the same values of n and F. The characterization of each term and the evaluation of $(\boldsymbol{J}\cdot\boldsymbol{I}_1)$ and $(\boldsymbol{J}\cdot\boldsymbol{I}_2)$, and hence of the energy levels, depend upon the ratio β_1/β_2 and require the application of methods similar to those used in the theory of complex atomic spectra involving a number of terms with the same angular momentum [6, p. 233]. The same holds for the extension of equation 13.

The author is indebted to Prof. I. I. Rabi and his associates for suggesting this work, for friendly discussions, and for hospitality in the Pupin Physics Laboratory.

VII. References

[1] F. Brouwer, Utrecht Dissertation (1930).
[2] I. I. Rabi, S. Millman, P. Kusch, and J. R. Zacharias, Phys. Rev. **55,** 526 (1939).
[3] H. K. Hughes, Phys. Rev. **70,** 570 (1946); **72,** 614 (1947).
[4] H. B. G. Casimir, Physica **2,** 719 (1935).
[5] E. Wigner, Gruppentheorie, p. 206 (Vieweg, Braunschweig, 1931).
[6] E. U. Condon and G. H. Shortley, Theory of Atomic spectra, p. 380 (Cambridge Univ. Press, Cambridge, England, 1935).

VIII. Appendix

The solution of the secular equation 10a for $n=1$ is obtained as follows. The total azimuthal quantum number M assumes all the values $|M|\leq I+1$. For $|M|=I+1$ the secular equation has only one row and column; its trivial solution is:

$$y=I(2I-1)+x, \text{ for } |M|=I+1. \tag{14a}$$

For $|M|=I$, the equation is quadratic:

$$\begin{vmatrix}[(I-3)(2I-1)+x]-y & 3(2I-1)I^{1/2}\\ 3(2I-1)I^{1/2} & -2[I(2I-1)+x]-y\end{vmatrix}=0,$$

and its solution is

$$y=-\frac{1}{2}\Big\{(I+3)(2I-1)+x\pm 3([(I-1)(2I-1)+x]^2+4[I(2I-1)]^{1/2}\Big\}, \text{ for } |M|=I. \tag{14b}$$

For $|M|<I$, the equation is cubic, having three rows and columns. Its solution can be indicated as

$$y=K_1+2K_2^{1/2}\cos[(\alpha+2p\pi)/3], \text{ for } |M|<I, \tag{14c}$$

where $p=0, 1, 2$, $\cos\alpha=-K_3/K_2^{3/2}$. K_1, K_2, K_3 are polynomials of first, second, and third degree in the elements of the determinant form of the secular equation, which can be given in terms of I, M and x:

$$K_1=2$$

$$K_2=[4I^2(I+1)^2+I(I+1)+1]+2[3M^2-I(I+1)+1]x+x^2$$

$$K_3=[8I^3(I+1)^3-24I^2(I+1)^2+(3/2)I(I+1)]-3[3M^2[2I(I+1)-7/2]-\tfrac{1}{2}I(I+1)[4I(I+1)+1]+1]x+3[3M^2-I(I+1)+1]x^2+x^3. \tag{15}$$

Figure 1 shows the plot of y as a function of x for $I=7/2$, corresponding to the Cs nucleus in the CsF molecule (F has no quadrupole moment), and for all values of M. The position of the energy levels for x greater than two or three times $I(2I-1)$ is already given with good accuracy by eq 7 and 9, which were calculated on the assumption of $\alpha^2\gg|\beta|$.

The derivation of the eq 15 is a purely algebraic but rather tedious and laborious process. This is probably true in general of the process of solving secular equations in which the matrix element are still functions of various pertinent parameters. It is not just the solution of the equation that is tedious, but especially the preliminary process of transforming the equation from its determinant form to a polynomial form. The labor involved increases rapidly with the degree of the equation. Therefore, whenever it is necessary to obtain a solution only for a few values of the parameters I and M and x, it is advisable to introduce these values in the matrix elements themselves, and to carry out the rest of the work numerically. Otherwise it may be advisable to consider other ways of reducing the equation to a polynomial form. For example, the coefficients of an algebraic equation can be expressed in terms of the sums of powers of its unknown solutions y_i. In the example above, $K_1=S_1/3$, $K_2=(S_2-S_1^2/3\cdot 6$, $K_3=((S_3-S_1S_2)/6)-S_1^3/27$, where $S_n=\Sigma_i y_i^n$. The quantity S_n is the trace of the matrix of the n-th power of the energy operator; it may well be simpler and safer from mistakes to calculate the necessary S_n than to expand the determinant form of the secular equation.

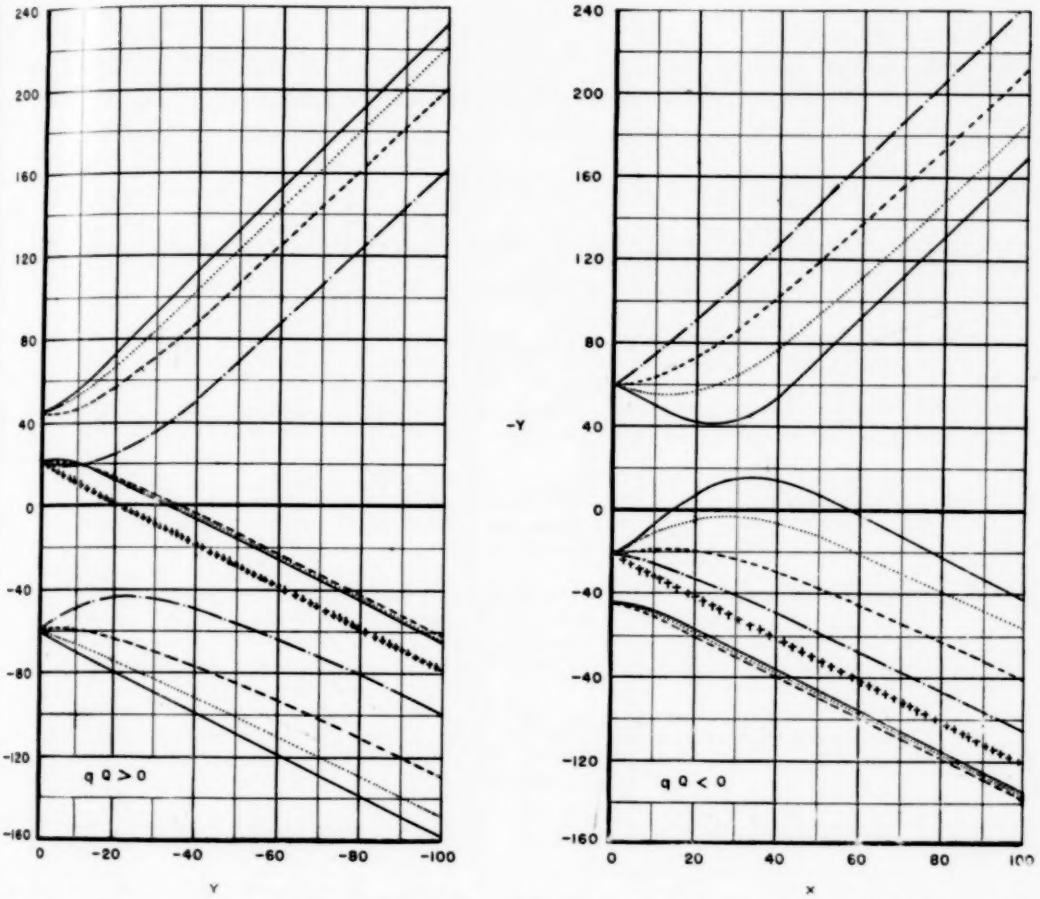

FIGURE 1.—*Plot of the energy levels W_n versus the square of the electric field, E^2, for $n=1$, $I=7/2$, $|M|\leq I+1=9/2$; coordinates are in dimensionless units:*

$$x=-21(lE)^2/e^2qQ(k^2/2A),\ y=420W/e^2qQ.$$

——, $M=\pm 1/2$; . . . , $M=\pm 3/2$; — — —, $M=\pm 5/2$; — · — · —, $M=\pm 7/2$; ++++, $M=\pm 9/2$.

WASHINGTON, March 31, 1947.

J. S. Department of Commerce
National Bureau of Standards

Research Paper RP1867
Volume 40, March 1948

Part of the Journal of Research of the National Bureau of Standards

Preliminary Study on Portions of the Systems Na_2O-CaO-Al_2O_3-Fe_2O_3 and Na_2O-CaO-Fe_2O_3-SiO_2

By William R. Eubank* and Robert H. Bogue*

Portions of the quaternary system Na_2O-CaO-Al_2O_3-Fe_2O_3 have been studied by the exploration of (1), the plane CaO-4CaO.Al_2O_3.Fe_2O_3-(Na_2O+3Al_2O_3) and (2), planes above the base system CaO-5CaO.3Al_2O_3-2CaO.Fe_2O_3 containing successively increasing amounts of Na_2O up to 6 percent. A portion of the quaternary system Na_2O-CaO-Fe_2O_3-SiO_2 has been studied by the exploration of a plane containing 5 percent of Na_2O above the base system CaO-2CaO.SiO_2-CaO.Fe_2O_3.

In the pseudo system CaO-4CaO.Al_2O_3.Fe_2O_3-(Na_2O+3Al_2O_3), the compound Na_2O.8CaO.3Al_2O_3 was found to exist as a primary phase, and the area in which the plane cuts the Na_2O.8CaO.3Al_2O_3 primary-phase volume was established. Three points on univariant curves were located. The iron phase (4CaO.Al_2O_3.Fe_2O_3 solid solution) was observed to exist in a solid-solution series.

In the system Na_2O-CaO-5CaO.3Al_2O_3-2CaO.Fe_2O_3, it was found that the compound Na_2O.8CaO.3Al_2O_3 appears at an Na_2O concentration of about 4.2 percent. However, because soda is taken into solid solution by other phases, it was not feasible at this time to determine the invariant point for Na_2O.8CaO.3Al_2O_3, 3CaO.Al_2O_3, 5CaO.3Al_2O_3, and 4CaO.Al_2O_3.Fe_2O_3 solid solution.

In the system Na_2O-CaO-2CaO.SiO_2-CaO.Fe_2O_3, no ternary compounds were observed up to the 5-percent limit of Na_2O employed. A soda-containing phase was found to occur in solid solution with α 2CaO.SiO_2, which may precipitate on cooling, forming inclusions in the β 2CaO.SiO_2, or enter into reaction with the glassy phase.

I. Introduction

The role of the alkali elements in portland ment has become of increasing interest in cent years, due to the importance attached by me investigators to a reaction that may take ace between the alkalies and certain siliceous ggregates [17, 14, 8].[1] The Portland Cement ssociation Fellowship, over a period of many ars, has conducted an intensive study of the fect of the alkali elements on the phase composi- on of cement clinker. Both potash [19, 20, 21] d soda [2, 6] have been so studied. In continua- on of this research, some of the preliminary vestigations incident to the examination of the inary system Na_2O-CaO-Al_2O_3-Fe_2O_3-SiO_2 have en completed and are herein reported.

Before direct attack can be made upon the inary system, it is necessary to know the phase relations of its boundary quaternary systems. There are five such boundary systems.[2] N-C-A-F; N-C-A-S; N-C-F-S; N-A-F-S; and C-A-F-S. One of these, N-A-F-S, contains no lime and can be considered, from the point of interest in portland cement, as not significant in the investigation. Studies on the system C-A-F-S have been reported by Lea and Parker [12] and by Swayze [18]. A portion of the system N-C-A-S has been explored by Greene and Bogue [7]. The remaining two systems, N-C-A-F and N-C-F-S, require further examination, which is the purpose of this paper.

Studies of the system C-F-S [9, 3] have shown no ternary-compound formation. In an investigation of the system C-A-F [10], the ternary compound C_4AF was reported as the end member of a solid-solution series between C_2F and hypothetical C_2A. Swayze [18] has shown that this series extends to the composition C_6A_2F. As it

*Research Associates at the National Bureau of Standards, representing Portland Cement Association.

[1] Figures in brackets indicate the literature references at the end of this paper.

[2] The following customary abbreviated symbols are used interchangeably with the conventional formulas: N=Na_2O; C=CaO; A=Al_2O_3; F=Fe_2O S=SiO_2; M=MgO; B=B_2O. Thus NC_4A_3=Na_2O.8CaO.3Al_2O_3, etc.

has not yet been found possible to define the precise composition of the solid solution resulting from the crystallization of a given melt in this area, the formula C_4AF *ss* will be employed herein to indicate this iron-containing solid-solution phase. A study [2] of the system N-C-A has revealed that a ternary compound, NC_8A_3, is stable in the high-lime region of those components in equilibrium with C_3A. A subsequent investigation [7] indicated that this compound is also stable, in the system N-C-A-S, in the presence of C_2S and C_3S. It remained to study the reactions of NC_8A_3 in systems containing the iron phase, and further to observe the effects of additions of Na_2O upon compositions in the systems C-A-F and C-F-S. This has been accomplished, and preliminary results are herein presented on three studies: 1. Pseudo system C-C_4AF-(NA_3)[3]; 2. Portion of the system N-C-C_5A_3-C_2F; 3. Portion of the system N-C-C_2S-CF.

II. Experimental Procedure

The phase-equilibrium relations of a four-component system may be expressed in various ways [12, 16]. In the present study two of these methods are employed. In the study of the pseudo-ternary system C-C_4AF-(NA_3), a plane was passed through the tetrahedron N-C-A-F in such a way as to cut the space model at the compositions C, (AF) and (NA_3), (see fig. 1). In the study of the systems N-C-C_5A_3-C_2F and N-C-C_2S-CF, planes were passed through the space model parallel to the soda-free surface (see figs. 3 and 4). In all cases the triangular diagrams obtained by these planes represent arbitrary pseudo-ternary systems. The advantage of this procedure is that the planes may thus be represented in the form of a ternary diagram (see fig. 2). However, it is evident that the information that can be obtained from the diagram of an arbitrary plane through a quaternary system is in general much more limited than that which can be derived from the diagram of a true ternary system. The course of crystallization upon cooling a given melt can be followed on the diagram of a ternary system, but usually this cannot be done for a plane through a quaternary system unless the plane represents a true ternary system.

[3] The parenthesized expressions (NA_3), (N_2A_5) and (AF) are used to indicate arbitrary compositions and are not intended to be understood either as compounds or phases.

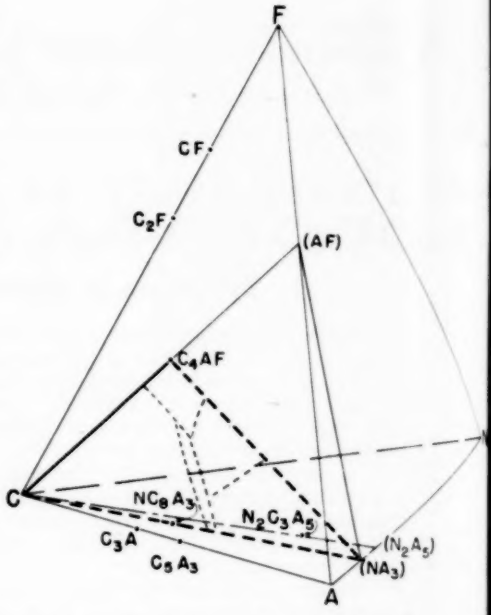

FIGURE 1.—*Tetrahedron, N-C-A-F, within which is the pseudoternary system,* C-C_4AF-(NA_3), *as a part of the plane cutting the tetrahedron at* C-(AF)-(NA_3).

This arises from the fact that crystalline phas in equilibrium with liquids at various temper tures usually have compositions outside t original plane. However, by judicious choice planes, these difficulties may be largely reduce

The quenching method of investigation [2, 1, was employed, except that in some cases t charge was allowed to cool slowly in order th secondary phases might be examined. The phas were identified by optical petrographic method

Both envelopes of platinum foil, and ope platinum pans as first used by Swayze and Brow [18], were employed in this study. It was foun that the alkali loss was much more rapid from th open pans. Therefore, in most cases, platinu envelops were used to hold the charges for burnin

Volatilization of small amounts of soda fro the charges during heating was found to occ when envelopes were employed, but could b controlled and provided for. The charges wer held at the reaction temperature for the shorte period consistent with complete reaction. Th period for equilibrium varied with composition and was usually short, only a few minutes, fo the high-fluidity iron-containing mixes. How

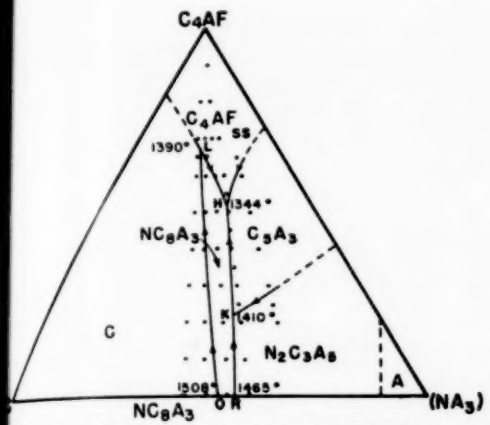

FIGURE 2.—*Field of intersection of the* C-C_4AF-(NA_3) *plane with the* NC_8A_3 *primary phase volume.*

The dots indicate compositions studied.

ver, in the absence of SiO_2 or in the presence of ss than 4 percent of Na_2O, longer periods, some- mes more than an hour, were required. The ss of soda was found to be less when it was dded in certain combined forms, as NA or NS_2. s the loss of soda was found to be proportional the concentration, a definite excess of Na_2O as provided in the preparation of the charges. nalytical checks indicated that the losses were tisfactorily compensated.

Raw materials were specially prepared and of nusually high purity. The Fe_2O_3 and SiO_2 were tter than 99.99 percent pure on a dry basis, and her reagents were better than 99.90 percent.

These raw materials were ground to pass a No. 0 sieve and, after proportioning, further ground an agate mortar. Microscopic examination owed satisfactory mixing. One-hundred gram uantities of C_3A_3, C_2S, (NA_3), C_2F, C_4AF, NA, d NS_2 were prepared. Each mix was given at ast two burns with intermediate grinding and ixing in each case. These materials, together ith $CaCO_3$, were then used as base mixes for reparing 1-g compositions to be studied by the uenching method. Because of the possible loss of da, no preliminary burns were given these mixes.

Water was found to be the most satisfactory uenching medium. Charges were removed from e water immediately after quenching and dried the top of the furnace. The hydration resulting om this procedure was insignificant, and the ficiency of cooling was superior to that obtained ith the use of mercury. The size of the charge was kept small (2 to 10 mg) to improve further the rapidity of freezing.

Permanent mounts of all charges were made, using Hyrax resin of refractive index 1.715. This procedure, which was emphasized by Brown [18], provides a permanent record of the investigation and permits the reexamination of specimens as the need arises.

In many cases, several quenches of a given mix were necessary before the temperature range was reached where the information obtained became pertinent to the investigation. Only those data that are of critical significance are herein recorded. In most instances, glass was the predominant phase, with small amounts of the various crystalline phases appearing embedded in the undercooled matrix.

The thermocouples were recalibrated at frequent intervals because of attack by the soda vapors. For this purpose pure diopside, CMS_2 (1391.5° C), or barium disilicate, BS_2 (1,418° C), were employed, the melting points of these compounds having been confirmed with a couple standardized by the National Bureau of Standards.

Special high-index media were prepared for measuring the refractive indices of the iron compounds. These were made by heating together purified piperine and a mixture of arsenic and antimony tri-iodides according to the method of Larsen and Merwin [11]. These media gave indices ranging from 1.88 to 2.06.

III. Experimental Results

1. Pseudo system C-C_4AF-(NA_3)

The reactions of NC_8A_3 in the presence of iron and alumina compounds, and the character of solid-solution formation between these compounds, were studied by an examination of the pseudo system C-C_4AF-(NA_3). The composition (NA_3) was selected as one of the component vertices so that the plane chosen would include the compound NC_8A_3. This is indicated in figure 1, where the pseudo system is shown to be a portion of a plane cutting the space model at the points C, (AF), and (NA_3). The pseudo system C-C_4AF-(NA_3), indicated in the figure as a scalene triangle within the tetrahedron, is shown to better advantage in figure 2, where it is reproduced as an equilateral triangle. The compositions studied are indicated by dots, and are defined in table 1, together with

TABLE 1.—*Results of quenches in the system* C-C_4AF-(NA_2)

No.	Composition				Temperature	Time	Petrographic examination
	Na_2O	CaO	Al_2O_3	C_4AF			
	NC_8A_3 FIELD						
	%	%	%	%	°C	*min*	
1	9.35	45.0	45.65	0	1,478	50	NC_8A_3, $N_2C_3A_5$, glass.
					1,489	60	NC_8A_3, trace $N_2C_3A_5$, glass.
					1,501	35	Glass, trace NC_8A_3.
2	8.45	40.5	41.05	10	1,461	65	NC_8A_3, $N_2C_3A_5$, glass.
					1,473	60	All glass.
3	7.45	36.0	36.55	20	1,433	55	NC_8A_3, $N_2C_3A_5$, glass.
					1,444	40	NC_8A_3, glass.
					1,463	30	Trace NC_8A_3, glass.
					1,470	30	All glass.
4	6.55	31.5	31.95	30	1,428	30	NC_8A_3, glass.
					1,439	35	All glass.
5	5.6	27.0	27.4	40	1,416	30	NC_8A_3, glass.
					1,423	35	All glass.
6	4.68	22.5	22.82	50	1,390	30	NC_8A_3, iron phase, glass.
					1,401	30	NC_8A_3, glass.
					1,417	35	All glass.
7	3.74	18.0	18.26	60	1,380	30	NC_8A_3, iron phase, glass.
					1,391	35	All glass.
16	4.25	25.0	20.75	50	1,429	30	Trace NC_8A_3, mostly glass.
					1,439	30	All glass.
17	3.4	20.0	16.6	60	1,380	30	NC_8A_3, glass.
					1,391	30	All glass.
35	5.1	20.0	24.9	50	1,340	40	NC_8A_3, C_3A_2, glass.
					1,346	30	All glass.
	C_4AF *ss* FIELD						
8	2.8	13.5	13.7	70	1,392	30	Iron phase, glass.
					1,404	35	All glass.
9	1.87	9.0	9.13	80	1,401	30	Iron phase, glass.
					1,412	35	All glass.
10	0.93	4.5	4.57	90	1,429	30	Iron phase, quench growth glass.
					1,438	30	All glass.
18	2.55	15.0	12.45	70	1,370	30	Iron phase, glass.
					1,380	30	All glass.
28	2.3	16.5	11.2	70	1,400	35	Iron phase, trace CaO, glass.
					1,412	35	All glass.
29	1.53	11.0	7.47	80	1,394	30	Iron phase, glass.
					1,408	20	All glass.
36	4.1	16.0	19.9	60	1,320	30	Iron phase, C_3A_2, glass.
					1,382	30	Small amt. iron phase, glass.
					1,395	30	All glass.
37	3.1	12.0	14.9	70	1,397	30	Trace iron phase, glass.
					1,411	35	All glass.
40	4.6	18.0	22.4	55	1,383	20	Trace iron phase, glass.
					1,395	40	All glass.
46	3.0	17.5	14.5	65	1,370	30	Iron phase, quench growths, glass.
					1,380	45	All glass.
55	4.2	16.0	20.8	65	1,395	35	Iron phase, quench growths, glass.
					1,404	32	All glass.
	C_3A_2 FIELD						
33	7.1	28.0	34.9	30	1,384	30	$N_2C_3A_7$, NC_8A_3, C_3A_2, glass.
					1,387	30	Trace C_3A_2, glass.
					1,391	30	All glass.
34	6.1	24.0	29.9	40	1,342	35	NC_8A_3, C_3A_2, quench growths, glass.
					1,352	55	C_3A_2, trace NC_8A_3, glass.
					1,360	30	All glass.
35	5.1	20.0	24.9	50	1,340	30	C_3A_2, NC_8A_3, glass.
					1,346	30	All glass.
38	7.6	30.0	37.4	25	1,381	30	C_3A_2, NC_8A_3, $N_2C_3A_5$, glass.
					1,390	30	Small amount C_3A_2, glass.
					1,400	30	All glass.

TABLE 1.—*Results of quenches in the system* C-C^{4}AF–(NA^3)—Continued

No.	Composition				Temperature	Time	Petrographic examination
	Na_2O	CaO	Al_2O_3	C_4AF			
C_3A_2 FIELD—Continued							
39	6.6	26.0	32.4	35	1,376	35	C_3A_2, NC_3A_2, glass.
					1,380	30	Trace C_3A_2, glass.
					1,385	30	All glass.
44	5.96	15.0	29.04	50	1,410	25	Trace C_3A_2, glass.
45	4.7	12.0	23.3	60	1,384	30	C_3A_2, iron phase, quench growths, glass.
					1,398	30	Small amount C_3A_2, glass.
					1,404	30	Trace C_3A_2, glass.
47	8.4	21.0	40.6	30	1,516	35	C_3A_2, $N_2C_3A_3$, glass.
					1,551	30	C_3A_2, glass.
48	7.1	18.0	34.9	40	1,454	30	C_3A_2, $N_2C_3A_3$, glass.
					1,470	30	C_3A_2, trace $N_2C_3A_3$, glass.
					1,488	35	Trace C_3A_2, glass.
50	8.1	12.0	39.9	40	1,498	35	C_3A_2, $N_2C_3A_3$, glass.
					1,540	45	C_3A_2, glass.
54	5.6	22.0	27.4	45	1,340	30	C_3A_2, NC_3A_2, glass.
					1,347	35	All glass.
$N_2C_3A_3$ FIELD							
30	10.2	40.0	49.8	0	1,485	30	$N_2C_3A_3$, glass.
					1,495	30	Do.
31	9.2	36.0	44.8	10	1,450	30	Do.
32	8.2	32.0	39.8	20	1,420	30	Do.
					1,430	30	All glass.
42	9.5	24.0	46.5	20	1,460	30	$N_2C_3A_3$, glass.
					1,490	35	Do.
43	8.9	22.5	43.6	25	1,495	45	Do.
CaO FIELD							
11	8.5	50.0	41.5	0	1,501	35	NC_3A_2, glass.
					1,514	35	CaO, NC_3A_2, glass.
					1,526	30	CaO, rounded grains, glass.
12	7.6	45.0	37.4	10	1,485	30	CaO, NC_3A_2, quench growths, glass.
					1,495	35	CaO, glass.
13	6.8	40.0	33.2	20	1,483	35	CaO, NC_3A_2, glass.
					1,495	30	Do.
					1,504	30	CaO, large grains, glass.
14	5.9	35.0	29.1	30	1,475	35	CaO, NC_3A_2, glass.
					1,487	30	Small amount CaO, glass.
15	5.1	30.0	24.9	40	1,439	35	NC_3A_2, CaO, glass.
					1,450	30	CaO, glass.
					1,461	30	All glass.
21	7.7	55.0	37.3	0	1,514	35	Small grains CaO, glass.
					1,526	30	Do.
22	6.9	49.5	33.6	10	1,485	30	CaO, NC_3A_2, quench growths, glass.
					1,495	35	Large rounded grains CaO, glass.
23	6.1	44.0	29.9	20	1,483	35	CaO, NC_3A_2, quench growths, glass.
					1,495	30	CaO, NC_3A_2, glass.
					1,504	30	Large grains CaO, glass.
24	5.4	38.5	26.1	30	1,475	35	CaO, quench growths, glass.
					1,487	30	Small amount CaO, glass.
25	4.6	33.0	22.4	40	1,439	35	CaO, small amount NC_3A_2, glass.
					1,461	30	CaO, glass.
26	3.8	27.5	18.7	50	1,439	30	CaO, NC_3A_2, quench growths, iron phase, glass.
					1,448	30	CaO, quench growths, glass.
27	3.1	22.0	14.9	60	1,391	30	CaO, quench growths, NC_3A_2, iron phase, glass.
					1,404	30	CaO, glass.
53	2.7	19.0	13.3	65	1,400	35	Do.
					1,409	35	All glass.

the heat treatments and the phases observed in the quenched charges.

From a study of about 50 compositions in this system, the boundaries defining the area of intersection of this plane with the primary-phase volume of NC_8A_3 were located. This field was found to be rather narrow and to extend from a point near the C_4AF vertex to the base line, C-(NA_3). As NC_8A_3 melts incongruently [2], its composition falls outside of the field for that compound. The boundary curves defining the area of NC_8A_3 in this system are indicated in the figures. The boundary curves extending away from that field, and originating at points on univariant curves, were not studied at length, and are indicated by dashed lines. The intersection point *H*, for C_5A_3, C_4AF *ss*, and NC_8A_3, was determined. Two other intersection points, *K* for C_5A_3, NC_8A_3, $N_2C_3A_5$, and *L* for CaO, C_4AF *ss*, NC_8A_3, also were located. The compositions and melting temperatures of these points, as of the points on the base-line, C-(NA_3) [7], are given in table 2.

TABLE 2.—*Intersection points in the pseudo system* C-C_4AF-(NA_3)

Point	Phases	Composition				Temperature
		CaO	Al_2O_3	Fe_2O_3	Na_2O	
COMPOSITIONS, EXPRESSED AS OXIDES						
		%	%	%	%	°C
H	C_5A_3, C_4AF *ss*, NC_8A_3	44.0	34.2	17.1	4.7	1,344±5
K	C_5A_3, NC_8A_3, $N_2C_3A_5$	42.8	42.8	7.2	7.8	1,410±10
L	C, C_4AF *ss*, NC_8A_3	48.4	26.8	22.3	2.5	1,390±10
O [2]	C, NC_8A_3	46.8	44.2	.....	9	1,508
R [2]	$N_2C_3A_5$, NC_8A_3	43.2	46.5	.....	10.3	1,465

COMPOSITIONS, EXPRESSED AS COMPONENTS			
Point	CaO	C_4AF	(NA_3)
	%	%	%
H	20	52	28
K	32	22	46
L	17	67	16

The curves in figure 2 are sections through bivariant surfaces in the quaternary system N-C-A-F. The intersections of these curves are points on univariant curves in the quaternary system. As the system C-C_4AF-(NA_3) is a pseudo system, none of these points can be considered to be invariant points. Such a point could be an invariant point, but only if the plane selected arbitrarily happened to pass through an invariant point. Intersection points *H* and *L* are on the univariant curves for C_4AF *ss*, C_3A and NC_8A_3 and for CaO, C_4AF *ss* and NC_3A, respectively.

A primary-phase region for C_3A exists in the plane C-AF-A (fig. 1), but is absent in the plane C-AF-(NA_3). On the other hand, a narrow region for NC_8A_3 exists in the plane C-AF-(NA_3), but is absent in the plane C-AF-A. It is to be expected, then, that between the two planes there is an Na_2O concentration at which the C_3A region disappears, and an Na_2O concentration at which the NC_8A_3 region appears. It is probable that these are the concentrations of Na_2O at invariant points. The Na_2O concentration at which NC_8A_3 appears is considered in the investigation of the system N-C-C_5A_3-C_2F.

The formation of iron-containing solid solution was observed by measurements of the refractive indices of the quenched charges. The α index (yellow-brown pleochroism) was measured in each case. Red filters, transmitting the equivalent wavelengths of red lithium light, were at first employed, but the values obtained were found not to differ from those obtained with unfiltered white light. It seems that the high-index media used, because of their reddish-brown color, act as filters, making the use of additional filters unnecessary. The refractive index of the crystalline pleochroic iron phase in this system was found to decrease with decreasing iron content of the charge. Thus, as the calculated percentage of C_4AF was reduced from 90 to 30 percent, the α index of the iron phase was lowered from 2.03 to 1.91.

Considerable difficulty was encountered in crystallizing the iron phase in the low-iron compositions of the NC_8A_3 field. Even when the charge was allowed to cool with the furnace, the cooling rate was still not slow enough to permit satisfactory crystallization of this phase. By a controlled slow cooling, effected by gradual reduction of electrical input into the furnace, the iron phase could be identified microscopically; but crystals large enough for index-of-refraction measurements could not be obtained in charges in which the calculated C_4AF concentration was below 30 percent.

The results of this study have located the

boundaries of the NC_8A_3 primary phase region in a system in which C_4AF is a component. The iron phase has been identified as a solid solution, the composition of which varies with the iron concentration. Evidence has previously been reported [6] leading to the suggestion that C_3A and NC_8A_3 form, under suitable conditions, a solid-solution phase at temperatures below the liquidus. No indication of this was found in the present study. However, in the following investigation, C_3A and NC_8A_3 were sometimes observed as what appeared to be mix-crystals.

2. Portion of the System N-C-C_5A_3-C_2F

From the study above reported, we learn that the soda compound NC_8A_3 exists at equilibrium on the liquidus over a part of the plane represented by the pseudo-ternary system C-C_4AF-(NA_3), as well as in the pseudo-binary system C-(NA_3), as shown by the diagram of figure 1. It was necessary to ascertain further the point in the quaternary system N-C-A-F where the soda compound NC_8A_3 first appears. From figure 1 it is obvious that this will be found within the wedge bounded by C, A, (NA_3) and (AF), i. e., in a region more remote from N than the plane previously studied. The procedure employed was to set up a space model of the system N-C-A-F as before, in which the ternary system C-C_5A_3-C_2F [18] appears on one of the faces, as shown in figure 3. A series of planes parallel to the above face was then drawn at specified Na_2O concentrations, each plane containing a fixed Na_2O value. These planes were arbitrarily spaced at Na_2O concentrations of 2, 4, and 6 percent, the intention being to continue study of successive planes until NC_8A_3 appeared as a primary phase. About 10 composition points were investigated in each soda plane as well as in the soda-free base plane.

It was found that the planes containing 2 percent and 4 percent of Na_2O did not show NC_8A_3 as a primary phase; but when the plane containing 6 percent of Na_2O was explored, it was found to cut the primary-phase volume of NC_8A_3 in a narrow elliptical section extending from about 3 to 22 percent of C_2F. Additional planes containing 5 and 4.5 percent of Na_2O were found also to cut the primary-phase volume of NC_8A_3, which locates between 4.0 and 4.5 percent the Na_2O concentration at which NC_8A_3 first appears. Further planes to locate this concentration more

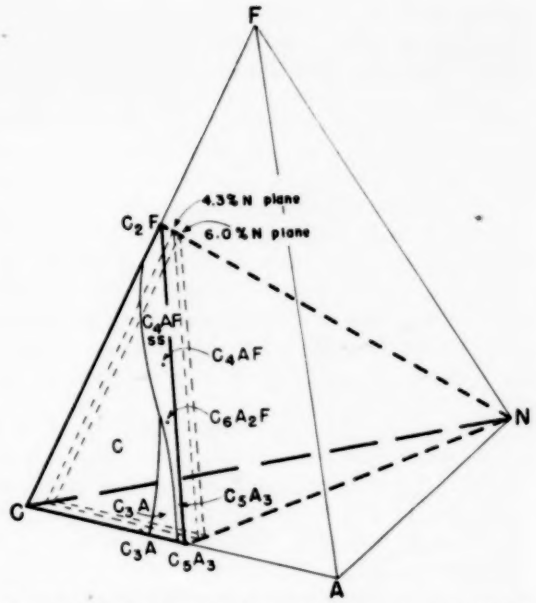

FIGURE 3.—*Tetrahedron, N-C-A-F, on one face of which is shown the ternary system* C-C_5A_3-C_2F [18], *and within which appears the quaternary system* N-C-C_5A_3-C_2F.

precisely were not explored; but it was concluded that the Na_2O concentration could be placed at about 4.2 percent.

These exploratory studies indicate that the temperature of the quaternary invariant point may be higher, rather than lower, than the 1,335° C [10, 18], reported for the soda-free, ternary invariant point for C_5A_3, C_3A, iron phase and liquid. The explanation appears to be that certain phases, especially C_5A_3 and the iron phase, are not pure and the resulting solid solutions may melt at higher temperatures than the pure compounds. It is theoretically possible for solid solution freezing-point curves to pass through either maxima or minima. The latter phenomenon, however, is the more common. Examples of each of these cases are discussed by Findlay [4] and others.

The effects of solid-solution formation have been noted by a number of investigators, and the readiness with which C_5A_3 enters into such solution has been reported. In the presence of Fe_2O_3, the refractive indices of the C_5A_3 phase have been found to be markedly raised [10]. As much as 8 percent of C_4AF may be taken up by C_5A_3, and up to 5 percent of C_5A_3 or C_3A may be

774908—48——5

taken up by C_4AF [13]. In the system N-C-A [2], the C_5A_3 phase crystallizes as a solid solution with Na_2O, and as little as 1 percent of Na_2O raises the melting point of C_5A_3 25 degrees. Likewise, in the system N-C-A-S [7], the invariant point for C_2S, C_3A, C_5A_3 and NC_8A_3 has been reported to occur at a temperature 30 degrees higher than that of the corresponding soda-free invariant point for C_2S, C_3A, and C_5A_3. From these results it appears that the formation of solid solutions involving C_5A_3 with Fe_2O_3 or Na_2O, as well as those concerned with the iron phase [18] may be responsible for the increased temperature in the compositions under discussion in the present investigation.

There seems to be some possibility of the existence of solid solution also in the case of C_3A and NC_8A_3. Occasionally, large isotropic grains of C_3A were seen to contain fine granules of grey birefringent material. The birefringence of this granular material corresponds to that for NC_8A_3. Such a large grain then has a mottled birefringence. This presents some evidence that fine grains of NC_8A_3 may be embedded in the C_3A matrix, resulting from a reaction of alkali with C_3A. Whether or not this is a solid solution is still not certain.

3. Portion of the System N-C-C_2S-CF

In former studies of the system C-F-S in the region of portland cement [9, 3], no ternary compounds were found. It was necessary, however, to extend that study by the introduction of Na_2O as a component. Accordingly, the quaternary system N-C-F-S was set up in a manner similar to that employed in the previous studies on the system N-C-A-F. Figure 4 shows the tetrahedron N-C-F-S on one face of which are given the boundary curves and joins of the system C-C_2S-CF [3]. A plane parallel to the plane of this system cutting the tetrahedron at 5-percent Na_2O concentration was explored, and is indicated on the diagram. Twenty compositions in this plane and five compositions in the soda-free plane were studied.

The burning and quenching techniques employed were the same as previously used, with the exception that additional burns of some mixes were made wherein the charge was allowed to cool slowly so that the secondary phases present might be examined.

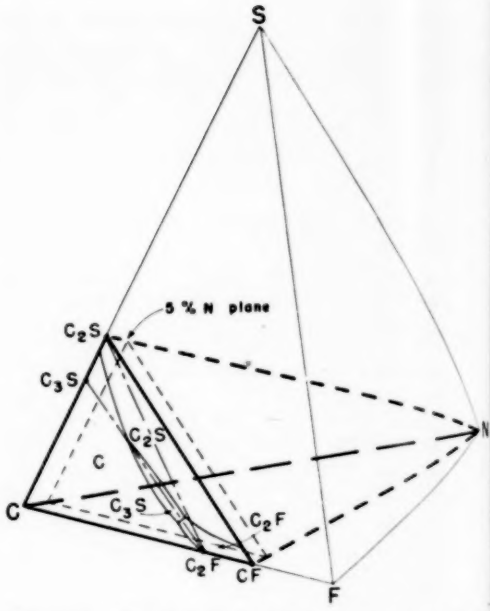

FIGURE 4.—*Tetrahedron, N-C-F-S, on one face of which is shown the ternary system,* C-C_2S-CF [3], *and within which appears the quaternary system* N-C-C_2S-CF.

It was observed that no ternary compounds were formed in this system with Na_2O additions of 5 percent. The temperature of liquid formation was lowered, however, due to the presence of Na_2O. Even in the presence of Na_2O, however, it was observed that charges near the C_2S-CF join and close to C_2S in composition were very refractory, showing little liquid at temperatures up to 1,550° C. As the composition moved away from the C_2S point and contained increasing concentrations of C_2F, the amount of liquid formed was found to increase. In a mix containing only 31.5 percent of CaO, the charge was completely liquid at 1,320°. In charges containing 15 percent or more of Fe_2O_3, it was noted that the C_2S grains were usually surrounded by a dark matrix which appeared more opaque as the iron concentration increased. This phase occurred in both the crystalline and glassy states; when crystalline, its birefringence was deep red. In many cases a region of higher birefringence (yellow to bright red) existed at the interface of this phase and the C_2S crystals, which would seem to indicate some reaction between the C_2S and the surrounding phase. It is possible that soda-contain-

g solid solutions within the C_2S react to some tent with the iron-containing matrix. Many he inclusions thought to contain soda were equently observed in the C_2S grains.

In this investigation soda was added as the lassy compound NS_2. As this compound crys-allizes only under carefully controlled conditions very slow cooling, no NS_2 crystals were ob-erved in any of the burns. However, only one quid phase was observed and, because a liquid hase was always present, it is probable that the oda was concentrated there.

No C_3S was observed in the 5-percent Na_2O lane studied. Apparently this compound is not able in the presence of Na_2O of that concentra-on. It has been observed that soda reacts ith C_3S, converting it to free CaO and C_2S, and hen enters into solid solution with the C_2S. ence soda causes free CaO to form, which would t otherwise appear, thus enlarging its primary-hase region. Conversely, the size of the C_3S rimary-phase region is decreased, or disappears ntirely as in the concentrations herein reported. he location of the C_2S and iron-phase fields ap-ear essentially unchanged in the 5-percent Na_2O lane.

IV. Discussion

In the investigations herein reported, SiO_2 and Al_2O_3 were not present together in any of the ompositions studied. The purpose, as already xplained, was to provide the necessary informa-on preliminary to the extension of the studies to he quinary system N-C-A-F-S.

The work has revealed that the extension of the eld of CaO due to the introduction of Na_2O, as reviously reported for the system N-C-A-S [7], pplies also in the systems and regions covered the present study. Also, the presence of soda as observed to lower the temperature of forma-on of first liquid. However, the influence of oda on the burnability of portland cement clinker annot be stated with assurance until the simulta-eous phase-equilibrium relations of all five omponents have been completed.

Likewise, the nature of the soda phase in port-and cement clinker cannot be stated with assur-nce until the completion of the quinary system. t the present state of information, it appears hat the phase NC_8A_3 is stable over a wide range and probably constitutes the principal soda phase in clinker, although soda has been observed to enter into several different solid solutions. It is possible that this phase may interact with calcium sulfate, as was found to be the case with the potash compound $KC_{23}S_{12}$ [21]. In that case we might expect Na_2SO_4 and C_3A to be produced, a reaction for which we have some evidence.

It had previously been shown [6] that soda enters into solid solution with α C_2S following interaction with C_3S by which CaO is liberated. When the α C_2S solid solution inverts to the β form on cooling, the soda appears to be precipitated, perhaps as NC_8A_3, and to remain as inclusions in the crystallized silicate grains. Further evidence of this reaction was obtained in the present study, where the C_2S phase was observed in all three of its polymorphic forms. Soda-containing charges that were rapidly quenched from 1,300° C or above were sometimes observed to contain α C_2S, characterized by its glassy appearance and α index close to 1.713 [6]. The crystals in many cases were found to contain very fine dark inclusions. The α to β inversion temperature was found to be lowered from 1,456° C, as reported by Newman and Wells [15]) by as much as 156 degrees. The β form of C_2S, readily identified by its twinned structure, was found in slowly cooled burns. These crystals contained inclusions of fairly large rounded grains that are believed to be due to the exsolution of a soda-containing phase. The slowly cooled charges contained considerable amounts of γ C_2S, and often dusted due to the inversion of the β C_2S to the gamma form.

Occasionally in charges of high-iron concentration, small areas of brighter color and higher birefringence were observed in the dark-brown glass surrounding the grains of dicalcium silicate. It appears probable that these areas are caused by an interaction of the soda (coming out of solution in the C_2S) with the surrounding glass.

The petrologic significance of certain ternary subsystems in the high-silica portion of the system N-C-A-S has recently been reported by Goldsmith [5]. Although these investigations consider concentrations of silica much higher than those encountered in this study, certain relations such as those of solid solution appear to be similar. The predominance of solid solutions in these sys-

tems is worthy of note. It was stated that the only substantially pure phase existing either in natural magmas or synthetic melts in this range of compositions is the mineral quartz. All other phases exist in some form of solid solution. A similar situation seems to exist in the systems under consideration here. In this case it is likely that the only pure phase encountered is free CaO, the remaining phases reacting with each other to a more or less extent to form solid solutions.

Certain of these solid solutions may be defined only in terms of the oxide components of the large quaternary system N-C-A-S. In other words, ternary subsystems having various compounds such as C_4AF or C_5A_3 as components may be nonternary. That is, phases encountered are not capable of being expressed in terms of the end members of the ternary system considered, and liquids formed upon crystallization of solid solutions fall outside that ternary system in composition. One reason for this appears to arise from the nature of these solid solutions, in which solution takes place in the form of the smaller oxide units, rather than the larger ones involving compounds.

At the liquidus, such systems may behave as ordinary ternary systems. However, as stated earlier, below the liquidus the composition of both solid solutions and liquids is usually outside the given plane. Courses of crystallization cannot be traced readily, and the phase-equilibrium relations in general increase in complexity in these systems containing solid solutions.

V. References

[1] L. T. Brownmiller, Am. J. Sci. **26,** 260 (1935), PCAF paper 30.

[2] L. T. Brownmiller and R. H. Bogue, Am. J. Sci. **23,** 501 (1932), PCAF paper 25.

[3] M. D. Burdick, J. Research NBS **25,** 475 (1940) RP1340.

[4] A. Findlay, The phase rule, 5th ed., pp. 145-149 (Longmans, Green & Co., New York, N. Y., 1923).

[5] J. R. Goldsmith, J. Geol. **55,** 381 (1947).

[6] K. T. Greene, J. Research NBS **32,** 1 (1944) RP1570, PCAF paper 45.

[7] K. T. Greene and R. H. Bogue, J. Research NBS **36,** 185 (1946) RP1699, PCAF paper 47.

[8] W. C. Hansen, J. Am. Concrete Inst. **40,** 213 (1944).

[9] W. C. Hansen and R. H. Bogue, J. Am. Chem. Soc. **48,** 1261 (1926), PCAF paper 1.

[10] W. C. Hansen, L. T. Brownmiller, and R. H. Bogue, J. Am. Chem. Soc. **50,** 396 (1928), PCAF paper 13.

[11] E. S. Larsen and H. E. Merwin, Am. J. Sci. **34,** 42 (1912).

[12] F. M. Lea and T. W. Parker, Proc. Royal Soc. [A] **234,** 1 (1934).

[13] H. F. McMurdie, J. Research NBS **18,** (1937), RP967.

[14] H. S. Meissner, J. Am. Concrete Inst. **37,** 549 (1941).

[15] E. S. Newman and L. S. Wells, J. Research NBS **36,** 137 (1946) RP1696.

[16] J. F. Schairer, J. Am. Ceramic Soc. **35,** 241 (1942).

[17] T. E. Stanton, Proc. Am. Soc. Civil Eng. **66,** 1781 (1940).

[18] M. A. Swayze, Am. J. Sci. **244,** 1, 65 (1946).

[19] W. C. Taylor, J. Research NBS **21,** 315 (1938) RP1131, PCAF paper 37.

[20] W. C. Taylor, J. Research NBS **27,** 311 (1941) RP1421, PCAF paper 40.

[21] W. C. Taylor, J. Research NBS **29,** 437 (1942) RP1512, PCAF paper 43.

WASHINGTON, August 11, 1947.

U. S. Department of Commerce
National Bureau of Standards

Research Paper RP1868
Volume 40, March 1948

Part of the Journal of Research of the National Bureau of Standards

Theory and Design of a Cavity Attenuator

By J. J. Freeman

The fields generated by an arbitrary current distribution exciting a piston-type or cavity attenuator are developed, and symmetric distributions exciting maximum amplitudes of the dominant mode and minimum amplitudes of unwanted modes are investigated. The relative error in voltage measurement due to spurious modes is computed as a function of spacing between exciting and receiving coils for certain simple current distributions. The relative merits of circular and rectangular attenuator cross sections are discussed.

I. Introduction

The cavity attenuator, also known as a piston or mutual inductance type attenuator, was first designed by Wheeler, Harnett, and Case [1][1] for use in signal generators, and has since found wide application. It consists of a hollow tube excited below its cut-off frequency and a coil or capacitor, which picks up the attenuated field. As the generated electromagnetic field falls off exponentially with distance from the exciting source, and as the attenuation constant may be computed from the dimensions of the tube, the ratio of any two voltages is reduced to a measurement of length.

Preparatory to the design and construction of such an attenuator, it was thought advisable to investigate the theory to determine the kind of excitation required for optimum mode purity, and an evaluation of the amplitudes of the unwanted modes, for different types of excitation. A rigorous solution of the problem is impossible, but an approximate solution that is useful consists in determining the field produced by an arbitrary-current distribution within a waveguide closed at both ends. Here the perturbation of the field by the receiving loop is neglected. It may also be assumed that the exciting current distribution is maintained by a constant-current generator.

Thus, given a distribution of current density, $\mathbf{J}(x', y', z')e^{-j\omega t}$, the field produced within a perfectly conducting cavity is sought. The scalar analogue, where $\mathbf{J}(x', y', z')$ is replaced by ρ, the charge density, is well known, and has been treated elegantly by Sommerfeld [2]. The vector problem is solved analogously, by expansion into orthogonal *vector* wave functions, and has been treated by Heitler [3], Condon [4], and others. For completeness, the method is outlined below.

[1] Figures in brackets indicate the literature references at the end of this paper.

II. Expansion of the Field into Normal Vector Functions

MKS units are used and the fields and source are assumed to vary as $e^{-j\omega t}$. Then, according to Maxwell's equations [5], one must find a solution for

$$\nabla\times\nabla\times\mathbf{E}-k^2\mathbf{E}=j\omega\mu\mathbf{J}, \tag{1}$$

subject to the boundary condition that $\mathbf{n}\times\mathbf{E}=0$ on the surface S of the cavity, where $\mathbf{n}$ is the normal on S. $\mathbf{E}$ is the electric field, $\mathbf{J}$ the impressed current density, and $k^2=\omega^2\mu\epsilon$. As any vector field may be shown to consist of two parts, one of zero curl, and the other of zero divergence, let $\mathbf{J}=\mathbf{J}_1+\mathbf{J}_2$, where curl $\mathbf{J}_1=0$, and div. $\mathbf{J}_2=0$. Let $\mathbf{E}=\mathbf{E}_1+\mathbf{E}_2$, where curl $\mathbf{E}_1=0$, and div $\mathbf{E}_2=0$. Then, if

$$\text{curl}^2\,\mathbf{E}_2-k^2\mathbf{E}_2=j\omega\mu\mathbf{J}_2 \tag{2}$$

and if

$$\mathbf{E}_1=-\frac{j\omega\mu}{k^2}\mathbf{J}_1, \tag{3}$$

then $\mathbf{E}=\mathbf{E}_1+\mathbf{E}_2$ satisfies eq 1.

If ψ_α is a solution of $\nabla^2\psi_\alpha+k^2{}_\alpha\psi_\alpha=0$, and $\psi_\alpha=0$ on S, the interior surface of the cavity, $\nabla\psi_\alpha\times\mathbf{n}=0$ on S. If the ψ_α are normalized and orthogonal, then $\frac{1}{k_\alpha}\nabla\psi_\alpha$ are normalized and orthogonal, because

$$\int\nabla\psi_\alpha\cdot\nabla\psi_\beta d\tau=\int(\nabla\cdot[\psi_\beta\nabla\psi_\alpha]-\psi_\beta\nabla^2\psi_\alpha)d\tau=$$

$$k_\alpha{}^2\int\psi_\alpha\psi_\beta d\tau.$$

Here $d\tau$ is an element of volume, and the integration is performed throughout the volume of the cavity.

Then if we call the normalized $\frac{1}{k_\alpha}\nabla\psi_\alpha=\mathbf{E}_\alpha$, an arbitrary irrotational vector function whose tangential component vanishes on S may be developed in terms of the $\mathbf{E}_\alpha$.

Thus,

$$\mathbf{E}_1=\sum_\alpha a_\alpha \mathbf{E}_\alpha,$$

where

$$a_\alpha=\int \mathbf{E}_1\cdot\mathbf{E}_\alpha d\tau$$

$$\mathbf{J}_1=\sum_\alpha \int \mathbf{J}_1\cdot\mathbf{E}_\alpha d\tau \mathbf{E}_\alpha$$

Substituting the above expression for $\mathbf{J}_1$ in eq 3,

$$\mathbf{E}_1(r)=-\frac{j\omega\mu}{k^2}\sum_\alpha \int \mathbf{J}_1(r')\cdot\mathbf{E}_\alpha(r')d\tau'\mathbf{E}_\alpha(r). \quad (4)$$

If one had a complete set of orthogonal vector wave functions $\mathbf{E}_\beta$, and if div $\mathbf{E}_\beta=0$, and $\mathbf{n}\times\mathbf{E}_\beta=0$, an arbitrary solenoidal vector, whose tangential component vanished on S, in particular $\mathbf{E}_2$, could be expanded in terms of the $\mathbf{E}_\beta$. Suppose the $\mathbf{E}_\beta$ are solutions of

$$\text{curl}^2\ \mathbf{E}_\beta-k_\beta^2\mathbf{E}_\beta=0,$$

where $\mathbf{n}\times\mathbf{E}_\beta=0$, and div $\mathbf{E}_\beta=0$. Then it may be shown that the $\mathbf{E}_\beta$ are orthogonal to each other, and to the $\mathbf{E}_\alpha$.

Let $\mathbf{E}_2=\Sigma e_\beta\mathbf{E}_\beta$, and let $\mathbf{J}_2=\Sigma j_\beta\mathbf{E}_\beta$. Then $j_\beta=\int \mathbf{J}_2\cdot\mathbf{E}_\beta d\tau$. Substituting the above values for $\mathbf{E}_2$ and $\mathbf{J}_2$ in eq 2,

$$\left.\begin{aligned} e_\beta&=\frac{j\omega\mu}{k_\beta^2-k^2}\int \mathbf{J}_2\cdot\mathbf{E}_\beta d\tau \\ \mathbf{E}_2&=j\omega\mu\sum_\beta \frac{\int \mathbf{J}_2(r')\cdot\mathbf{E}_\beta(r')}{(k_\beta^2-k^2)}\ d\tau'\mathbf{E}_\beta(r) \end{aligned}\right\} \quad (5)$$

Since the $\mathbf{E}_\alpha$ are orthogonal to the $\mathbf{E}_\beta$, and the $\mathbf{E}_\alpha$ and $\mathbf{E}_\beta$ are assumed complete for expansions of electric fields of zero curl and zero divergence, respectively, $\int \mathbf{J}_2\cdot\mathbf{E}_\alpha d\tau=\int \mathbf{J}_1\cdot\mathbf{E}_\beta d\tau=0$. Accordingly, we may drop the subscripts in $\mathbf{J}_1$ and $\mathbf{J}_2$ in eq 4 and 5, and substitute the total current density, $\mathbf{J}$. Thus

$$\left.\begin{aligned} \mathbf{E}_1(r)&=\frac{-j\omega\mu}{k^2}\sum\int \mathbf{J}(r')\cdot\mathbf{E}_\alpha(r')d\tau'\mathbf{E}_\alpha(r) \\ \mathbf{E}_2(r)&=j\omega\mu\sum\frac{\int \mathbf{J}(r')\cdot\mathbf{E}_\beta(r')d\tau'}{(k_\beta^2-k^2)}\ \mathbf{E}_\beta(r) \end{aligned}\right\} \quad (6)$$

III. Attenuators of Circular Cross Section

The normal vector modes are now considered for the circular cylinder of radius a, and length d, where $\mathbf{i}_1$, $\mathbf{i}_2$ and $\mathbf{k}$ are the unit vectors in the directions of increasing r, θ and z.

Orthogonal vector wave functions have been treated by Stratton [6], and the normal vector modes are most easily obtained by following his treatment, and satisfying the appropriate boundary conditions. For the interior of a circular cylinder,

$$\begin{aligned} \mathbf{E}\alpha=\mathbf{E}_{\substack{e\\ nml}}&=\frac{F_{\substack{e\\ nm}}}{\sqrt{\lambda^2_{nm}+\frac{l^2\pi^2}{d^2}}} \\ &\left[\left\{\lambda_{nm}J_n'(\lambda_{nm}r)\begin{pmatrix}\cos n\theta\\ \sin n\theta\end{pmatrix}\mathbf{i}_1+\right. \\ &\left.\frac{n}{r}\begin{pmatrix}-\sin n\theta\\ \cos n\theta\end{pmatrix}J_n(\lambda_{nm}r)\mathbf{i}_2\right\}\sin\frac{l\pi z}{d}+ \\ &\begin{pmatrix}\cos n\theta\\ \sin n\theta\end{pmatrix}J_n(\lambda_{nm}r)\frac{l\pi}{d}\cos\frac{l\pi z}{d}\mathbf{k}\Bigg] \end{aligned} \quad (7)$$

Here,

$$\lambda_{nm}=\frac{u_{nm}}{a}, \text{ where } J_n(u_{nm})=0 \quad (8)$$

and

$$k_\alpha^2=k_{nml}^2=\lambda_{nm}^2+\left(\frac{l\pi}{d}\right)^2 \quad (9)$$

J_n is the nth order Bessel function. The normalizing factor, F_{nm} is

$$F_{\substack{e\\ nm}}=\begin{pmatrix}\sqrt{4-2\delta_0^n}\\ \sqrt{4-4\delta_0^n}\end{pmatrix}\frac{1}{a\sqrt{\pi d}|J_{n-1}(\lambda_{nm}a)|}, \quad (10)$$

where $\delta_0^n=0$, for $n\neq 0$, and $\delta_0^n=1$, for $n=0$

The normal vector modes $\mathbf{E}_\beta$, consist of two independent, mutually orthogonal sets, the transverse electric type, which we designate as $\mathbf{M}_\beta$ and the transverse magnetic type, which we designate as $\mathbf{N}_\beta$.

$$\mathbf{M}_\beta=\mathbf{M}_{\substack{e\\ nml}}=A_{\substack{e\\ nm}}\left[\frac{n}{r}\begin{pmatrix}-\sin n\theta\\ \cos n\theta\end{pmatrix}J_n(\delta_{nm}r)\mathbf{i}_1-\delta_{nm}J_n'(\delta_{nm}r)\begin{pmatrix}\cos n\theta\\ \sin n\theta\end{pmatrix}\mathbf{i}_2\right]\times\sin\frac{l\pi z}{d} \quad (11)$$

Here, $\delta_{nm}=\frac{v_{nm}}{a}$, $J_n'(v_{nm})=0$

and $k_{nml}^2=\delta_{nm}^2+\left(\frac{l\pi}{d}\right)^2$ (12)

The normalizing factor is

$$A_{nm}^{e}=\frac{2}{\sqrt{\pi d(1+\delta_0^n)}\sqrt{v_{nm}^2-n^2J_n(v_{nm})}} \quad (12a)$$

$$\mathbf{M}_{nml}^{e}=N_{nml}=\frac{F_{nm}^{e}}{\lambda_{nm}\sqrt{\lambda_{nm}^2+\frac{l^2\pi^2}{d^2}}\sqrt{1+\delta_0^l}}\left[-\frac{l\pi}{d}\sin\frac{l\pi z}{d}\left\{\begin{pmatrix}\cos n\theta\\ \sin n\theta\end{pmatrix}\lambda J_n'(\lambda_{nm}r)\mathbf{i}_1+\frac{n}{r}\begin{pmatrix}-\sin n\theta\\ \cos n\theta\end{pmatrix}J_n(\lambda_{nm}r)\mathbf{i}_2+\right.\right.$$

$$\left.\left.\lambda_{nm}^2\cos\frac{l\pi z}{d}J_n(\lambda_{nm}r)\begin{pmatrix}\cos n\theta\\ \sin n\theta\end{pmatrix}\mathbf{k}\right]\right. \quad (13)$$

When no ambiguity results, the subscripts l, m, are omitted and λ_{nm}, is written, for instance, as λ. The even, odd designations $\binom{e}{o}$, are also omitted and one writes $\mathbf{m}_o^e$ as $\mathbf{m}$, the even, odd designation being implied.

Substituting eq 11 and 13 in eq 6,

$$\mathbf{E}_2=j\omega\mu\sum_{n,m,l}\frac{\int\mathbf{J}(r').M_0^e(r')d\tau'M_0^e(r)}{\delta^2+\left(\frac{l\pi}{d}\right)^2-k^2}+$$

$$j\omega\mu\sum_{n,m,l}\frac{\int\mathbf{J}(r')\cdot\mathbf{N}_0^e(r')d\tau'\mathbf{N}_0^e(r).}{\lambda^2+\left(\frac{l\pi}{d}\right)^2-k^2} \quad (14)$$

Call the first summation **A**, the second **B**, so that

$$\mathbf{E}_2=\mathbf{A}+\mathbf{B}.$$

$$\text{Let } \mathbf{M}_{nml}^{e}=A_{nm}\mathbf{m}_{nm}^{e}\sin\frac{l\pi z}{d}$$

where

$$\mathbf{m}_{nm}^{e}=\frac{n}{r}\begin{pmatrix}-\sin n\theta\\ \cos n\theta\end{pmatrix}J_n(\delta r)\mathbf{i}_1-\begin{pmatrix}\cos n\theta\\ \sin n\theta\end{pmatrix}\delta J_n'(\delta r)\mathbf{i}_2$$

Then

$$\mathbf{A}=j\omega\mu\sum_{n,m}A_{nm}^2\int\mathbf{J}(r').\mathbf{m}(r')\mathbf{m}(r)\sum_{l=1}^{\infty}\frac{\sin\frac{l\pi z'}{d}\sin\frac{l\pi z}{d}}{\delta^2-k^2+\left(\frac{l\pi}{d}\right)^2}d\tau' \quad (15)$$

In appendix I, it is shown that

$$\sum_{l=1}^{\infty}\frac{\sin\frac{l\pi z'}{d}\sin\frac{l\pi z}{d}}{\delta^2-k^2+\left(\frac{l\pi}{d}\right)^2}=S_1=$$

$$\frac{d}{2\gamma}\sinh\gamma z'\left(\frac{1-e^{-2\gamma(d-z)}}{1-e^{-2\gamma d}}\right)e^{-\gamma z},$$

where $\gamma_{nm}=\sqrt{v_{nm}^2-k^2}$

Substituting the above in eq 15, and substituting the value of A_{nm} given in eq 12*a*.

$$\mathbf{A}=j\omega\mu\sum_{n=0}^{\infty}\sum_{m=1}^{\infty}\frac{2e^{-\gamma z}\left(\frac{1-e^{-2\gamma(d-z)}}{1-e^{-2\gamma d}}\right)}{\pi(1+\delta_0^n)(v_{nm}^2-n^2)J_n^2(v_{nm})\gamma}\int\mathbf{J}(r').\mathbf{m}(r')\mathbf{m}(r)\sinh\gamma z'd\tau' \quad (16)$$

Let

$$\mathbf{n}_{o}^{enm}=\left[-\lambda_{nm}J_n'(\lambda r)\begin{pmatrix}\cos n\theta\\ \sin n\theta\end{pmatrix}\mathbf{i}_1+\right.$$

$$\left.\begin{pmatrix}\sin n\theta\\ -\cos n\theta\end{pmatrix}\frac{n}{r}J_n(\lambda r)\mathbf{i}_2\right] \quad (17)$$

and

$$\mathbf{p}_{o}^{enm}=\begin{pmatrix}\cos n\theta\\ \sin n\theta\end{pmatrix}J_n(\lambda r)\mathbf{k} \quad (18)$$

Substituting eq 17 and eq 18 in the second sum of eq 14, we get

$$\mathbf{B}=j\omega\mu\int\mathbf{J}(r').\sum_{n,m}\frac{F_{0,m}^{e}}{\lambda^2}$$

$$\left\{\mathbf{n}(r')\mathbf{n}(r)\sum_{l=1}^{\infty}\frac{\left(\frac{l\pi}{d}\right)^2\sin\frac{l\pi z'}{d}\sin\frac{l\pi z}{d}}{\left(\lambda^2+\frac{l^2\pi^2}{d^2}\right)\left(\lambda^2-k^2+\frac{l^2\pi^2}{d^2}\right)}+\right.$$

$$\lambda^2\mathbf{n}(r')\mathbf{p}(r)\sum_{l=1}^{\infty}\frac{\frac{l\pi}{d}\sin\frac{l\pi z'}{d}\cos\frac{l\pi z}{d}}{\left(\lambda^2+\frac{l^2\pi^2}{d^2}\right)\left(\lambda^2-k^2+\frac{l^2\pi^2}{d^2}\right)}+$$

$$\lambda^2\mathbf{p}(r')\mathbf{n}(r)\sum_{l=1}^{\infty}\frac{\frac{l\pi}{d}\cos\frac{l\pi z'}{d}\sin\frac{l\pi z}{d}}{\left(\lambda^2+\frac{l^2\pi^2}{d^2}\right)\left(\lambda^2-k^2+\frac{l^2\pi^2}{d^2}\right)}+$$

$$\lambda^4\mathbf{p}(r')\mathbf{p}(r)$$

$$\left.\sum_{l=0}^{\infty}\frac{\cos\frac{l\pi z'}{d}\cos\frac{l\pi z}{d}}{\left(\lambda^2+\frac{l^2\pi^2}{d^2}\right)\left(1+\delta_0^l\right)\left(\lambda^2-k^2+\frac{l^2\pi^2}{d^2}\right)}\right\}d\tau' \quad (19)$$

Similarly, if eq 17, 18, and 7 are substituted in eq 6,

$$\mathbf{E}_1=-\frac{j\omega\mu}{k^2}\int\mathbf{J}(r')\cdot\sum_{n,m}F_{nm}^2$$
$$\left\{\mathbf{n}(r')\mathbf{n}(r)\sum_{l=1}^{\infty}\frac{\sin\frac{l\pi z'}{d}\sin\frac{l\pi z}{d}}{\lambda^2+\frac{l^2\pi^2}{d^2}}-\mathbf{n}(r')\mathbf{p}(r)\right.$$
$$\sum_{l=1}^{\infty}\frac{\frac{l\pi}{d}\sin\frac{l\pi z'}{d}\cos\frac{l\pi z}{d}}{\lambda^2+\frac{l^2\pi^2}{d^2}}-\mathbf{p}(r')\mathbf{n}(r)$$
$$\sum_{l=1}^{\infty}\frac{\frac{l\pi}{d}\cos\frac{l\pi z'}{d}\sin\frac{l\pi z}{d}}{\lambda^2+\frac{l^2\pi^2}{d^2}}+\mathbf{p}(r')\mathbf{p}(r)$$
$$\left.\sum_{l=1}^{\infty}\frac{\frac{l^2\pi^2}{d^2}\cos\frac{l\pi z'}{d}\cos\frac{l\pi z}{d}}{\lambda^2+\frac{l^2\pi^2}{d^2}}\right\}d\tau' \qquad (20)$$

With a little manipulation, $\mathbf{E}_1$ and $\mathbf{B}$ may be combined to give

$$\mathbf{E}_1+\mathbf{B}=\frac{j}{\omega\epsilon}\int\mathbf{J}(r')\cdot\sum_{n,m}F^2$$
$$\left\{\mathbf{n}(r')\mathbf{n}(\mathbf{r})\frac{k^2-\lambda^2}{\lambda^2}\sum_{l=1}^{\infty}\frac{\sin\frac{l\pi z'}{d}\sin\frac{l\pi z}{d}}{\lambda^2-k^2+\frac{l^2\pi^2}{d^2}}+\right.$$
$$\mathbf{n}(r')\mathbf{p}(r)\sum_{l=0}^{\infty}\frac{\frac{l\pi}{d}\sin\frac{l\pi z'}{d}\cos\frac{l\pi z}{d}}{\lambda^2-k^2+\frac{l^2\pi^2}{d^2}}+$$
$$\mathbf{p}(r')\mathbf{n}(r)\sum_{l=1}^{\infty}\frac{\frac{l\pi}{d}\cos\frac{l\pi z'}{d}\sin\frac{l\pi z}{d}}{\lambda^2-k^2+\frac{l^2\pi^2}{d^2}}+$$
$$\mathbf{p}(r')\mathbf{p}(r)\sum_{l=0}^{\infty}\left(k^2-\frac{l^2\pi^2}{d^2}\right)$$
$$\left.\frac{\cos\frac{l\pi z'}{d}\cos\frac{l\pi z}{d}}{\left(\lambda^2-k^2+\frac{l^2\pi^2}{d^2}\right)(1+\delta_0^l)}\right\}d\tau' \qquad (21)$$

Thus the contribution to the field from $\mathbf{E}_1$ is exactly equal and opposite to part of the contribution arising from $\mathbf{B}$, so that the total field may now be divided into two parts (1) a transverse electric field, $\mathbf{E}_{TE}$, which corresponds at low frequencies to inductive coupling, and (2) a transverse magnetic field, $\mathbf{E}_{TM}$, which corresponds at low frequencies to capacitative coupling. Thus

$$\mathbf{E}_{TE}=\mathbf{A},$$
$$\mathbf{E}_{TM}=\mathbf{E}_1+\mathbf{B}, \text{ and}$$
$$\mathbf{E}_{Total}=\mathbf{E}_{TE}+\mathbf{E}_{TM}.$$

The various infinite sums are evaluated in appendix I and II. When the values of these summations are substituted in eq 15 and eq 21, we get for $z>z'$,

$$\mathbf{E}_{TE}=\mathbf{A}=j\omega\mu\sum_{n=0}^{\infty}\sum_{m=1}^{\infty}\frac{2e^{-\gamma_{nm}z}(1-e^{-2\gamma_{nm}(d-z)})}{\pi(1+\delta_0^n)(v_{nm}^2-n^2)J_n^2(v_{nm})\gamma_{nm}(1-e^{-2\gamma_{nm}d})}[\int\mathbf{J}(r')\cdot\mathbf{m}_{omn}^{e}(r')\mathbf{m}_{omn}^{e}(r)\sinh\gamma_{nm}z'd\tau'] \qquad (22)$$

$$\mathbf{E}_{TM}=\mathbf{E}_1+\mathbf{B}=-\frac{j}{\omega\epsilon}\sum_{n=0}^{\infty}\sum_{m=1}^{\infty}\frac{(2-\delta_0^n)e^{-\eta_{nm}z'}}{\pi u_{nm}^2J_{n-1}^2(u_{nm})(1-e^{-2\eta_{nm}d})}\left[(1-e^{-2\eta_{nm}(d-z)})\int\mathbf{J}(r')\cdot\right.$$
$$[\mathbf{n}_{nm}(\mathbf{r}')\mathbf{n}_{nm}(\mathbf{r})\eta_{nm}\sinh\eta_{nm}z'-\lambda_{nm}^2\mathbf{p}_{nm}(r')\mathbf{n}_{nm}(r)\cosh\eta_{nm}z']d\tau'+(1+e^{-2\eta_{nm}(d-z)})\int\mathbf{J}(r')\cdot$$
$$\left.\left[\lambda_{nm}^2\eta_{nm}(r')\mathbf{p}(r)\sinh\eta_{nm}z'-\lambda_{nm}^4\mathbf{p}_{nm}(r')\mathbf{p}(r)\frac{\cosh\eta_{nm}z'}{\eta_{nm}}\right]d\tau'\right], \qquad (23)$$

where $\eta_{nm}=\sqrt{\lambda_{nm}^2-k^2}$

The field for $z<z'$ is obtained by interchanging z and z' in eq 22 and 23.

It is noticed first that the various modes are either in phase or 180 degrees out of phase, which is, of course necessary, since we have neither resistive nor radiation losses. Also, the field does not decrease exponentially with z, but contains a factor, $(1\pm e^{-2\gamma(d-z)})$ which is insignificant at small values of attentuation, but becomes appreciable as the receiving loop approaches the end of the cavity. If the attenuator were used in this way, its calibration in decibels would not be linear with variation of z. This nonlinearity can be avoided if the attenuator is constructed as illustrated in figure 1. The exciting loop is fixed relative to a fixed end of the cavity, and the receiving loop is fixed to the other end which may slide within the cavity, varying its length, so that $d-z$ is a constant. Since

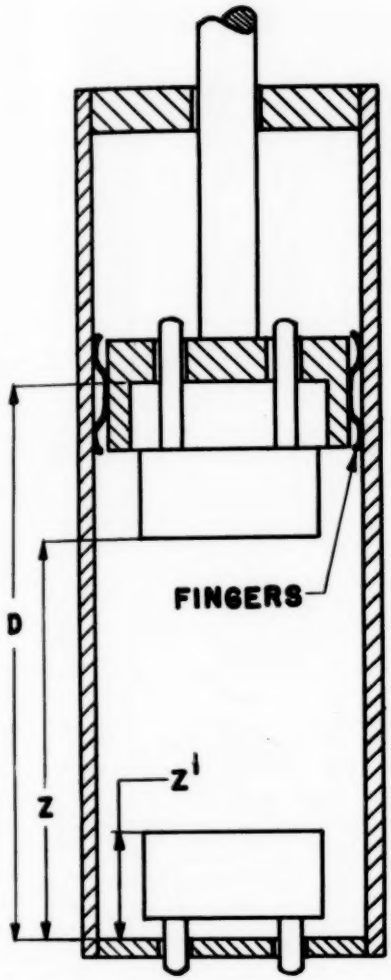

FIGURE 1.—*Schematic drawing of attenuator.*

$e^{-2\gamma_1 d} \ll 1$, the denominator is independent of d and the ratio of E_{TE} for a given mode, for two positions of the receiving loop, z_1 and z_2, is $e^{-\gamma(z_1-z_2)}$, and the nonlinearity is eliminated.

In general, an infinite number of modes are excited, so that the best one can do to insure purity of mode is to use symmetry of excitation which will not excite those unwanted modes with the lowest attenuation factor, and to use large enough values of z, such that the unwanted modes are sufficiently attentuated. For low enough frequency,

$$\gamma_{nm} = \sqrt{\frac{v_{nm}^2}{a^2} - k^2} \simeq \frac{v_{nm}}{a}, \text{ where } J_n(v_{nm}) = 0;$$

$$\eta_{nm} = \sqrt{\frac{u_{nm}^2}{a^2} - k^2} \simeq \frac{u_{nm}}{a}, \text{ where } J_n(u_{nm}) = 0.$$

The first few values of v_{nm} and u_{nm} are as follows:

$u_{01} = 2.405$	$v_{11} = 1.841$
$u_{11} = 3.832$	$v_{21} = 3.05$
$u_{21} = 5.136$	$v_{01} = 3.832$
$u_{02} = 5.520$	$v_{12} = 5.33$
$u_{12} = 7.016$	$v_{20} = 7.016$

From the above values of u_{nm} and v_{nm} it is at once apparent that maximum purity of mode can be achieved by exciting the TE_{11} mode, and eliminating the TE_{01}, TE_{21}, and TM_{01} modes through symmetry considerations.

Consider the exciting current distribution in a plane perpendicular to the axis of the cylinder, figure 2. Assume that corresponding to every

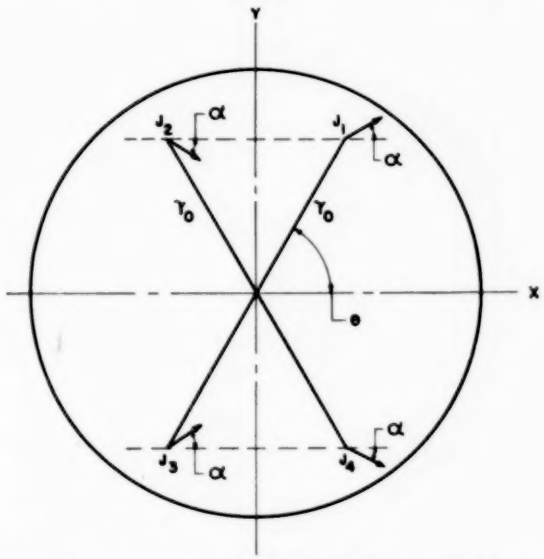

FIGURE 2.—*Current distribution in plane perpendicular to axis of cylinder.*

current element, $\mathbf{J}_1(r_0, \theta, \alpha)$, where r_0 is the distance of the element from the axis of the cylinder, θ is the angular displacement of its position vector with respect to the x-axis, and α is the angle between $\mathbf{J}$, and the x-axis, there exist corresponding current elements,

$$\mathbf{J}_2(r_0, \pi-\theta, -\alpha),\ \mathbf{J}_3(r_0, \pi+\theta, \alpha),\ \mathbf{J}_4(r_0, 2\pi-\theta, -\alpha).$$

Then, it immediately follows that

$$\int_0 \mathbf{J} \cdot \mathbf{n}_{nm}^* d\tau = \int_0 \mathbf{J} \cdot \mathbf{m}_{nm}^* d\tau = 0 \text{ for } n \text{ even}.$$

Further, if corresponding to a positive z-component of current at $(r_0, 2\pi-\theta)$ and (r_0, θ), there exist equal negative z-components of current at $(r_0, \pi-\theta)$ and $(r_0, \pi+\theta)$, then $\int \mathbf{J}\cdot\mathbf{p}^*_{nm} d\tau = 0$, for n even.

In general, if the exciting current symmetry is such that the distribution for $x<0$ is the negative mirror image of that for $x>0$, and if the distribution for $y<0$ is the positive mirror image of that for $y>0$, then only those modes will be excited for which n is odd.

A convenient index of attenuator performance is the percentage error made in a measurement of voltage as a function of the distance between exciting and receiving coils. The computed value

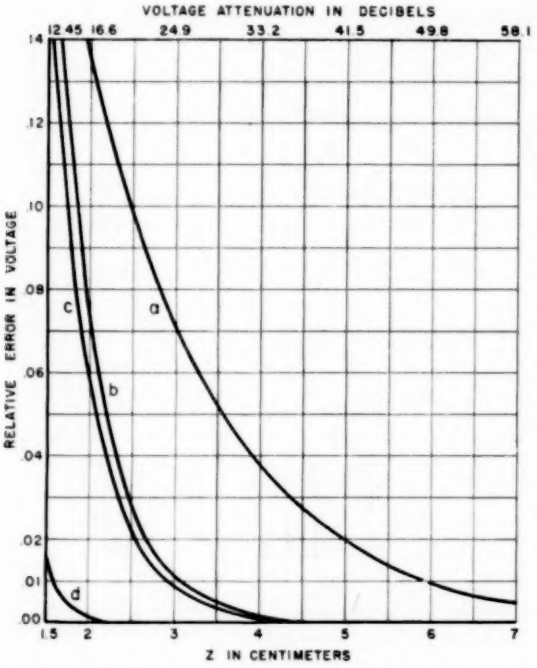

FIGURE 3.—*Relative error in measurement of voltage due to the presence of unwanted modes.*

a, Unsymmetric source in circular guide (fig. 5b); b, symmetric source in circular guide (fig. 5a); c, symmetric source in rectangular guide (fig. 6a); d, symmetric source in rectangular guide chosen to eliminate TE_{10} modes (fig. 6b).

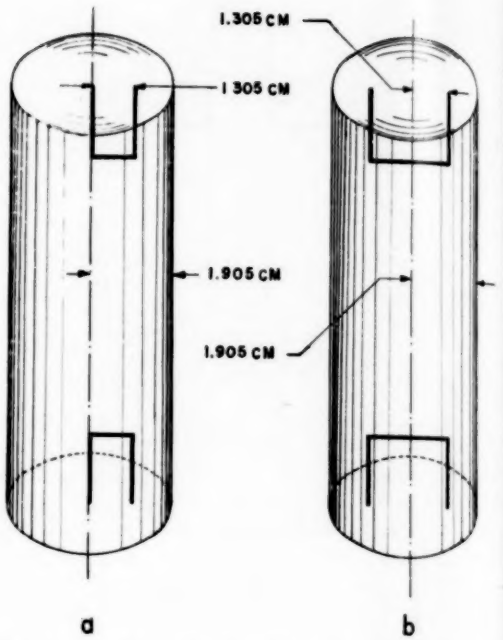

FIGURE 4.—*Schematic of exciting and receiving loops in circular guide.*

a, Unsymmetric loop; b, symmetric loop.

of this error at 500 megacycles per second is shown by curves a and b in figure 3 for an attentuator with symmetrical and unsymmetrical receiving and exciting loops (fig. 4). Figure 3 shows that a symmetrical exciting source permits a considerable decrease in the insertion loss for a given accuracy tolerance, over that of an unsymmetrically excited attenuator.

IV. Attenuators of Rectangular Cross Section

Attenuators of rectangular cross section may be treated similarly to those of circular cross-section. For a rectangular cavity, whose x, y, z, dimensions are a, b, c, with the origin of coordinates taken at a corner, the normalized vector wave function of zero curl is

$$\mathbf{E}_{lmn}=\sqrt{\frac{8}{abc}}\frac{1}{\sqrt{\frac{l^2}{a^2}+\frac{m^2}{b^2}+\frac{n^2}{c^2}}}\left[\frac{l}{a}\cos\frac{l\pi x}{a}\sin\frac{m\pi y}{b}\sin\frac{n\pi z}{c}\mathbf{i}+\frac{m}{b}\sin\frac{l\pi x}{a}\cos\frac{m\pi y}{b}\sin\frac{n\pi z}{c}\mathbf{j}+\right.$$

$$\left.\frac{n}{c}\sin\frac{l\pi x}{a}\sin\frac{m\pi y}{b}\cos\frac{n\pi z}{c}\mathbf{k}\right] \qquad (24)$$

The two independent normalized vector wave functions of zero divergence are

$$\mathbf{M}_{lmn}=\sqrt{\frac{8}{abc}}\,\frac{1}{\sqrt{\frac{l^2}{a^2}+\frac{m^2}{b^2}}}\left[-\frac{m}{b}\sin\frac{m\pi y}{b}\cos\frac{l\pi x}{a}\,\mathbf{i}+\frac{l}{a}\sin\frac{l\pi x}{a}\cos\frac{m\pi y}{b}\,\mathbf{j}\right]\sin\frac{n\pi z}{c}, \tag{25}$$

and

$$\mathbf{N}_{lmn}=\sqrt{\frac{8}{abc}}\,\frac{1}{\sqrt{\frac{l^2}{a^2}+\frac{m^2}{b^2}+\frac{n^2}{c^2}}}\,\frac{1}{\sqrt{\frac{l^2}{a^2}+\frac{m^2}{b^2}}}\,\frac{1}{\sqrt{1+\delta_0^n}}\left[\begin{aligned}&-\frac{ln}{ac}\cos\frac{l\pi x}{a}\sin\frac{m\pi y}{b}\sin\frac{n\pi z}{c}\,\mathbf{i}\\&-\frac{mn}{bc}\sin\frac{l\pi x}{a}\cos\frac{m\pi y}{b}\sin\frac{n\pi z}{c}\,\mathbf{j}\\&+\left(\frac{l^2}{a^2}+\frac{m^2}{b^2}\right)\sin\frac{l\pi x}{a}\sin\frac{m\pi y}{b}\cos\frac{n\pi z}{c}\,\mathbf{k}\end{aligned}\right]$$

Again, when we solve for the field excited by a distribution of current, $\mathbf{J}(r')$, part of the field developed into $\mathbf{N}_{lmn}$ functions exactly cancels that part of the field whose curl is zero, so that the resultant field, $\mathbf{E}$, may be expressed as the sum of transverse electric and transverse magnetic components.

$$\mathbf{E}=\mathbf{E}_{TE}+\mathbf{E}_{TM},$$

$$\text{where } \mathbf{E}_{TE}=\frac{4j\omega\mu}{ab}\int\mathbf{J}(r')\cdot\sum_{lm}\frac{\mathbf{P}_{lm}(r')\mathbf{P}_{lm}(r)\,\sinh\eta z'}{\eta_{lm}\left(\frac{l^2}{a^2}+\frac{m^2}{b^2}\right)}\left[\frac{e^{-\eta z}}{1-e^{-2\eta c}}\,(1-e^{-2\eta(c-z)})\right]d\tau'$$

$$\mathbf{E}_{TM}=\frac{-4j}{\omega\epsilon ab}\int\mathbf{J}(r')\cdot\sum_{lm}\frac{e^{-\eta z}}{1-e^{-\eta c}}\left[\left\{\frac{\mathbf{S}(r')\mathbf{S}(r)\eta\,\sinh\eta z'}{\left(\frac{l^2}{a^2}+\frac{m^2}{b^2}\right)}+\pi\mathbf{Q}(r')\mathbf{S}(r)\cosh\eta z'\right\}(1-e^{-2\eta(c-z)})-\right.$$

$$\left.\left\{\pi\mathbf{S}(r')\mathbf{Q}(r)\,\sinh\eta z'+\pi^2\left(\frac{l^2}{a^2}+\frac{m^2}{b^2}\right)\mathbf{Q}(r')\frac{\mathbf{Q}(r)\cosh\eta z'}{\eta}\right\}(1+e^{-2\eta(c-z)})\right]d\tau'$$

$$\mathbf{P}_{lm}=\left[-\frac{m}{b}\sin\frac{m\pi y}{b}\cos\frac{l\pi x}{a}\,\mathbf{i}+\frac{l}{a}\sin\frac{l\pi x}{a}\cos\frac{m\pi y}{b}\,\mathbf{j}\right],\ \eta_{lm}=\sqrt{\left(\frac{\pi l}{a}\right)^2+\left(\frac{\pi m}{b}\right)^2-k^2}$$

$$\mathbf{S}_{lm}=\left[\frac{l}{a}\cos\frac{l\pi x}{a}\sin\frac{m\pi y}{b}\mathbf{i}+\frac{m}{b}\sin\frac{l\pi x}{a}\cos\frac{m\pi y}{b}\mathbf{j}\right],\ \mathbf{Q}_{lm}=\sin\frac{l\pi x}{a}\sin\frac{m\pi y}{b}\,\mathbf{k},$$

r' and r refer respectively to the position coordinates of $\mathbf{J}$, and the point at which the field is evaluated.

It will be noticed that $\mathbf{E}_{TE}$ and $\mathbf{E}_{TM}$ have the same value of attentuation constant, for the same mode numbers, l, m.

Also, in line with our previous discussion, we shall assume that the receiving coil is rigidly fixed to the movable end of the cavity, so that the factor $(1\pm e^{-2\eta(c-z)})$ is cancelled out in the measurement of the ratio of any two voltages. The magnitude of the error introduced by the factor $(1-e^{-2\eta c})$ is such, that if the smallest value of c used is always greater than 1.5 times the larger dimension of cross section, the factor will introduce an error of less than 1 part in 10,000 for the TE_{01} mode, and less for higher modes.

One advantage of an attenuator tube with rectangular cross section over that with circular cross section is that for the former, there is no need to discriminate between TE and TM type modes, for the same index numbers, l, m, since for given values of l and m, the voltage induced in the collecting coil will vary as $e^{-\sqrt{\frac{\pi^2l^2}{a^2}+\frac{\pi^2m^2}{b^2}-k^2}\,z}$ for TM and TE type modes, alike. Of course, for tubes of circular cross section this is not true, except for cases of accidental degeneracy.

Furthermore, for tubes of rectangular cross section, it is possible to secure greater suppression of unwanted modes by a suitable choice of ratio of the two dimensions of cross section. The following table enumerates the ratios of attenuation

constants for various modes to that of the lowest mode, for various ratios of rectangular cross section dimensions and for circular cross section.

It becomes apparent that the optimum practical ratio in the above table is $b/a=3$, and that this choice allows the unwanted modes to decay much faster than for circular cross section.

TABLE 1.—*Ratio of attenuation constant of higher modes to that of the dominant mode*

Rectangular waveguide					Circular waveguide	
Mode	$\frac{\alpha}{\alpha_{TE_{01}}}$	$\frac{\alpha}{\alpha_{TE_{01}}}$	$\frac{\alpha}{\alpha_{TE_{01}}}$	$\frac{\alpha}{\alpha_{TE_{01}}}$	$\frac{\alpha}{\alpha_{TE_{11}}}$	Mode
	$a=b$	$a=0.9b$	$a=\frac{b}{2}$	$a=\frac{b}{3}$		
TE_{01}	1	1	1	1	1	TE_{11}
TE_{02}	2	2	2	2	1.31	TM_{01}
TE_{03}	3	3	3	3	1.66	TE_{21}
TE_{10}	1	1.1	2	3	2.08	TE_{01}, TM_{11}
TE_{20}	2	2.2	4	6	2.79	TM_{21}
TE_{11}, TM_{11}	1.41	1.5	2.2	3.1	2.90	TE_{12}
TE_{21}, TM_{21}	2.2	2.4	4.1	6.1	3.0	TM_{12}

If the exciting current distribution is chosen, so that to each element of current corresponds its negative mirror image with respect to the plane $x=\frac{a}{2}$, and its positive mirror image with respect to the plane $y=\frac{b}{2}$, then it is easily seen that

$$\left.\begin{aligned} &\int \mathbf{J}(r')\cdot\mathbf{P}_{lm}d\tau' \\ &\int \mathbf{J}(r')\cdot\mathbf{S}_{lm}d\tau' \\ &\int \mathbf{J}(r')\cdot\mathbf{Q}_{lm}d\tau' \end{aligned}\right\}=0, \text{ for } l \text{ odd or } m \text{ even.}$$

The advantages of employing this type of symmetrical source distribution becomes apparent when we consult table 1, and recognize that it eliminates four out of the first six spurious modes.

Another advantage of rectangular attenuators over those of circular cross section is the ease with which current distributions of slightly higher symmetry may be used to eliminate further spurious modes, by placing the current elements at the nodal points of the undesired modes. The relative voltage error for a rectangular attenuator with a simple symmetric loop source, and a double loop source, (fig. 5) whose position is so chosen that modes for which $m=3$ are not excited, is graphed in figure 3.

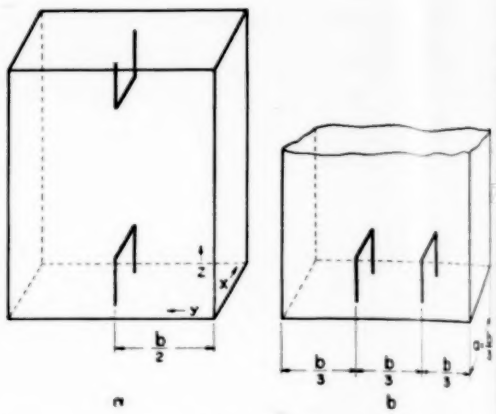

FIGURE 5.—*Schematic of exciting and receiving loops in rectangular guide.*

a, Symmetric loop; b, symmetric double loop placed at nodes so that no modes are excited, for which $m=3$.

V. Conclusion

It may be concluded, in general, that attenuators of rectangular cross section have two advantages over those of circular cross section:

1. Greater symmetry with respect to the dominant mode in the rectangular guide permit one to eliminate more spurious modes; 2. a slight departure from symmetry in the rectangular guide is not so serious as in the circular guide, as the spurious modes decay more rapidly in the former.

The author expresses his thanks to Dr. Harold Lyons for his interest and helpful discussions during the course of this investigation.

VI. References

[1] D. E. Harnett and N. P. Case, IRE **23** 578 (June 1935).
[2] Deutsche Mathematiker—Vereinigung Jahresbericht **21** 309 (1912).
[3] W. Heitler, Quantum theory of radiation, p. 47 (Oxford Univ. Press, 1944).
[4] E. U. Condon, Rev. Mod. Phys. **14,** 341 (Oct. 1942).
[5] J. A. Stratton, Electromagnetic theory, p. 465 (McGraw-Hill Book Co., New York, N. Y., 1941).
[6] J. A. Stratton, Electromagnetic theory, p. 392 (Mcgraw-Hill Book Co., New York, N. Y., 1941).
[7] T. M. McRobert, Functions of a complex variable, p. 115 (MacMillan Co., New York, N. Y., 1933).

VII. Appendix I

1. Let $S_1=\sum_{l=1}^{\infty}\frac{\sin\frac{l\pi z'}{d}\sin\frac{l\pi z}{d}}{\gamma^2+\frac{l^2\pi^2}{d^2}}=\frac{d^2}{\pi^2}\sum_{l=1}^{\infty}\frac{\sin\frac{l\pi z'}{d}\sin\frac{l\pi z}{d}}{\frac{d^2\gamma^2}{\pi^2}+l^2}$.

2. Let $\frac{d\gamma}{\pi}=\beta$.

3. $S_1=\frac{d^2}{2\pi^2}\sum_{l=1}^{\infty}\frac{\cos\frac{l\pi}{d}(z-z')-\cos\frac{l\pi}{d}(z+z')}{\beta^2+l^2}=$

$\frac{d^2}{4\pi^2}\sum_{l=-\infty}^{\infty}\frac{\cos\alpha l-\cos\alpha' l}{\beta^2+l^2}$.

4. Where $\alpha=\frac{\pi(z-z')}{d}$, $\alpha'=\frac{\pi(z+z')}{d}$.

5. Consider $f(z)=\frac{e^{jaz}}{(\beta^2+z^2)\,(e^{2\pi jz}-1)}$,
let $z=R\,(\cos\theta+j\sin\theta)$.

Then $\lim_{R\to\infty}|Zf(z)|=0$, and $\lim_{R\to\infty}zf(z)=0$, provided $0\leq a\leq 2\pi$.

Then, [7] the line integral of $f(z)$ around an infinite circle enclosing the complex plane vanishes.

6. $\lim_{R\to\infty}\oint f(z)dz=0$.

Since $f(z)$ has poles at $\pm j\beta$, 0, ± 1, ± 2. . . . .

7. $0=\sum_{l=-\infty}^{l=\infty}\frac{e^{jal}}{\beta^2+l^2}+\frac{\pi}{\beta}\left\{\frac{e^{-a\beta}}{e^{-2\pi\beta}-1}-\frac{e^{a\beta}}{e^{2\pi\beta}-1}\right\}$.

8. or $\sum_{-\infty}^{\infty}\frac{\cos al}{\beta^2+l^2}=\frac{\pi}{\beta}\left[\frac{e^{a\beta}}{e^{2\pi\beta}-1}-\frac{e^{-a\beta}}{e^{-2\pi\beta}-1}\right]$.

On substituting eq 8 in eq 3, with a little algebra we get immediately,

9. $S_1=\frac{d}{2\gamma}\frac{\sinh\gamma z'(1-e^{-2\gamma(d-z)})}{1-e^{-2\gamma d}}e^{-\gamma z}$, for $z>z'$.

VIII. Appendix II

1. Let $S_2=\sum_{l=0}^{\infty}\frac{\frac{l\pi}{d}\sin\frac{l\pi z'}{d}\cos\frac{l\pi z}{d}}{\gamma^2+\left(\frac{l\pi}{d}\right)^2}$.

2. Then $S_2=\frac{dS_1}{dz}=\frac{d}{-2}\sinh\gamma z'\left[\frac{e^{\gamma z}}{e^{2\gamma d}-1}-\frac{e^{-\gamma z}}{e^{-2\gamma d}-1}\right]$.

3. Let $S_3=\sum_{l=1}^{\infty}\frac{\frac{l\pi}{d}\cos\frac{l\pi z'}{d}\sin\frac{l\pi z}{d}}{\gamma^2+\left(\frac{l\pi}{d}\right)^2}$.

4. Then $S_3=\frac{dS_1}{dz'}=\frac{-d}{2}\cosh\gamma z'\left[\frac{e^{\gamma z'}}{e^{2\gamma d}-1}+\frac{e^{-\gamma z}}{e^{-2\gamma d}-1}\right]$.

5. Let $S_4=\sum_{0}^{\infty}\frac{\left(\frac{l\pi}{d}\right)^2\cos\frac{l\pi z}{d}\cos\frac{l\pi z'}{d}}{\gamma^2+\left(\frac{l\pi}{d}\right)^2}$.

6. Then $S_4=\frac{dS_2}{dz'}=\frac{-\gamma d}{2}\cosh\gamma z'\left[\frac{e^{\gamma z}}{e^{2\gamma d}-1}-\frac{e^{-\gamma z}}{e^{-2\gamma d}-1}\right]$.

WASHINGTON, September 23, 1946.

U. S. Department of Commerce
National Bureau of Standards

Research Paper RP1869
Volume 40, March 1948

Part of the Journal of Research of the National Bureau of Standards

Theory of Wagner Ground Balance for Alternating-Current Bridges

By Richard K. Cook

A method is described for getting the Wagner ground balance of an alternating-current bridge when used with any three-terminal source. The basic idea is to insert impedances between the two ungrounded terminals of the source, and the corresponding terminals of the Wagner ground arm and the bridge, so as to "balance" approximately the currents from the source. The method is applicable to high-voltage type Schering bridges. Such a bridge, incorporating the principles of the new method for securing the Wagner ground balance, has been designed and built principally for measurement of the small capacitances, about 50 $\mu\mu$f, of some types of condenser microphones.

I. Introduction

A Wagner ground is used sometimes with alternating current bridges in order to eliminate the effects of capacity to ground. The same end can be achieved by a system of electrostatic shielding, but the required shielding can become very complicated. With a Wagner ground, it is possible to secure high precision with simple shielding.

The object of this paper is to show how almost any available three-terminal source can be used with a Wagner-grounded bridge. The simple theory that is usually given assumes that the source has only two accessible output terminals, which are connected to the two ungrounded input terminals of the bridge [1] [1]. The Wagner ground balance is readily found theoretically, but sometimes it is difficult or impossible to find experimentally, particularly in the case of high-voltage type Schering bridges used to measure small capacitances.

Ogawa [2] has pointed out that the experimental difficulty is due to the fact that available sources really have three output terminals, and the simple theory of a two-terminal source does not apply. He has given a comprehensive treatment of the general theory of Wagner-grounded alternating-current bridges and has solved the difficulty of securing balance by means of a specially constructed transformer satisfying an electrical condition which simplifies the Wagner ground balance equation. The theory has been applied by Astin [3] to a Schering bridge used for precision measurement of the power factors of air capacitors.

The theory given below shows how almost any available three-terminal source can be used, thus obviating the need for a special transformer. The theory is applied to the design of a high-voltage type Schering bridge for measurement of the small capacitances of condenser microphones at frequencies between 500 and 10,000 c/s. Such capacitance measurements are required when making absolute calibrations of condenser microphones by the reciprocity technique.

It should be pointed out that there are other ways of securing Wagner ground balance. For example, in a high-voltage type Schering bridge for capacitance measurements at power-supply frequencies, which has recently become commercially available [4], the Wagner ground balance is obtained by adjustment of the amplitude and phase (relative to ground) of the voltage applied to one of the input terminals of the bridge.

II. Theory of a Wagner-grounded Bridge

The basic idea of the new way for getting Wagner ground balance is as follows: In the circuit shown in figure 1, suppose the bridge to be balanced, so that points B_1 and B_2 are at the

[1] Figures in brackets indicate the literature references at the end of this paper.

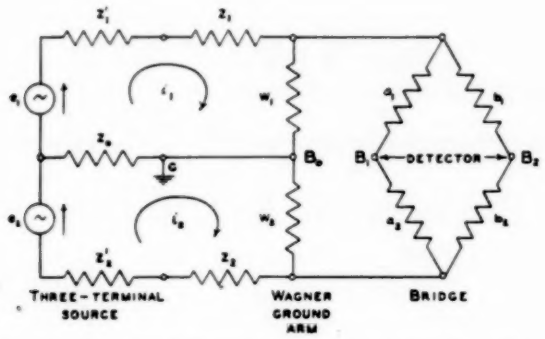

FIGURE 1.—*Circuit diagram of Wagner-grounded alternating-current bridge.*

same potential. Hence $a_1b_2=a_2b_1$. Suppose also that $i_1=i_2$; the wire B_0G will then carry no current. This will be referred to as the balanced ground-current condition. It is clear that this assumption eliminates the effect of z_0, so that the simple bridge theory will apply. The third assumption is that $a_1w_2=a_2w_1$. Then it follows from these three assumptions that the Wagner ground is balanced, or that points B_0 and B_1 are at the same potential. If $e_1=e_2$, the balanced ground-current condition can be realized by adjusting z_1 and z_2 so that z_1+z_1' plus the parallel combination of a_1, b_1, and w_1, is equal to z_2+z_2' plus the parallel combination of a_2, b_2, and w_2.

The mathematics needed for proof of the foregoing statements can be obtained from Ogawa's article, but a simplified derivation might be of interest. We assume a more general condition in which the ground-current might not be balanced, so that i_1 is not necessarily equal to i_2, but in which the potentials at B_0, B_1, and B_2 are the same (Wagner ground and bridge balanced). Also, we assume e_1 is not necessarily equal to e_2.

Before proceeding, a few words about three-terminal sources are in order. Ogawa has shown by a generalization of Thévenin's theorem that any three-terminal source can be represented by the network shown in figure 1. Subsequently a more general proof was given by Starr [5]. An equivalent network of this type applies whenever the potentials of the terminals are linear functions of the three currents through the terminals. Whether or not the network can be applied to a source that is available in the laboratory is a question that can, of course, be answered only by experiment. The simple bridge theory which is usually given tacitly assumes that $z_0=\infty$.

By virtue of the bridge balance, the circuit of figure 1 can be replaced by the simpler circuit of figure 2, in which the impedance s_1 is the parallel combination of a_1 and b_1, and s_2 is the parallel combination of a_2 and b_2. Also, $Z_1=z_1+z_1'$, $Z_2=z_2+z_2'$. As in figure 1, the detector impedance is not indicated, as it has no current at balance. Application of Maxwell's loop equations to the network yields the following equations:

$$\left.\begin{aligned}(w_1+Z_1+z_0)i_1-z_0i_2-w_1i_3-e_1&=0\\ -z_0i_1+(w_2+Z_2+z_0)i_2-w_2i_3-e_2&=0\\ w_1i_1+0-(w_1+s_1)i_3+0&=0\\ 0+w_2i_2-(w_2+s_2)i_3+0&=0.\end{aligned}\right\}\quad(1)$$

As these equations are linear and homogeneous in $(i_1, i_2, i_3, 1)$, the necessary and sufficient condition for a nonzero solution for $(i_1, i_2, i_3, 1)$ is the vanishing of the determinant of the coefficients:

$$\begin{vmatrix} w_1+Z_1+z_0 & -z_0 & -w_1 & -e_1\\ -z_0 & w_2+Z_2+z_0 & -w_2 & -e_2\\ w_1 & 0 & -(w_1+s_1) & 0\\ 0 & w_2 & -(w_2+s_2) & 0\end{vmatrix}=0.\quad(2)$$

Expansion of the determinant yields the fundamental balance equation,

$$e_1\left[s_2+Z_2+\frac{s_2Z_2}{w_2}+\left(\frac{s_2}{w_2}-\frac{s_1}{w_1}\right)z_0\right]=e_2\left[s_1+Z_1+\frac{s_1Z_1}{w_1}-\left(\frac{s_2}{w_2}-\frac{s_1}{w_1}\right)z_0\right],\quad(3)$$

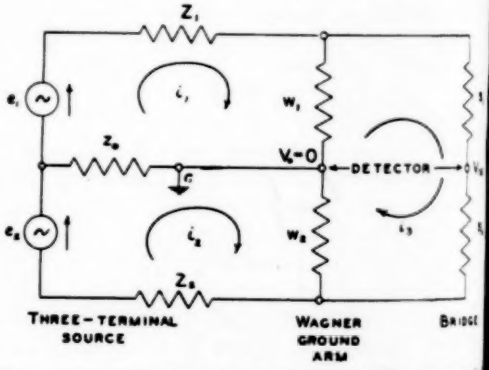

FIGURE 2.—*Simplified circuit diagram of Wagner-grounded bridge.*

which is basically the same as Ogawa's eq 62.

If $i_1=i_2$, then eq 1 show it is necessary that

$$\frac{s_2}{w_2}=\frac{s_1}{w_1}. \tag{4}$$

If in addition, $e_1=e_2$, then eq 3 reduces to

$$Z_2+\frac{s_2 w_2}{s_2+w_2}=Z_1+\frac{s_1 w_1}{s_1+w_1}. \tag{5}$$

This is the algebraic form of the statement made in the first paragraph of this section.

Suppose that $z_0\to\infty$. Then it is found that eq 3 reduces to eq 4, provided $e_1+e_2\neq 0$. This is the usual Wagner ground balance condition obtained by application of the simple theory.

We define the unbalance voltage to be the amount by which V_{12} exceeds ground potential when the Wagner ground is not balanced. This quantity is needed for studying the convergence of the sequence of balancing operations. It is justifiable to ignore the impedance of the amplifier-detector system which might be employed to observe V_{12}. The reason for this is that the impedance will affect only the magnitude and phase of V_{12}, and will not affect the convergence of the sequence of balancing operations when the unbalance current is small in comparison with the main bridge currents. We find

$$V_{12}=\frac{1}{\Delta}\left\{e_1\left[s_2+Z_2+\frac{s_2 Z_2}{w_2}+\left(\frac{s_2}{w_2}-\frac{s_1}{w_1}\right)z_0\right]-\right.$$
$$\left. e_2\left[s_1+Z_1+\frac{s_1 Z_1}{w_1}+\left(\frac{s_1}{w_1}-\frac{s_2}{w_2}\right)z_0\right]\right\}, \tag{6}$$

where

$$\Delta=\left(Z_1+s_1+\frac{Z_1 s_1}{w_1}\right)\left(1+\frac{Z_2}{w_2}+\frac{z_0}{w_2}\right)+$$
$$\left(Z_2+s_2+\frac{Z_2 s_2}{w_2}\right)\left(1+\frac{Z_1}{w_1}+\frac{z_0}{w_1}\right)+$$
$$z_0\left(\frac{Z_1}{w_1}+\frac{s_2}{w_2}+\frac{Z_1 s_2}{w_1 w_2}+\frac{Z_2}{w_2}+\frac{s_1}{w_1}+\frac{Z_2 s_1}{w_2 w_1}\right).$$

The way in which eq 3 was derived shows it to be a necessary condition for Wagner ground balance. Equation 6 shows that eq 3 is also sufficient, if $\Delta\neq 0$.

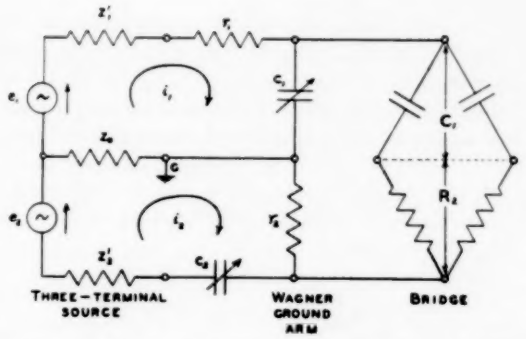

FIGURE 3.—*High-voltage type Schering bridge with Wagner ground.*

III. Application to a Schering Bridge

The application of the Wagner-grounding technique described above to a high-voltage type Schering bridge, which is useful for measuring the capacitance of condenser microphones, is easily accomplished. A circuit diagram for such a bridge is shown in figure 3. Here C_1 is the parallel combination of the two capacitances in the high-voltage arms, and R_2 is the parallel combination of the two resistances in the low-voltage arms.

It is important to study how the Wagner ground balance is obtained when the circuit parameters are varied. A practical advantage of the Schering bridge is that balance can be obtained by variation of capacitance only. The Wagner ground balance of the Schering bridge circuit shown in figure 3 can also be obtained by variation of capacitance only, as the following analysis shows.

As before, we shall suppose that both the bridge and the Wagner ground are balanced. Also, we make the following simplifying assumptions, which can be readily fulfilled experimentally. (1) The three-terminal source is the secondary of a center-tapped transformer. (2) The transformer is symmetrical enough so that $e_2=(1+\alpha+j\beta)e_1$, where $\alpha\ll 1$ and $\beta\ll 1$. (3) The terminals of the transformer secondary are externally connected to the center tap by equal low resistances, so that $z_1'\approx z_2'$, and $z_0\approx\frac{-z_1'}{2}$. z_1' and z_2' are positive resistances, but z_0' is a negative resistance. In what follows there will be no loss of generality in supposing that z_1' is included in r_1, and z_2' is included in the residual of c_2. (4) c_1, c_2, and C_1

are variable capacitors whose residuals are small, and r_1, r_2, and R_2 are fixed resistors whose residuals are small.

First we shall suppose that all the small quantities α, β, and the residuals of the impedances are zero. Hence $\epsilon_1=\epsilon_2$. The object of this is to find the approximate values of the adjustable capacitances c_1 and c_2. Application of eq 3 to the circuit yields

$$\left.\begin{aligned} R_2&=r_1+\left(\frac{c_1}{C_1}\right)r_1-2z_0\left(\frac{R_2}{r_2}-\frac{c_1}{C_1}\right);\\ \frac{1}{\omega c_2}\left(1+\frac{R_2}{r_2}\right)&=\frac{1}{\omega C_1}. \end{aligned}\right\} \tag{7}$$

The first of these corresponds to the real part of eq 3, and the second corresponds to the imaginary part. Solutions of eq 7 for c_1 and c_2 are as follows:

$$\left.\begin{aligned} c_1&=\left(\frac{R_2-r_1+\dfrac{2z_0R_2}{r_2}}{r_1+2z_0}\right)C_1;\\ c_2&=\left(\frac{R_2}{r_2}+1\right)C_1. \end{aligned}\right\} \tag{8}$$

These equations indicate that if

$$r_1+2z_0>0, \text{ and } R_2-r_1+\frac{2z_0R_2}{r_2}>0, \tag{9}$$

the Wagner ground balance can be obtained by variation of capacitance only. The balance is independent of frequency.

It is to be noted that c_1 can be adjusted to satisfy the real part of eq 3, and c_2 can be separately adjusted to satisfy the imaginary part. This, together with eq 6, shows that the Wagner ground unbalance voltage, which is a vector in the complex plane, can be reduced to zero by a series of steps, successive steps being mutually perpendicular. This is a highly desirable property of a sequence of balancing operations for an alternating-current bridge.

The unbalance voltage can be reduced to zero by adjustment of other pairs of parameters besides c_1 and c_2. Equations 7 show that variation of r_1 and c_2 will also yield successive voltage steps that are mutually perpendicular. However, all other pairs will yield successive steps, which in general are not mutually perpendicular, an example of which is the combination r_2 and c_1. The pair r_1, c_1 cannot be used at all to get balance, as the second eq 7 contains neither of these parameters.

A more detailed analysis in which α, β, and the residuals are not assumed to be zero shows that the Wagner ground balance can still be secured by variation of the capacitances c_1 and c_2 only. However, the successive steps in the unbalance voltage, obtained by varying c_1 and c_2 successively, are vectors which are not quite perpendicular to one another.

It might be inconvenient to select the circuit parameters so that the inequalities (9) hold if a center-tapped transformer is used as a source, as for such a transformer, z_0 is a negative resistance. An examination of the fundamental balance eq 3 shows that the effect of z_0 disappears if the condition given by eq 4 holds. When this condition is applied to the Schering bridge circuit discussed above, we find

$$c_1=\frac{R_2}{r_2}C_1,\ r_1=\frac{r_2R_2}{r_2+R_2},\ c_2=c_1+C_1. \tag{10}$$

It is understood that r_1 includes the resistive impedance z_1'. The ground current is balanced in this case.

Another possibility is to introduce a positive external resistor, whose magnitude is $|z_0|$, at the center tap of the transformer. This would, in effect, reduce z_0 to zero, and the terms in eq 3 containing z_0 would vanish.

Still another possibility is to use two similar transformers driven by the same oscillator. The transformers would have to be arranged so that there is no mutual induction between them. The use of buffer amplifiers might also be required between the oscillator and transformers. The whole arrangement can be converted into a three-terminal source having $z_0=0$ by connecting a terminal on the secondary of one transformer to a terminal on the other.

IV. Description of a Bridge

A Wagner-grounded Schering bridge, based on the principles outlined above, has been constructed in our Sound Laboratory. The bridge is the high-voltage type and has been used mainly to measure condenser-microphone capacitances, which are about 50 $\mu\mu$f, at frequencies ranging from 500 to 10,000 c/s. Accuracy of the order of 0.1 per-

ent can be obtained, but the microphones must f course be converted into three-terminal im-edances by means of a grounded shield in order o realize this accuracy. The source is the center-apped output transformer of a commercially vailable beat-frequency oscillator. The circuit f the high-voltage type bridge easily allows the troduction of the direct-current polarizing volt-ge needed for condenser microphones.

The resistance arms of the bridge are fixed esistors, each of about 50,000 ohms. The apacitance arms have the unknown condenser, sually about 50 $\mu\mu$f, and a standard condenser, ariable over the range 40 to 60 $\mu\mu$f. Hence C_1 ee fig. 3) is about 100 $\mu\mu$f, and R_2 is about 25,000 hms. The condensers c_1 and c_2 are variable up o about 1,000 $\mu\mu$f, and r_1 and r_2 are each ap-roximately 3,000 ohms.

The three-terminal source has z_1' and z_2', which are mainly resistive, both approximately 800 ohms. The impedance z_0 is also mainly resistive, and is approximately -400 ohms. The voltages e_1 and e_2 are closely equal, both in magnitude and phase, and are about 8 volts for frequencies between 500 and 10,000 c/s.

V. References

[1] B. Hague, Alternating-current bridge methods, 5th ed., pp. 542–546 (Sir Isaac Pitman & Sons, Ltd., London, 1946).

[2] K. Ogawa, General theory and earthing device for alternating current bridges, Researches of the Electrotechnical Laboratory, Tokyo, Japan, No. 254 (1929).

[3] A. V. Astin, J. Research NBS **21,** 425 (1938) RP1138.

[4] Modified Schering bridge, Catalog E–54 (2) 1945 of the Leeds and Northrup Co., Philadelphia, Pa.

[5] A. T. Starr, J. Inst. Elec. Engrs. (London) **73,** 303 (1933).

Washington, September 8, 1947.

U. S. Department of Commerce
National Bureau of Standards

Research Paper RP1870
Volume 40, March 1948

Part of the Journal of Research of the National Bureau of Standards

Correlations of the Gel Strength of Paste Walls and the Shelf Life of Electric Dry Cells

By Walter J. Hamer

Paste walls of most dry cells consist of starch-flour gels. Their characteristics were studied by means of gel-strength measurements and correlated with the shelf life of dry cells. Interactions were observed between the paste wall and the dry-cell electrolyte and the depolarizing mix of manganese dioxide. Attempts were made to eliminate or retard these reactions. These included the use of addition agents, of different varieties of starches and flours, of modified starches, and of fractions of natural starch and natural flour. Only the flour fractions, gliadin and mesonin, in different states of polymerization were found to give an increase in the electrical output of dry cells. No significant differences were found in the electrical output of dry cells made with different starches, and the use of modified starches and starch fractions decreased the electrical output of dry cells. The beneficial effects of the flour fractions were attributed to their action in curtailing the local action at the zinc anodes of dry cells.

I. Introduction

One of the reasons advanced for the decreased shelf life of electric dry batteries at high temperatures is the deterioration of the paste wall, or its interaction with various constituents of the cell. A Leclanché dry cell consists of a zinc positive element, a carbon negative element surrounded by a depolarizing mix of manganese dioxide, and a paste-wall separator usually consisting of starch-flour gels. An electrolyte of saturated ammonium chloride with low concentrations of zinc chloride is generally used. Acetylene black is added to the depolarizing mix to render it more conducting and absorptive.[1]

Otto, Vinal, and Ostrander [1][2] have shown by digestion experiments that the paste walls of dry cells react with the depolarizing mix of manganese dioxide. As digestion experiments cannot be used to determine the rate of duration of the interaction, another method, such as the measurement of gel strength, must be used for this purpose. One of the purposes of this paper is to show how gel-strength measurements may be applied to studies of the paste wall of dry cells. Characteristics of the paste wall determined in this way are then correlated with the shelf life of the dry cells.

Because of the interaction of the paste wall and other constituents of the dry cell, it would appear that substitutes for the starch-flour paste wall would be the answer to the deterioration of batteries at elevated temperatures. However, other materials have, in general, proved to be even less satisfactory, either because they are corrosive, increase the internal resistance of the cell, exhibit syneresis, or are precipitated or otherwise affected by the cell electrolyte. For this reason, a thorough study of the characteristics of starch-four gels was undertaken and the results are presented in this paper.

The paste wall is made in a number of ways, and various formulas are used in its preparation. In this work a definite formula was rigorously adhered to throughout, so that interpretations of the results could be readily made. The paste walls consisted of approximately 8 g of zinc chloride, 30 g of ammonium chloride, 66 g of distilled water, 0.1 g of mercuric chloride, and 29 g of a mixture of cornstarch and wheat flour in a total volume of 108 ml.

[1] For a description of a Leclanché dry cell, including a diagram, see E. Otto C. K. Morehouse, and G. W. Vinal, Trans. Electrochem. Soc. Preprint 90-17, 235, (1946), or pamphlets of battery manufacturers.

[2] Figures in brackets indicate the literature references at the end of this paper.

II. Experimental Procedures

1. Stability [3] of Starch Gels in Presence of Dry-Cell Constitutents

A large number of gels, simulating the paste wall as to composition, were prepared, and after aging their gel strengths were measured by a method previously described [3]. These data served as standards or controls. Then gels were made in like manner in which various constituents of the dry cell were incorporated. The strengths of these were also measured after aging and compared with the standards. Data are given in table 1 for temperatures of 25° and 54° C. As starch gels are irreversible, each value represents a single measurement on an individual gel. A temperature of 54° C was chosen for the tests, because temperatures this high were encountered in the tropics during the past war. Comparisons of the strengths of gels containing no salts with those that do, show that the zinc and ammonium chlorides of the dry-cell electrolyte cause a decrease in the strength of starch gels, presumably because of some interaction between these salts and the cereal. Additions of MnO_2 or acetylene black, which are insoluble, give an apparent increase in the strength of starch gels, because they contribute to the concentration of the gels as would additional cereal.

Interactions between the paste wall and other constituents of the dry cell are more clearly shown by relative changes in the strength of the gels with time. In figure 1, the ratios of the strength of aged gels to unaged ones of the same composition, expressed as percentages, are shown as a function of aging or storage time. The figure is largely self-explanatory. All gels decrease in strength as they are aged owing to deterioration of the starch, and the rate is approximately the same for the control gels as for those made with zinc dust or stored in zinc cans, and for those in which acetylene black is incorporated. Consequently, interactions between the paste wall and zinc or acetylene black must be slight. On the other hand, the gels containing no salts decrease in strength less rapidly and those containing MnO_2 more rapidly than the standards.

[3] One of the factors affecting the stability of gels is syneresis. Therefore, the syneresis of a large number of gels was measured by the mothod of Chapman and Buchanan [2]. None of the gels presented in this work, whether or not they contained zinc, acetylene black, or MnO_2, exuded water over a period of 1 year. Only when the concentration of the cereal in the gels was less than 8 to 9 percent was synersis observed, and this concentration of cereal is much less than that used in the preparation of paste walls of dry cells.

TABLE 1.—*Gel strength* measured at 25° C of paste walls mixed with constituents of dry cells*

Type of paste wall	Composition of paste wall[a]				Days of storage								
	Weight, starch	Weight, water	Weight, $ZnCl_2$	Weight, NH_4Cl	0	4	7	14	21	30	45	60	90
	g	*g*	*g*	*g*	*g/cm²*	*g/cm²*	*g/cm²*	*g/cm²*	*g/cm²*	*g/cm²*	*g/cm²*	*g/cm²*	*g/cm²*
Control at 25° C	29.20	65.67	8.13	30.27	526	520	520	505	487	481	468	475	96
Control at 54° C	29.20	65.67	8.13	30.27	526	520	499	506	482	468	445	461	43
Starch alone without electrolytes at 25° C	29.20	88.17	0.00	0.00	671	655	651	649	651	665	641	657	62
Starch alone without electrolytes at 54° C	29.20	88.17	.00	.00	671	670	658	656	627	640	634	621	62
Control+10 grams of MnO_2 at 54° C	28.66	64.45	7.98	29.71	916	.....	860	778	712	700	630	621	68
Control+10 grams of MnO_2+10 grams of Na_2SO_3 at 54° C	27.67	62.19	7.70	28.67	927	.....	906	840	829	752	691	.....	62
Control+10 grams of MnO_2+1.9 grams of borax at 54° C	28.36	62.89	7.90	29.40	886	.....	858	809	763	745	644	645	98
Control+10 grams of MnO_2+10 grams of glucose at 54° C	26.90	60.50	7.49	27.89	[b] 872	.....	589	311	.....	.....	.....	.....	.....
Control+10 grams of MnO_2+10 grams of dextrose at 54° C	26.90	60.50	7.49	27.89	[b] 877	.....	572	285	.....	.....	.....	.....	.....
Control+1 gram of acetylene black[c] at 54° C	28.66	64.45	7.98	29.71	551	547	.....	505	.....	494	.....	.....	.....
Control in zinc can at 54° C	29.20	65.67	8.13	30.27	526	520	508	[d] • 470	[d] [f] 379	463	467	.....	.....
Control+1 gram of zinc dust at 54° C	28.66	64.45	7.98	29.71	492	485	.....	461	.....	435	.....	.....	69

[a] All pastes contained 0.1 g of $HgCl_2$, which acts as a preservative.
[b] Gassed with evolution of CO_2.
[c] Acetylene black does not wet well. A few drops of butyl cellusolve, a wetting agent, were added.
[d] Adhesion between zinc and gel was poor.
[e] 12 days.
[f] 18 days.
* Weight of mercury divided by area of disk having a diameter of 0.95 cm (⅜ in.).

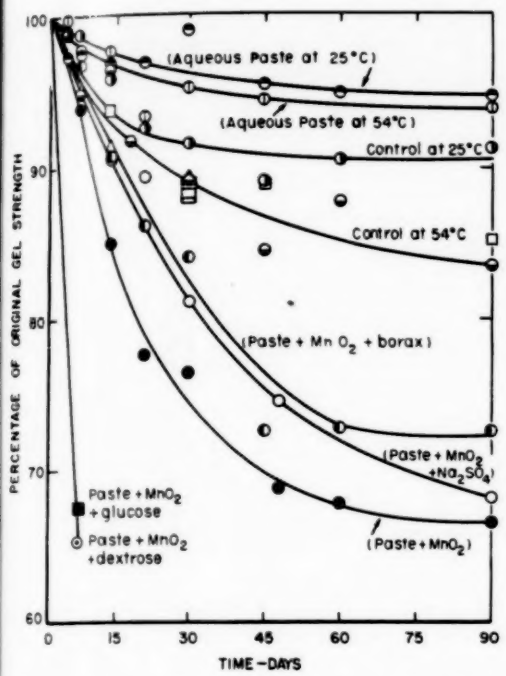

FIGURE 1.—*Percentage decrease in gel stength of cornstarch paste walls in presence of constituents of dry cells at 25° and 54° C.*

◑, Control at 25° C; ◒, control at 54° C; ◓, starch paste wall without electrolytes at 25° C; ◐, starch paste wall without electrolytes at 54° C; ●, control with 10 g of MnO_2 added at 54° C; ○, control with 10 g of MnO_2 and 10 g of Na_2SO_4 added at 54° C; ◐, control with 10 g of MnO_2 and 1.9 g of borax added at 54° C; ■, control with 10 g of MnO_2 and 10 g of glucose added at 54° C; ⊖, control with 10 g of MnO_2 and 10 g of dextrose added at 54° C; △, control with 10 g of acetylene black added at 54° C; □, control stored in zinc can or with 1 g of zinc dust added at 54° C.

Therefore, the salts ($ZnCl_2$ and NH_4Cl) and MnO_2 apparently react with the cereal causing a decrease in the strength of the gels. MnO_2 must react either directly with the starch or its hydrolytic products. When glucose or dextrose, hydrolytic products, are incorporated in starch gels containing MnO_2, there is a rapid evolution of CO_2 with an attendant large and rapid decrease in the strength of the gel. The decrease in gel strength is caused in part by the fact that the evolution of gas makes the gels porous.

All gels whether or not they contain constituents of the dry cell seem to attain stability within 60 to 90 days, as the decrease in gel strength ceases within this time. Tests for much longer periods of time at 54° C could not be made, because gels become desiccated after 4 to 5 months at this temperature. However, the reaction between MnO_2 and starch is quite marked during the first 60 days, and the problem resolves itself into finding ways by which this interaction may be either eliminated or retarded. Possible approaches to this problem include (1) the use of addition agents that will retard the hydrolysis of the starch, (2) the use of other types of starch or flour instead of cornstarch or wheat flour, (3) modifications of the starch to decrease its reducing power and hence its interaction with MnO_2, (4) the use of the amylose or amylopectin fractions of starch, or (5) the use of the constituents of flour, namely gluten or its protein fractions, rather than the natural flour. Each of these possibilities is considered in the following sections.

2. Stability of Starch Gels in Presence of Addition Agent and Inhibitors

Neutral sulfates are believed to retard the hydrolysis of starch [4], and borax is known to increase the viscosity and adhesiveness of starch pastes. However, neither of these salts was effective in retarding the hydrolysis of starch. The slight benefits of these salts indicated in figure 1 are not significant, because these salts raise the strength of starch gels not containing MnO_2. Other salts might be used, but in general most addition agents decrease the stability of starch gels and have deleterious effects on dry cells. Therefore, this approach to the elimination of interactions between the paste wall and the constitutents of the dry cell is not promising.

In preparations of the paste wall, mercuric chloride (see formula given in the introduction) is frequently added for the purpose of reducing the local action at the zinc anode. Chromates or chromate films are sometimes used in place of mercuric chloride. Neither amalgamation nor chrome films are as effective as is essential for good shelf-life at high temperatures [5] and other materials have been suggested as inhibitors of the corrosion of zinc. Their choice is largely a matter of trial and error and to study a large number would be a prohibitive task. An elimination may first be made by studying the effects of the inhibitors on the paste wall.

The inhibitors were incorporated into the paste wall by grinding the inhibitor with the starch using a minimum of alcohol, which was then

allowed to evaporate at room temperature. Heating of an alcoholic-inhibitor-starch mixture causes a decrease in the strength of the starch and was avoided. The starch-inhibitor pastes (pastes *A*) were made using the formula given in the introduction, corrections being made for the amount of inhibitor added, so that the ratio of starch to $ZnCl_2$, NH_4Cl, and H_2O and the concentrations of $ZnCl_2$ and NH_4Cl were the same as in the non-inhibitor pastes. Data for starch gels containing inhibitors are given in table 2, and for wheat-flour gels containing inhibitors in table 3. Data on pastes (pastes *B*) made using the formula given in the introduction without regard to density corrections are given for the starch gels. Data for pastes *A* and *B* are not very different.

TABLE 2.—*Data showing the effect of inhibitors on the strength of cornstarch gels at 25° C*

Inhibitor	Grams of inhibitor per 100 g of starch	Weight of mercury required to pull disk from gels		Gel strength [a]	
		Paste A [b]	Paste B [c]	Paste A	Paste B
	g	g	g	g/cm²	g/cm²
Control	0.00	375	375	526	526
$K_2Cr_2O_7$	1.00	431	.....	604	.....
Do	2.00	454	.....	637	.....
Do	3.00	467	.....	655	.....
Do	5.00	481	.....	675	.....
$Na_2Cr_2O_7.2H_2O$	2.28	452	.....	634	.....
Do	5.69	479	.....	672	.....
$(NH_4)_2Cr_2O_7$	3.00	465	.....	652	.....
Do	5.00	478	.....	670	.....
K_2CrO_4	3.00	446	.....	626	.....
Do	5.00	452	.....	634	.....
Do	10.00	404	.....	567	.....
$ZnCrO_4$	5.00	457	.....	641	.....
Do	10.00	446	.....	626	.....
Furfural	0.50	389	380	546	533
Do	5.00	514	561	721	787
Do	10.00	524	371	735	520
Hydrofuramide	0.50	358	362	502	508
Do	3.00	286	309	401	433
Quinaldine	2.00	395	.....	554	.....
Do	5.00	361	.....	506	.....
Proprietary compounds of unknown composition.	5.00	20	33	28	46
	5.00	101	114	142	160
	5.00	133	143	187	201
	5.00	176	198	247	278
	5.00	260	292	365	410
	2.00	340	355	477	498
	5.00	318	357	446	501
	3.00	249	266	349	373
	5.00	192	216	269	303

[a] Weight of mercury divided by area of disk having a diameter of 0.95 cm (⅜ in.).

[b] Corrections for densities of constituents of paste were made.

[c] Corrections for densities of constituents of paste were not made.

TABLE 3.—*Data showing the effect of inhibitors on the strength of wheat flour gels at 25° C*

Inhibitor	Inhibitor per 100 g of flour	Weight of mercury required to pull disks from gels [a]	Gel strength [a]
	g	g	g/cm²
Control	0.00	226	317
$K_2Cr_2O_7$	3.00	226	373
Do	5.00	270	379
Do	10.00	242	339
$Na_2Cr_2O_7.H_2O$	3.81	278	390
Do	5.69	282	396
Do	11.38	252	353
$(NH_4)_2Cr_2O_7$	8.00	282	396
Do	10.00	276	387
K_2CrO_4	3.00	241	338
Do	5.00	243	341
Do	10.00	229	321
$ZnCrO_4$	5.00	237	332
Do	8.00	249	349
Do	10.00	269	377
Furfural	5.00	294	412
Hydrofuramide	5.00	219	307
Quinaldine	5.00	239	335
CKM wheat flour [c]	0.00	259	363
Proprietary compounds of unknown composition.	.50	258	362
	1.00	257	360
	1.00	233	327
	3.00	234	328
	5.00	227	318
	5.00	166	233
	5.00	180	252

[a] Corrections for densities of constituents of paste were made.

[b] Weight of mercury divided by area of disk having a diameter of 0.95 cm (⅜ in.).

[c] Treated with methanol; prepared by C. K. Morehouse.

The chromates and dichromates increase the strength of both types of gels, and the increase is about the same for cations K^+, Na^+, NH_4^+, or Zn^{++}. On the other hand, with the exception of furfural and possibly quinaldine, the other inhibitors (proprietary compounds of unknown composition) lower the strength of gels. This decrease in the strength of starch-inhibitor gels indicates an interaction between the starch and the inhibitor. Dry cells made with paste walls of starch-inhibitor gels were not satisfactory and gave less electrical output than cells without inhibitors [5]. Cells made with furfural and quinaldine, substances which increase the strength of the paste wall, had low flash currents indicating high internal resistance [5].

3. Paste Walls of Different Starch Types

Different varieties of starches or flours may function differently as paste walls. Therefore, a number of gels, simulating the paste wall of dry

cells as to composition, were made with different varieties of starch or flour and aged for 1 day. Their strengths were then measured using disks having a diameter of 0.95 cm (⅜ in.). The data are given in table 4 and are shown in figure 2 as

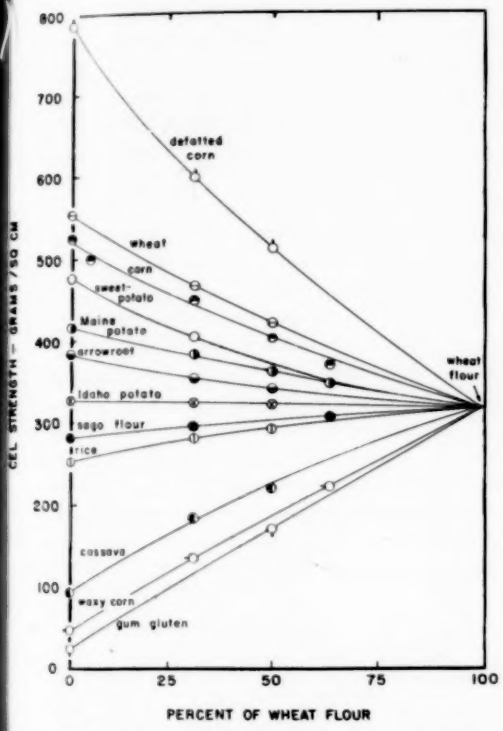

FIGURE 2.—*Gel strengths at 25° C. of various paste walls as a function of the percentage of wheat flour in the paste wall.*

a function of the percentage of wheat flour in the gels. Paste walls of widely different strengths may, therefore, be made by varying the percentage of flour in them or by using different kinds of starch. Very rigid gels are obtained with defatted cornstarch, and nonrigid and tacky gels are obtained with waxy cornstarch. Addition of flour lowers the strength of defatted cornstarch gels and raises the strength of gels made of waxy cornstarch.

In figure 3 the resistance to deformation of gels made of pure starch or flour is shown. The method by which these curves are obtained was described previously [3]. The slope up to the break in the curve gives an indication of the resistance a gel offers to deformation. A large slope means that the gel is less rigid than one having a small slope. Thus waxy cornstarch makes paste walls that can be easily deformed, whereas cornstarch gels resist deformation.

TABLE 4.—*Gel strengths at 25° C of several standard pastes for construction of dry cells*

Starch or sample	Weight of sample	Weight of wheat flour	Weight of mercury required to pull disks from gels	Gel strength [a]
	g	*g*	*g*	*g/cm²*
Cornstarch	29.20	0.00	375	526
	26.28	2.92	356	499
	19.67	9.53	320	449
	14.60	14.60	287	403
	9.53	19.67	263	369
Wheat flour	29.20	.....	226	317
Wheat starch	29.20	0.00	396	555
	19.67	9.53	333	467
	14.60	14.60	301	422
Waxy cornstarch	29.20	0.00	34	48
	19.67	9.53	96	135
	9.53	19.67	158	222
Cassava starch	29.20	0.00	67	94
	19.67	9.53	131	184
	14.60	14.60	158	221
Arrowroot starch	29.20	0.00	274	384
	19.67	9.53	254	356
	14.60	14.60	244	342
Idaho potato starch	29.20	0.00	233	328
	19.67	9.53	231	324
	14.60	14.60	231	324
Maine potato starch	29.20	0.00	297	417
	19.67	9.53	273	383
	14.60	14.60	258	362
	9.53	19.67	248	348
Sweetpotato starch	29.20	0.00	340	477
	19.67	9.53	289	406
	9.53	19.67	250	350
Rice starch	29.20	0.00	180	253
	19.67	9.53	200	281
	14.60	14.60	208	292
Sago flour	29.20	0.00	202	283
	19.67	9.53	210	295
	9.53	19.67	219	307
Gum gluten	29.20	0.00	18	25
	14.60	14.60	121	171
Defatted cornstarch	29.20	0.00	561	787
	19.67	9.53	428	600
	14.60	14.60	366	513

[a] Weight of mercury divided by area of disk of diameter 0.95 cm (⅜ in.).

To ascertain if the shelf life of dry cells is dependent on the strength of the paste wall, or if the extent of the interactions between the paste wall and dry-cell electrolytes and MnO_2 may be different for various varieties of starches, a number of *D*-size dry cells[4] (1¼ in. diameter and 2¼ in. in height) were constructed with paste walls of

[4] See Letter Circular 267, National Bureau of Standards (1941) for a classification of electric dry cells of the Leclanché type.

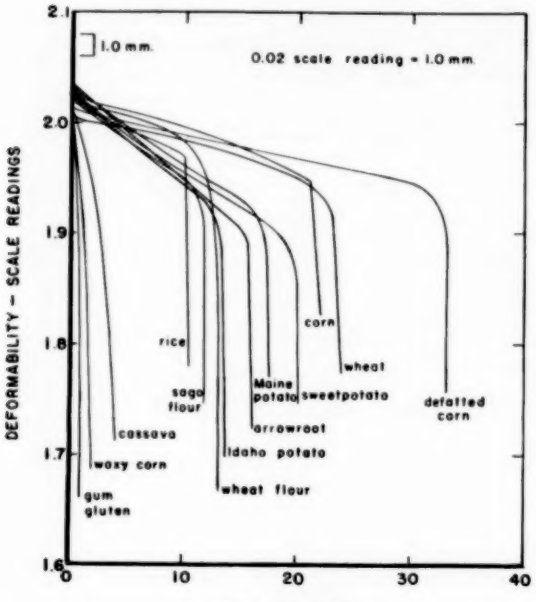

FIGURE 3.—*Deformability (scale reading) of paste walls of different starches at 25° C.*

different starch type. Shelf-life data are given in table 5 for a storage period up to 2 years. The data do not indicate that one or another type of starch is preferable for construction of paste walls nor that the interactions between the paste walls and the other constituents of the cell are significantly different for various varieties of starches. Cells with paste walls of waxy cornstarch of low gel strength performed similarly to those with paste walls of cornstarch of high gel strength. Consequently, the shelf life of dry cells is not dependent on the strength of the gel, providing it retains stability. This does not imply that discharge characteristics under various current drains will be the same for different kinds of starch; the data here obtained apply only to shelf life.

4. Paste Walls of Modified Starches

In section I, it is shown that natural starches and MnO_2 react chemically, and in section II, 3, natural starches of various kinds behave similarly in dry cells. Starch granules consist of chains of glucose residues with primary and secondary alcohol groups, glycol groups, and reducing aldehyde end groups. Reaction of MnO_2 and starch may be at any of these groups [6], but it is probably most pronounced at the aldehyde end group. It is possible, therefore, that dry cells with better characteristics would result if the starch used in the paste wall were modified to decrease its reducing power.

A number of modified starches were studied. Each one was characterized by the strength of its gel (table 6) and the resistance each gel offered to deformation (fig. 4). The method of modification of the starch is listed in the second column of table 6. The strength of starch gels is increased when the fats adsorbed on the starch granules are removed. The strengths of the gels made with the other modified starches are less than those made with unmodified starches. Apparently, most modifications of starch fracture the starch granules causing a decrease in their strength.

A number of *D*-size dry cells were made with paste walls of modified starches. Data for a storage period up to 2 years are given in table 7 for modified starches, and in table 8 for starches plus wheat gluten or fats. Dry cells made with defatted starches and 4601 cornstarch have shelf-life data comparable with that of dry cells made with natural starches. On the other hand, dry cells made with paste walls of other modified starches were less satisfactory than cells contain-

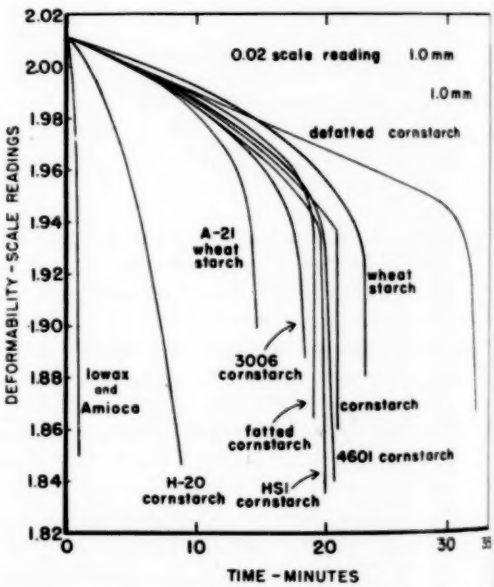

FIGURE 4.—*Deformability (scale readings) at 25° C. of paste walls of different modified starches.*

TABLE 5.—*Shelf life data at 21° C of D-size dry cells containing different kinds of starches and flours*[a]

Test	Composition of the paste wall	Number of cells	Storage period																			
			1 week		1 month		3 months		6 months		9 months		1 year		15 months		18 months		21 months		2 years	
			OCV[b]	FC[c]	OCV	FC	OCV	FC	OCV	FC	OCV	FC	OCV	FC	OCV	FC	OCV	FC	OCV	FC	OCV	FC
			v	*amp*	*v*	*amp*	*v*	*amp*	*v*	*amp*	*v*	*amp*	*v*	*amp*	*v*	*amp*	*v*	*amp*	*v*	*amp*	*v*	*amp*
1	Cornstarch, 67% Wheat flour, 33%	48	1.63	6.7	1.59	6.1	1.58	5.6	1.58	5.0	1.57	5.1	1.57	4.4	1.56	3.7	[d]1.54	3.5	[d]1.54	2.7	.....	.....
2	Cornstarch, 30% Waxy cornstarch, 17% Wheat flour, 33%	4	1.64	7.0	1.60	6.8	1.58	6.0	1.58	5.3	1.57	5.0	1.57	4.9	1.56	4.4	1.55	5.0	1.57	5.1	.....	.....
3	Cornstarch, 33.3% Waxy cornstarch, 33.3% Wheat flour, 33.3%	5	1.64	7.1	1.60	6.7	1.58	5.4	1.58	4.1	1.58	3.6	1.57	3.0	1.56	2.0	(e)	.....	.....	.....	.....	.....
4	Cornstarch, 17% Waxy cornstarch, 50% Wheat flour, 33%	6	1.64	7.9	1.61	7.2	1.58	6.4	1.58	5.9	1.58	5.4	1.57	5.1	1.56	4.2	1.56	[f]3.4	1.57	[f]3.2	.....	.....
5	Waxy cornstarch 67% Wheat flour, 33%	61	1.63	6.7	1.60	6.5	1.58	6.0	1.58	5.7	1.58	5.0	1.58	4.7	1.56	5.0	1.56	4.9	1.55	4.8	1.56	4.4
6	Sweetpotato starch, 67% Wheat flour, 33%	18	1.62	6.2	1.59	6.0	1.58	6.0	1.58	6.2	1.57	6.1	1.57	5.9	1.56	5.0	1.55	3.9	1.55	2.1	.....	.....
7	Waxy cornstarch, 67% Sago flour, 33%	[g]5	1.64	8.1	.....	.....	.....	.....	.....	.....	.....	.....	.....	.....	.....	.....	.....	.....	.....	.....	.....	.....
8	Cornstarch, 100%	4	1.64	6.4	1.60	6.6	1.60	5.7	1.58	5.9	1.57	5.7	1.56	5.2	(e)	.....	.....	.....	.....	.....	.....	.....
9	Waxy cornstarch, 100%	18	1.64	7.1	1.61	6.6	1.59	6.1	1.58	5.4	1.58	5.0	1.58	4.3	1.56	3.0	.....	.....	[h]1.55	5.4	1.56	4.3

Test No.	Light industrial flashlight test (LIF) (after 1 week)	4-ohm continuous test (after 1 week)	Current maintenance (percent)									
	min	*min*	*min*	*min*	*min*	*min*	*min*	*min*	*min*	*min*	*min*	*min*
1	980	645	100	91	84	75	76	66	55	52	40	.....
2	1,012	645	100	97	86	76	71	70	63	71	73	.....
3	1,005	683	100	94	76	58	51	42	28	(e)	.....	.....
4	1,120	675	100	91	81	75	68	65	53	43	41	.....
5	909	698	100	97	90	85	75	70	75	73	72	66
6	816	705	100	97	97	100	98	95	81	63	34	.....
7	1,196	673	100	.....	.....	.....	.....	.....	.....	.....	.....	.....
8	921	.....	100	103	89	92	89	81	(e)	.....	.....	.....
9	964	.....	100	93	86	76	70	61	42	.....	[h]76	[h]60
Avg	991	675	100	95	86	80	75	69	57	60	[i]52	.....

[a] The data used in constructing this table were supplied by Earl Otto, Clarence K. Morehouse, Jacqueline M. Pritchard, Woodward G. Eicke, Ray Lasky, Frances McPherson, Mary J. Gleason, and Margaret E. Dekle.

[b] Open-circuit voltage.

[c] Flash or short-circuit current.

[d] 32 cells.

[e] Scrapped; cells were perforated and gave poor service.

[f] Perforated.

[g] All cells were used for the LIF and 4-ohm test.

[h] 6 cells.

[i] Does not include the value for test number 9.

TABLE 6.—*Gel strength of modified starches at 25° C*

Starch [a]	Modification	Weight of mercury	Gel strength [b]
		g	*g/cm²*
Natural Buffalo cornstarch.	No modification	375	526
Defatted Buffalo cornstarch.	Extractions with 85% of methanol.	561	787
H-20 cornstarch [c]	To resist oxidation	193	271
4601 cornstarch [d]	do	356	499
3006 cornstarch [d]	To resist zinc chloride	316	443
HSI cornstarch [e]	Treated with chlorine dioxide.	343	481
CKM cornstarch [f]	Mixed with ethanol and heated at 80° C.	352	494
Soft white wheat starch	Slotter and Langford [g] method.	396	555
A-21 wheat starch (General Mills).	Unknown treatment	261	366
Fatted Buffalo cornstarch.	1% of corn oil added	327	459
Natural waxy cornstarch.	No modification	34	48
Amioca	do	30	42
Iowax [h]	Washed with distilled water.	39	55
Amidex (a dextrine)	Acid-treated and heated	0	0

[a] All of the pastes were made with 29.2 g of starch, 8.133 g of $ZnCl_2$, 30.267 g of NH_4Cl, and 65.57 g of distilled water.

[b] Weight of mercury divided by area of disk of diameter 0.95 cm (⅜ in.).

[c] Supplied by American Maize Products Co., Roby, Ind.

[d] Supplied by the Corn Products Laboratories, treatments unknown.

[e] Prepared by H. S. Isbell, National Bureau of Standards.

[f] Prepared by C. K. Morehouse, formerly of the National Bureau of Standards.

[g] R. L. Slotter and C. T. Langford, Ind. & Eng. Chem. **36**, 404 (1944).

[h] Supplied by the Northeastern Regional Laboratory of the U. S. Department of Agriculture, Peoria, Ill.

ing paste walls of natural unmodified starches. Apparently, the modifications fracture the glucose chains of the starch granules, shown by the gel-strength measurements, giving more reducing aldehyde end groups, and consequently increased interaction between the starch and MnO_2. Even those treatments intended to convert the aldehyde end groups to nonreducing carboxyl groups [7] must instead fracture the starch granule, thereby giving more instead of less aldehyde end groups. Probably most chemical modifications will affect starch in like fashion. Hence, modified starches will probably be less satisfactory than natural starches for use in dry cells.

Dry cells made with various starches, plus wheat gluten or fats, compare favorably with those prepared with wheat flour, providing the amount of fats or oils added was not excessive. Cells prepared with soybean flour gave less current maintenance than the others, probably because of the large amounts of fats and oils in soybean flour.

5. Fractionation of Starch

Starch granules consist of straight chained (amylose) and branched chained (amylopectin) glucose units. Only 0.4 percent of glucose units in amylose contain aldehyde end groups and 4 percent of the glucose units of amylopectin contain aldehyde end groups [8]. Therefore, amylose should be less subject to oxidation by MnO_2 than amylopectin. The common starches, corn, wheat, and potato consist of about 20 percent of amylose and 80 percent of amylopectin, whereas waxy cornstarch is 100 percent amylopectin. Hence, waxy cornstarch should be more easily oxidized than the common starches. Otto, Vinal, and Ostrander [1] have shown that this is the case at 100° C. However, shelf-life data given above for cells made with paste walls of waxy cornstarch and ordinary cornstarch were not appreciably different. However, the amylose content in cornstarch may be too low to expect any noticeable difference. Consequently, *D*-size cells were made with paste walls of corn amylose.

Cornstarch was first defatted by the methanol method of Schoch [9]. Then corn amylose was obtained from the defatted cornstarch by the butanol isoamyl alcohol method of Wilson, Schoch, and Hudson in which a starch paste is first autoclaved for 2 to 3 hours at 18 to 20 pounds per square inch [10]. The amylose was partially dehydrated by tritulation with methanol and butanol, maintained in a water-soluble state by keeping it moist with butanol, and its purity determined by the colorimetric method of McCready and Hassid [11]. A purity of 90 percent was found by this method for the sample by Harriet L. Frush of this Bureau. As this purity was adequate for the present purpose, no further purification was made.

Pastes were made of pure amylose and of mixtures of amylose and cornstarch. The strengths of these pastes are given in table 9, together with data on mixtures of cornstarch and waxy cornstarch. No exact correlation between gel strength and the percentage of amylose in the paste was found. However, it is a question whether these amylose pastes are true gels. Brimhall and Hixon [12] have stated that starches autoclaved at high temperatures possess little rigidity and hence would not form gels. However, when corn amylose, wet with butanol, is heated at 100° C, it

TABLE 7.—*Shelf life data at 21° C of D-size dry cells containing modified starches* [a]

Test No.	Type of modified starch	Number of cells	Storage period																			
			1 week		1 month		3 months		6 months		9 months		1 year		15 months		18 months		21 months		2 years	
			OCV [b]	FC [c]	OCV	FC	OCV	FC	OCV	FC	OCV	FC	OCV	FC	OCV	FC	OCV	FC	OCV	FC	OCV	FC
			v	*amp*	*v*	*amp*	*v*	*amp*	*v*	*amp*	*v*	*amp*	*v*	*amp*	*v*	*amp*	*v*	*amp*	*v*	*amp*	*v*	*amp*
10	Defatted cornstarch	15	1.63	6.5	1.59	5.7	1.58	5.3	[d] 1.57	5.7	1.56	4.7	[e] 1.56	5.3	.....	.....	[e] 1.54	4.1	[e] 1.54	3.5	[e] 1.54	2.5
11	3006 Cornstarch	10	1.63	6.6	1.59	6.4	1.58	5.3	1.58	4.4	1.57	4.4	1.55	3.0	1.55	2.3	[f]	.....	.....	.....	.....	.....
12	4601 Cornstarch	10	1.64	6.7	1.60	6.4	1.58	5.8	1.58	5.4	1.57	4.9	1.55	4.8	1.55	4.3	1.56	4.3	.....	.....	.....	.....
13	H-20 Cornstarch	3	1.65	8.0	1.62	5.7	1.59	5.8	1.59	4.8	1.58	4.6	1.57	3.6	1.56	3.1	[f]	.....	.....	.....	.....	.....
14	H8I Cornstarch	5	1.62	7.4	1.60	6.8	[f]	.....	.....	.....	.....	.....	.....	.....	.....	.....	.....	.....	.....	.....	.....	.....
15	H-20 Cornstarch, 67%; Wheat flour, 33%	44	1.62	7.5	1.60	6.9	1.59	6.0	1.58	4.1	1.57	3.1	1.56	2.6	1.56	1.8	1.56	1.2	[f]	.....	.....	.....

Test No.	Light industrial flashlight test (LIF) (after 1 week)	4-ohm continuous test (after 1 week)	Current maintenance (percent)									
	Min.	*Min.*										
10	893	--	100	88	82	88	72	82	.....	63	54	38
11	.....	--	100	97	80	67	67	46	35	[f]	.....	.....
12	.....	--	100	96	87	81	73	72	64	64	.....	.....
13	951	--	100	71	73	60	58	45	39	[f]	.....	.....
14	.....	--	100	92	[f]	.....	.....	.....	.....	.....	.....	.....
15	928	705	100	92	80	55	41	35	24	16	[f]	.....
Avg.	924	--	100	89	80	70	62	56	41	.....	.....	.....

[a] Data used in constructing this table were obtained by Earl Otto, Clarence K. Morehouse, Jacqueline M. Pritchard, Woodward G. Eicke, and Ray Lasky.

[b] Open-circuit voltage.

[c] Flash or short-circuit current.

[d] 6 cells.

[e] 4 cells.

[f] Scrapped; cells were perforated and gave poor service.

dissolves completely to form a clear solution. On cooling, the amylose appears from solution in the form of a very rigid mass, probably retrograded amylose, which could be used as a paste wall in dry cells.

Data on *D*-size dry cells made with paste walls of corn amylose are given in table 10. The initial flash or short-circuit current was low, and the current maintenance poor. There are probably two reasons for this poor behavior. First, the amylose must be kept moist with butanol, and second, the amylose pastes are not true gels. Butanol has a deleterious effect on the dry cell, and amylose pastes not being true gels do not retain cell electrolyte well and give up their water and electrolyte to the depolarizing mix of the cell. Attention, therefore, was given to the flour portion of the paste wall.

6. Fractionation of Flour

Crude gluten was obtained from wheat flour by the method of Dill and Alsberg [13], in which the starch was washed away with a synthetic tap water of pH 6.8. The various proteins were then obtained from the crude gluten by a modification of the combined methods of Stockelbach and Bailey [14] and of Haugaard and Johnson [15]. Crude gluten (200 g) was added to 3.5 liters of 0.1 *N* acetic acid to which 7 g of K_2SO_4 were slowly added. After 24 hours of stirring, the glutenin was dispersed with 3.5 liters of 95-percent ethanol. After a few hours the dispersed glutenin was recovered using a laboratory centrifuge (rpm = 2,000). The glutenin became hard and brittle when air-dried and was unsuitable for use in dry cells. After an additional 24 hours at room temperature, a second syrupy mass settled from the acetic acid-alcohol mixture. This fraction was designated mesonin but probably was contaminated with glutenin.

The other proteins were obtained from the supernatant liquid by a cooling process, first for 2 days at 13° C, next for 1 day at 4° C, and finally for 2 days at −10° C. Syrupy masses were ob-

TABLE 8.—*Shelf life data at 21° C of D-size dry cells containing starches plus gluten or fats* [a]

Test No.	Composition of the paste wall	Number of cells	Storage period																	
			1 week		1 month		3 months		6 months		9 months		1 year		15 months		18 months		21 months	
			OCV[b]	FC [c]	OCV	FC	OCV	FC	OCV	FC	OCV	FC	OCV	FC	OCV	FC	OCV	FC	OCV	FC
			v	*amp*	*v*	*amp*	*v*	*amp*	*v*	*amp*	*v*	*amp*	*v*	*amp*	*v*	*amp*	*v*	*amp*	*v*	*amp*
16	Cornstarch 67%; soybean [d] flour, 33%.	3	1.60	6.2	1.57	4.7	1.55	2.3	(•)											
17	Waxy cornstarch, 99.5%; corn oil, 0.5%.	12	1.65	7.1	1.62	6.1	1.59	5.7	1.57	6.0	1.57	5.4			1.54	5.1	1.54	4.7	1.55	4.5
18	Cornstarch, 67%; wheat gluten, 33%.	3	1.65	8.2	1.62	7.5	1.59	7.1	1.58	6.3	1.58	5.8	1.57	5.0	1.55	4.2	1.56	3.3	1.56	2.7
19	Waxy cornstarch, 67%; wheat gluten, 33%.	4	1.65	8.0	1.62	7.4	1.59	6.9	1.58	6.0	1.58	5.6	1.56	5.0	1.56	4.4	1.56	3.9	1.56	3.2

Test No.	Light industrial flashlight test (LIF) (after 1 week)	4-ohm continuous test (after 1 week)	Current maintenance (percent)								
	min	*min*									
16	723		100	76	37	(•)			72	66	63
17		468	100	86	80	85	76	61	51	40	33
18	879	720	100	91	87	77	71	63	55	49	40
19	1,092	660	100	93	86	75	70				
Average	898	616	100	87	73	79	72	62	59	51	45

[a] Data used in constructing this table were obtained by Earl Otto, Clarence K. Morehouse, Jacqueline M. Pritchard, Woodward G. Eicke, and Ray Lasky.

[b] Open-circuit voltage.

[c] Flash or short-circuit current.

[d] Contained 46% fats and oils.

• Scrapped; cells were perforated and gave poor service.

TABLE 9.—*Data on the gel strength of aqueous mixtures of cornstarch and corn amylose, and cornstarch and waxy cornstarch*

[Moisture contents: Cornstarch=12.8%; waxy cornstarch=13.5%; corn amylose=86.9% butanol.]

Weight of cornstarch	Weight of corn amylose	Weight of water	Weight of dry sample per 100 ml of paste	Percent of amylose	Weight of mercury	Gel strength [a]
g	*g*	*g*	*g*		*g*	*g/cm²*
11.50	0.00	141.0	6.7	21.0	236	83
9.17	15.27	126.9	6.7	34.8	463	162
6.88	30.53	114.0	6.7	48.6	526	185
4.59	45.80	101.0	6.7	62.4	682	239
0.00	76.34	75.0	6.7	90.0	859	301
	Weight of waxy cornstarch					
	g					
12.84	0.00	138.4	7.6	21.0	272	95
9.63	3.24	138.3	7.6	15.7	106	37
6.42	6.47	138.3	7.6	10.5	34	12
3.21	9.71	138.3	7.6	5.3	13	5
0.00	12.95	138.3	7.6	0.0	0	0

[a] Weight of mercury divided by the area of the disk of diameter 1.9 cm (¾ in.).

tained at the end of each day and were, respectively, mesonin I, mesonin II, 4° C-gliadin, and −10° C-gliadin (fraction obtained in last 2 days of cooling). Only a very small fraction (residual gliadin) and insufficient for use in dry cells was was obtained, when the ethanol was removed from the acetic acid-alcohol mixture by distillation. Each fraction was washed with distilled water and used to line 12 *D*-size zinc cans by the mere expedient of allowing the pastes to stand in the cans for 12 hours. On pouring the pastes from the cans after 12 hours, a very sticky and adhering film remained on the wall of each can. Part of the 4° gliadin was neutralized to a phenolphthalein end point with sodium hydroxide. Cells were also made with this neutralized gliadin. Nine *D*-size cells were also lined with a sample of commercial gliadin dissolved in 60-percent ethanol.

Shelf-life data for dry cells made with the various gluten fractions are given in table 10. The average current maintenance (ratio of flash currents of aged cells to initial flash current of same cells) of the seven types of gluten fractions is given in

TABLE 10.—*Shelf life data at 21° C of D-size dry cells made with cornstarch and wheat flour fractions* [a]

Test No.	Starch or flour fraction or addition to paste wall of dry cells	Number of cells	Storage period													
			1 week		1 month		3 months		6 months		9 months		1 year		15 months	
			OCV[b]	FC[c]	OCV	FC	OCV	FC	OCV	FC	OCV	FC	OCV	FC	OCV	FC
			v	*amp*	*v*	*amp*	*v*	*amp*	*v*	*amp*	*v*	*amp*	*v*	*amp*	*v*	*amp*
20	Corn amylose	2	1.44	4.8	1.38	1.8	[d]									
21	Pure cornstarch	13	1.64	7.1	1.59	6.8	1.58	6.7	1.57	6.3	1.56	5.9	1.56	5.3		
1	Cornstarch 67% wheat flour 33%	48	1.63	6.7	1.59	6.1	1.58	5.6	1.58	5.0	1.57	5.1	1.57	4.4	1.56	3.7
18	Cornstarch 67% wheat gluten 33%	3	1.65	8.2	1.62	7.5	1.59	7.1	1.58	6.3	1.58	5.8	1.57	5.0	1.56	3.9
22[e]	Film of gliadin on zinc can	9	1.66	4.9	1.62	4.8	1.58	4.9	1.57	5.0	[f] 1.56	3.6	[f] 1.57	4.1	[f] 1.55	4.2
23[e]	Film of neutralized 4° gliadin on zinc can.	6	1.65	7.9	1.60	7.4	1.58	7.0	1.56	6.9	[g] 1.55	6.8	[g] 1.56	6.3	1.57	5.9
24[e]	Film of −10° gliadin on zinc can	7	1.66	6.6	1.62	6.2			1.56	6.1	1.56	5.7	1.56	5.7	1.57	5.5
25[e]	Film of 4° gliadin on zinc can	5	1.66	4.8	1.62	4.9			1.57	4.2	1.56	4.5	1.57	4.5	1.57	4.2
26[e]	Film of mesonin on zinc can	9	1.66	6.2	1.62	5.8	1.58	5.6	1.56	4.9	1.56	4.3	[f] 1.57	5.0	[f] 1.57	4.4
27[e]	Film of mesnin I on zinc can	9	1.65	5.7	1.62	5.4	1.58	5.0	1.57	4.8	[h] 1.56	3.8	[d]			
28[e]	Film of mesonin II on zinc can	2	1.65	5.7	1.60	5.2	1.58	5.2	1.57	4.7	[i]	[i]	[i]	[i]	[i]	[i]

Test No.	Light industrial flashlight test (LIF)		4-ohm continuous test (1 week)	Current maintenance (percent)						
	1 week	6 months								
	Minutes	*Minutes*	*Minutes*							
20				100	38	[d]				
21	921			100	96	94	89	83	75	
1	980		645	100	91	84	75	76	66	55
18	879		720	100	91	87	77	71	[f] 61	[j] 51
22	808	794		100	98	100	102	[e] 73	[e] 84	94
23	767	777		100	94	89	87	86	80	[e] 75
24	802	746		100	94		92	86	86	83
25	837	841		100	102		88	94	[j] 94	88
26	716	753		100	94	90	79	69	81	[j] 71
27	879	747		100	95	88	84	[h] 67		
28	919	720		100	91	91	82	[i]	[i]	[i]
Avg of 22 to 28.	814	767		100	95	92	87	79	85	[j] 79

[a] Data used in constructing this table were obtained by Clarence K. Morehouse and Jacqueline M. Pritchard.
[b] Open-circuit voltage.
[c] Flash or short-circuit current.
[d] Scrapped; cells gave poor service.
[e] All cells contained a paste wall of cornstarch, 67% and wheat flour, 33%.
[f] Data for 7 cells; 2 cells were removed for LIF tests.
[g] Data for 4 cells, 2 cells were removed for LIF tests.
[h] Perforated.
[i] Removed for LIF tests.
[j] Value not included in average.

figure 5 for a period of 15 months, and compared with similar data for eight natural starches (table 5) and five modified starches (table 7). At the end of 15 months, cells made with paste walls of the gluten fractions, natural starches, and modified starches gave current maintenances, respectively, of 79, 57, and 41 percent. On the average, cells with modified starches give lower current maintenance than those with natural starches, whereas the gluten fractions show beneficial effects in dry cells. Many commercial cells will show higher current maintenance than the experimental cells reported here, but identical procedures were followed in making all of the cells reported in this paper, and comparisons must be made with the experimental cells and not with commercial ones. It is known that gluten and its protein fractions are inhibitors of the corrosion of zinc [5], and their beneficial effects in the dry cells may be interpreted in this light. Therefore, the properties of the paste wall of dry cells may be improved, not by changes in the starch content, but by changes in the flour content wherein the protein constituent is either modified or used as a film.

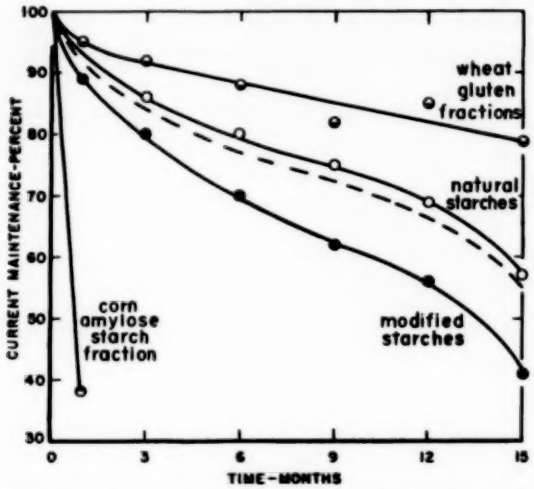

FIGURE 5.—*Current maintenance of D-size flashlight cells stored at 21° C and made with paste walls of natural starches, modified starches, and gluten fractions.*

◒, 7 gluten fractions (45 cells); ○, 8 starch-flour combinations (169 cells); ●, 5 modified starches (42 cells); ◓ amylose (2 cells); — — — —, cornstarch-wheat flour (48 cells).

III. Conclusions

The results of this investigation have shown that the paste walls of dry cells react for a time with the depolarizing mix of manganese dioxide, and to a lesser degree with the zinc and ammonium chlorides of the electrolyte. It was shown that these reactions could not be eliminated or curtailed by using different varieties of starches, modified starches of low reducing power, starch fractions of low reducing power, or by the use of addition agents. Improvements in dry cells could be made, however, by using protein films on the surface of the zinc anode of a dry cell. These films decrease the local action at the anodes whereby the gassing and the drying out of the dry cell and the desiccation of the paste wall are retarded. This suggests that these latter factors are more critical than the deterioration, or the interaction of the paste wall with the constituents of the dry cell, in determining the shelf life of dry batteries in hot and humid climates.

Acknowledgment is gratefully given to George W. Vinal for his interest and suggestions during the course of this investigation, to Harriet L. Frush for the determination of the purity of amylose, to H. S. Isbell for the preparation of a modified starch, and to Earl Otto and C. K. Morehouse and their associates for many of the electrical measurements reported in this paper.

IV. References

[1] E. Otto, G. W. Vinal, and E. Ostrander, Trans. Electrochem. Soc. **86,** 235 (1944).
[2] O. W. Chapman and J. H. Buchanan, Iowa State College, J. Sci. **4,** 441 (1930).
[3] W. J. Hamer, J. Research NBS **39,** 29 (1947) RP1810.
[4] E. Angelescu and O. Manolescu, Bul. Soc. Chim. Romania **11,** 99 (1930).
[5] C. K. Morehouse, W. J. Hamer, and G. W. Vinal, J. Research NBS **40,** 149 (1948) RP 1863.
[6] G. Felton, F. F. Farley, and R. M. Hixon, Cereal Chem. **15,** 678 (1938).
[7] H. S. Isbell. Unpublished.
[8] K. H. Meyer, Advances in colloid science, p. 182, edited by E. O. Kraemer (Interscience Pub. Inc., New York, N. Y., 1941).
[9] T. J. Schoch, J. Am. Chem. Soc. **60,** 2824 (1938).
[10] E. J. Wilson, Jr., T. J. Schoch, and C. S. Hudson, J. Am. Chem. Soc. **65,** 1380 (1943).
[11] R. M. McCready and W. J. Hassid, J. Am. Chem. Soc. **65,** 1154 (1943).
[12] B. Brimhall and R. M. Hixon, Ind. Eng. Chem., Anal. Ed. **11,** 358 (1939).
[13] D. B. Dill and C. L. Alsberg, Cereal Chem. **1,** 229 (1924).
[14] L. S. Stockelbach and C. H. Bailey, Cereal Chem. **15,** 801 (1938).
[15] G. Haugaard and A. H. Johnson, J. Biol. Chem. **93,** 677 (1931).

WASHINGTON, October 7, 1947.